2018

Prelimbic Cortical Synaptic and Structural Plasticity Following Cocaine Self-administration and Abstinence in Rats: Role of Glutamatergic Pathway Specificity

Benjamin Michael Siemsen
Medical University of South Carolina

Prelimbic Cortical Synaptic and Structural Plasticity Following Cocaine Self-administration and Abstinence in Rats: Role of Glutamatergic Pathway Specificity

Benjamin Michael Siemsen
Department of Neuroscience
2018

A dissertation submitted to the faculty of the Medical University of South Carolina in partial fulfillment of the requirements for the degree of Doctor of Philosophy in the College of Graduate Studies.

Approved by:

Chairperson, Advisory Committee — Jacqueline F. McGinty

Peter W. Kalivas

John J. Woodward

William C. Griffin, III

Paul J. Lombroso

Joseph B. Blumer

Acknowledgements

The work presented herein is dedicated to all of those who have helped me grow intellectually over the past five years.

I would first like to thank my friend and mentor Dr. Jacqueline McGinty for providing an excellent mentoring environment. Dr. McGinty provided not only careful and planned mentoring to ensure my success, but also encouraged my growth by challenging me intellectually; whether it be through data interpretation or planning of experiments. Obviously, this work could not have been completed without her guidance and support along the way.

I would also like to extend my gratitude to three specific colleagues who have helped me along the way. First, I would like to thank Dr. Sarah Barry. As a fellow graduate student in the McGinty lab, Dr. Sarah Barry provided me with outstanding training in the use of the Wes™ system used throughout this dissertation and several of the experiments could not have been accomplished without her help. Second, I would like to thank Dr. Giuseppe Giannotti. As a former postdoctoral scholar in the McGinty lab, Dr. Giannotti and I developed an extremely close working relationship, particularly with the use of chemogenetic vectors. Third, I would like to thank Dr. Michael Scofield for his dedication to the collaboration that led to the development of techniques presented in Chapter four.

I would like to thank my committee members for their insightful comments and for providing alternative interpretations for data presented at various seminars and committee meetings.

Additional thanks go out to all the rotating graduate students, undergraduate scholars and volunteers, and technicians that I have worked with over the years. These people have been critical for the success of several of the experiments presented within this dissertation.

I would also like to thank my family and friends who have supported me throughout this endeavor. My mother and father have always encouraged me to do my best, honest work throughout life, and this has extended into my time in graduate school at MUSC.

I would like to thank my NIDA funding sources: RO1 DA033479, P50-DA015369, T32 DA07288, and F31 DA041021.

Finally, I would like to extend my utmost gratitude to my fiancé Amelia Smith for always being there for me through thick and thin over these last five years. I could not have gotten through the tough times without her.

Table of contents

List of figures

BENJAMIN MICHAEL SIEMSEN. Prelimbic cortical synaptic and structural plasticity following cocaine self-administration and abstinence in rats: Role of glutamatergic pathway specificity. (Under the direction of JACQUELINE F. MCGINTY)

Abstract

The primary goal of this dissertation is to further examine the role of the prelimbic (PrL) subdivision of the rodent medial prefrontal cortex in relapse to cocaine seeking following abstinence, and to extend our understanding of pathway-specific adaptations in the PrL cortex projection to the nucleus accumbens (NAc) core that drives relapse. Previous findings indicate that the PrL cortex shows a biphasic response to abstinence from cocaine exposure. Specifically, early withdrawal (two hours after the final self-administration session) results in dephosphorylation of glutamate NMDA receptors and glutamate signaling regulators including extracellular signal-regulated kinase and the downstream transcription factor cAMP response-element binding protein (CREB). One week of abstinence enhances p-CREB and AMPA receptor subunit GluA1 phosphorylation in the PrL cortex, and Synapsin I in the NAc core. Interventions that act to normalize glutamate transmission in the PrL cortex during early withdrawal provide an enduring suppression of drug-seeking by normalizing activity in the PrL-NAc core pathway. Using a combination of biochemical and behavioral pharmacology techniques, we have found that the cocaine-induced activation of STriatal-Enriched protein tyrosine Phosphatase in the PrL cortex during early withdrawal plays a role in subsequent cocaine seeking by dephosphorylating extra-cellular

signal-regulated kinase. We also show that chemogenetic-mediated activation of the PrL cortex, or PrL-NAc core neurons, immediately after self-administration transiently reduces drug seeking which is not sustained. Finally, using an array of immunohistochemistry, pathway-specific viral vectors, and high-resolution confocal microscopy techniques, we provide evidence that PrL-NAc core neurons show reduced immunoreactivity of the activity markers Fos and p-CREB, reduced dendritic spine head diameter, and reduced GluA1/2 expression in subsets of dendritic spines during early withdrawal. The opposite effect was found after one week of abstinence. At this timepoint, PrL-NAc core neurons showed heightened nuclear p-CREB, spine head diameter, and GluA1/2 expression in dendritic spines. These findings suggest that the PrL cortex, and specifically PrL-NAc core neurons, undergoes an abstinence duration-dependent transformation in glutamate transmission which may be regulated by the activation of STEP during early withdrawal.

Chapter 1: General Introduction

The role of the prefrontal cortex in drug-seeking behavior: Findings from clinical studies

Illicit drug use in general is a major societal concern and in 2007 alone was estimated to cost the United States economy 193 billion dollars annually in costs related to crime, health, and productivity. For comparison, costs related to treatment and management of diabetes in the United States was 173 billion dollars in 2007 (NDIC, 2011). In 2011, approximately half of all emergency department visits were related to illicit drug misuse. Importantly, cocaine misuse in particular was responsible for approximately 40% of the emergency department visits related to illicit drug misuse (SAMHSA, 2011). From the perspective of an addicted patient, illicit drug abuse not only produces great external society harm, but also produces internal harm by increasing the risk of developing a Substance Use Disorder (SUD). Globally, of the total percentage of individuals initially experimenting with illicit drug use, approximately 20% will meet criteria for diagnosis of a SUD (Degenhardt and Hall, 2012).

A major clinical issue in the treatment of SUDs is the relatively high propensity for relapse, even after prolonged periods of abstinence (Sinha, 2011). In a metanalysis examining relapse rates of treatment-engaged patients, it was found that following 50 days of discharge from a treatment center, less than half of cocaine-addicted patients remain abstinent. Remarkably, after one year only approximately 12.5% of patients remained abstinent (Sinha, 2011). Thus, a major goal of drug addiction research is determining neural mechanisms underlying

relapse and finding pharmacological targets to prevent relapse. Craving, a necessary precursor to relapse, can result from exposure of an addict to drug-associated contexts or cues, invigorating the unmanageable desire to seek and ultimately use drugs (Kalivas, 2009). In clinical studies, the prefrontal cortex has emerged as a critical regulator of relapse behavior (Goldstein and Volkow, 2011) which is attributed to its downstream innervation of limbic-motor regions implicated in the execution of motivated behavior, such as the ventral striatum (Kalivas and Volkow, 2011). Furthermore, human addicts observing cocaine-related videos show hyperactivation of the prefrontal cortex in response to cues (i.e. paraphernalia), which positively correlates with self-reported craving (Robbins et al., 1999; Garavan et al., 2000).

Interestingly, similar prefrontal cortical regions show reduced glucose metabolism using Positron-Emission Tomography (PET) following several weeks of abstinence from cocaine use (Volkow et al., 1992) a phenomena termed ‘hypofrontality’. This decreased activity is likely important for relapse because repetitive transcranial magnetic stimulation (rTMS), a technique to elevate neuronal activity in defined brain regions, of the dorsolateral prefrontal cortex during abstinence appears to reduce cocaine use as well as craving (Terraneo et al., 2016). Additionally, hypoactivity of the medial prefrontal cortex (mPFC) during a cognitive challenge task correlates with propensity for relapse (Brewer et al., 2008).

Structurally, grey matter volume is reduced in the mPFC in cocaine abusing patients relative to healthy controls (Ersche et al., 2011), and grey matter volume

negatively correlates with years of use (Ide et al., 2014). However, grey matter volume normalizes after 6 months of abstinence (Parvaz et al., 2017). Collectively, these findings indicate that cocaine use produces maladaptive structural and functional alterations in prefrontal regions, which may serve as biomarkers for relapse propensity. However, these cocaine-induced structural adaptations appear to be plastic such that the recovery process during abstinence involves reorganization of these regions involved in behavioral control, which may be important for successful relapse prevention. Although neuroimaging and clinical neuropsychological measurements of addicted patients are critical for the development of pharmacological treatments for preventing relapse, preclinical models have provided a wealth of knowledge pertaining to neurotransmitters and circuitry involved in relapse-like events. Accordingly, animal models of addiction remain essential for furthering our understanding of drug-induced adaptations and how contexts and cues associated with drug reward gain salience to drive craving and ultimately relapse (Garcia Pardo et al., 2017).

Role of the prefrontal cortex in relapse to cocaine seeking: Findings from preclinical studies

Several decades of work have led to the conclusion that cocaine-induced elevations in extracellular dopamine (Everitt and Wolf, 2002) within limbic-reward regions are critical for not only the rewarding characteristics of acute cocaine, but also the reinforcement learning that occurs between contexts, cues, and the interoceptive state induced by cocaine (Wise et al., 2008; Volkow et al., 2017). Chronic elevations in dopamine lead to increased transcription of genes involved in reinforcement learning, facilitating the encoding of the association between the

rewarding characteristics of drugs of abuse and contexts or cues (Pulipparacharuvil et al., 2008; Taniguchi et al., 2017). Ultimately, this produces heightened sensitivity to glutamatergic inputs, as discussed in detail below.

Preclinical models of addiction using self-administration (SA), followed by extinction and reinstatement, in rodents have revealed a critical role for dopamine release in the prelimbic (PrL) cortex (McGlinchey et al., 2016; James et al., 2018) and the nucleus accumbens core (NAc core) (Shen et al., 2014a) in reinstating cocaine seeking. However, the induction of cocaine seeking is dependent on elevated PrL glutamate release in the NAc core (Figure 1.1) (Kalivas et al., 2005; Kalivas, 2009). Thus, cocaine experience produces profound alterations in glutamatergic plasticity, which may be due to chronic dopamine elevations, in both the NAc core as well as the upstream PrL cortex, changes which are critical for subsequent relapse following presentation of drug-associated stimuli (Kalivas, 2009).

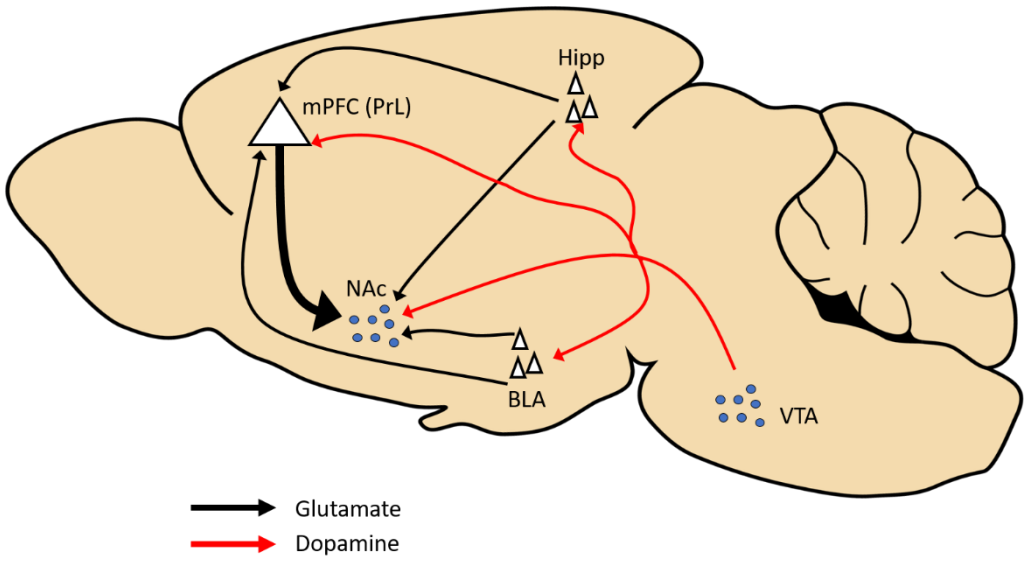

Figure 1.1. Dopamine and glutamate pathways within the brain reward circuitry. Cocaine-induced adaptations in dopamine transmission in the NAc core and PrL

cortex induce alterations in glutamatergic transmission in the NAc core. Heightened glutamate release in the NAc core arising from the PrL cortex is highly implicated in relapse to cocaine seeking following re-exposure to conditioned contexts or cues after abstinence.

These findings suggest that targeting corticostriatal glutamatergic dysfunction during abstinence may provide an enduring reduction in relapse vulnerability following presentation of cocaine-associated contexts and stimuli. Indeed, treatments which normalize corticostriatal glutamate transmission, such as N-acetylcysteine (NAC) provide an enduring suppression of relapse in preclinical models (Moussawi et al., 2009). However, such treatments have provided mixed results in promoting abstinence in clinical populations (McClure et al., 2014). Regardless, it is well-accepted that treatment approaches to promote abstinence in human populations should be directed towards normalizing glutamate transmission between the PFC and NAc core.

Several lines of evidence implicate heightened glutamatergic transmission arising from PrL afferents in the NAc core as a mediator of cocaine-seeking behavior. For example, optogenetic-mediated inactivation of the PrL, the NAc core, or PrL axon terminals within the NAc core, immediately prior to a cue-induced relapse test in rats suppresses cocaine seeking (Stefanik et al., 2013). Additionally, glutamate release arising from PrL afferents in the NAc core mediates cocaine prime-induced reinstatement, and glutamate levels in the NAc core are suppressed following chronic cocaine SA and extinction training (McFarland et al., 2003). However, other glutamatergic inputs to the NAc core are critical for cue-induced reinstatement, including basolateral amygdala (BLA) afferents within the NAc core (Stefanik and Kalivas, 2013).

However, in most experiments interrogating cocaine-induced plasticity in corticostriatal circuits, interventions have been performed immediately prior to relapse testing in rats. This approach has informed our understanding of plasticity that mediates relapse occurring at this abstinence timepoint. However, this approach may not be beneficial for preventing relapse in clinical populations because neuroadaptations involved in relapse in brain reward circuitry have fully developed and may be less malleable relative to earlier abstinence timepoints. Relatively less is known about how chronic cocaine SA in rats alters excitatory transmission between the PrL and the NAc core during early withdrawal, a timepoint which may be particularly useful for interventions in clinical populations (McGinty et al., 2015). Indeed, the early hours of drug withdrawal have been found to be a critical timepoint for relapse prevention in preclinical models.

Early withdrawal, PrL cortex, and BDNF

In the last decade our laboratory has vigorously investigated alterations in glutamatergic transmission within the PrL cortex during early withdrawal (i.e. two hours after the final cocaine SA session). Several lines of evidence have shown that this timepoint is critical for relapse prevention. First, we have found that a single infusion of brain-derived neurotrophic factor (BDNF) into the PrL cortex immediately after the final of 14 daily cocaine SA sessions provides an enduring suppression of relapse to contexts, cues, as well as a priming injection of cocaine for at least three weeks after the infusion (Berglind et al., 2007). Second, this intervention normalizes glutamatergic neurotransmission within the NAc core following extinction and prevents the cocaine prime-induced elevation in

extracellular glutamate in the NAc core (Berglind et al., 2009). This is associated with a normalization of augmented Synapsin phosphorylation, and presumably glutamate release probability, in the NAc core during early withdrawal (Sun et al., 2014a), suggesting BDNF normalizes PrL-NAc core glutamate transmission. Third, the suppressive effect of PrL BDNF on cocaine seeking relies on the normalization of a cocaine-induced dephosphorylation of several key glutamatergic signaling entities in the PrL cortex during early withdrawal; including extracellular signal-regulated kinase 2 (ERK2), the downstream transcription factor cAMP response-element binding protein (CREB), as well as the N-Methyl-D-Aspartate (NMDA) receptor subunits, GluN2A and GluN2B (Whitfield et al., 2011; Go et al., 2016; Barry and McGinty, 2017). Specifically, preventing BDNF from reversing the cocaine-induced dephosphorylation of these signaling molecules with selective antagonists and kinase inhibitors prevents intra-PrL BDNF from suppressing cocaine seeking (Go et al., 2016; Barry and McGinty, 2017). Interestingly, these dephosphorylation events are transient in nature such that the ERK2 dephosphorylation is normalized 24 hours after the final SA session (Whitfield et al., 2011). A major question resulting from this body of work is how chronic cocaine SA results in these dephosphorylation events, and specifically, what phosphatase might be activated in the PrL cortex during this early withdrawal timepoint to drive these dephosphorylation events.

Striatal-enriched protein tyrosine phosphatase as a likely mediator of PrL dysfunction during early withdrawal

The STriatal-Enriched protein tyrosine Phosphatase (STEP) has arisen as an important regulator of ERK2 (Paul et al., 2003), GluN2B (Braithwaite et al., 2006),

and more recently, GluN2A (Tian et al., 2016) tyrosine phosphorylation. GluN2A^{Y1325} phosphorylation potentiates NMDA-mediated excitatory currents by increasing GluN2A open channel probability (Taniguchi et al., 2009). GluN2B^{Y1472} phosphorylation inhibits internalization of GluN2B-containing NMDA receptors, enhancing synaptic activity (Carreno et al., 2011). Dephosphorylation of these NMDA receptor subunits would therefore likely produce a suppression of NMDA-receptor mediated currents in the PrL cortex during early withdrawal from cocaine SA, although this has yet to be shown.

Previous studies indicate that NMDA or glutamate stimulation in cultured neurons leads to a rapid but transient NMDA receptor-dependent elevation in ERK2 phosphorylation (Paul et al., 2003). The rapid rise in ERK2 phosphorylation is GluN2A-dependent, whereas the subsequent dephosphorylation of ERK2 is GluN2B-dependent (Paul and Connor, 2010). Finally, our lab has previously shown that cocaine SA leads to STEP dephosphorylation in the PrL cortex during early withdrawal, resulting in STEP activation (Sun et al., 2013).

Apart from its role in regulating glutamatergic neurotransmission, STEP also plays a role in actin depolymerization following NMDA receptor stimulation *in vitro*. Specifically, NMDA receptor activation in cultured neurons activates STEP and leads to the STEP-dependent dephosphorylation of the actin binding protein, SH3 protein interacting with NCK of 90 kD (SPIN90) (Cho et al., 2013). When tyrosine is phosphorylated by Src family kinases (SFKs), SPIN90 acts as a potent inhibitor of the actin-depolymerizing factor, cofilin, in dendritic spine heads.

However, when dephosphorylated by STEP, SPIN90 translocates to the dendritic shaft, allowing for cofilin-mediated actin depolymerization in dendritic spine heads.

Thus, it is possible that the activation of STEP during early withdrawal in the PrL cortex may be accompanied by actin depolymerization, leading to shrinkage of dendritic spine heads. Moreover, STEP dephosphorylates C-terminal tyrosine residues of the GluA2 subunit of AMPA receptors, promoting endocytosis of GluA2-containing AMPA receptors (Zhang et al., 2008). Collectively, these findings indicate that STEP not only functions to limit excitatory neurotransmission via dephosphorylation of key tyrosine residues on both AMPA and NMDA receptors, but that STEP activation also facilitates actin depolymerization through interactions with actin binding proteins. See Figure 1.2 for a diagram summarizing the consequences of increased STEP activity on glutamate signaling. Such alterations in actin polymerization may result in changes in the morphology of dendritic spines, and presumably the activity state of neurons as discussed below.

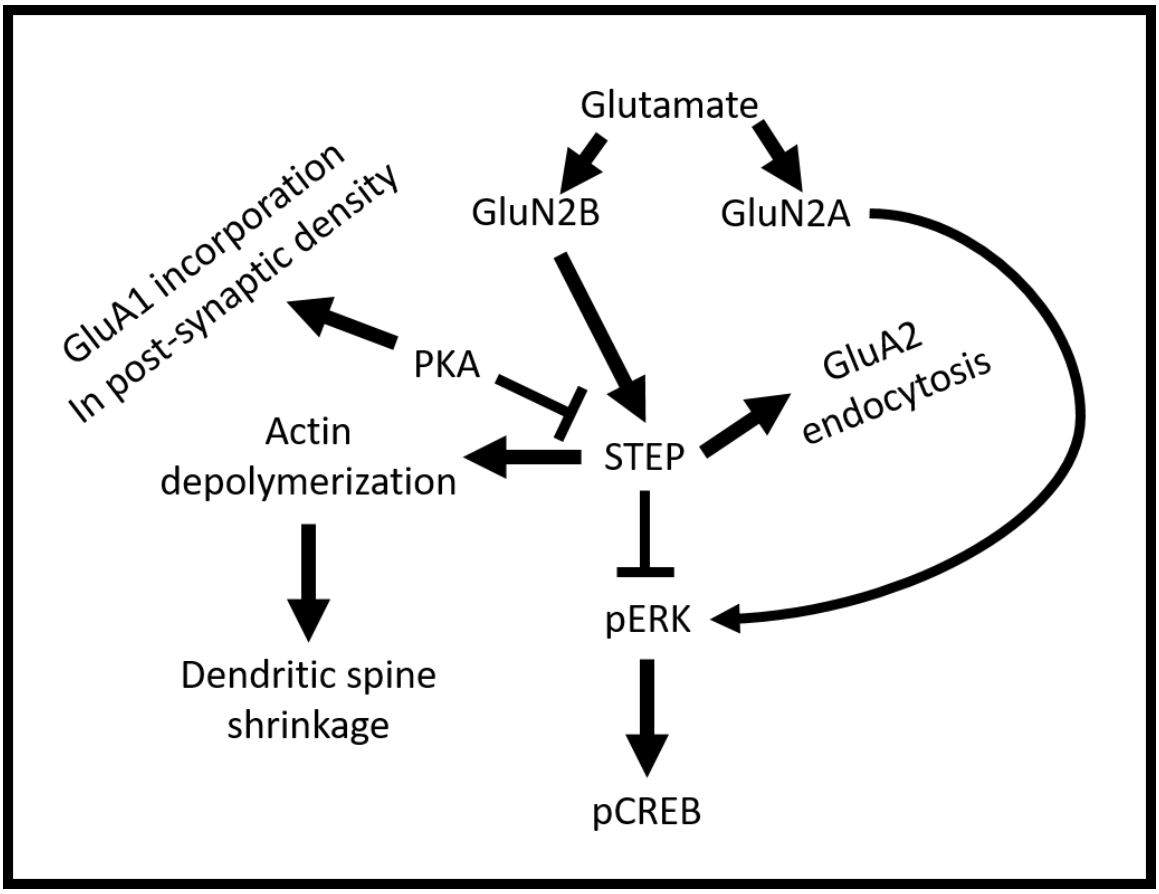

Figure 1.2 Diagram summarizing consequences of STEP activation on glutamate signaling. STEP activation suppresses ERK signaling and promotes endocytosis of GluA2-containing AMPA receptors. STEP also interacts with the actin binding protein substrate SPIN90 (not shown) to facilitate actin depolymerization leading to shrinkage of dendritic spines.

Dendritic spine morphology as an index of neuronal physiology

Dendritic spines are small protrusions arising from dendrites that are enriched in f-actin, actin binding proteins, post-synaptic receptors, as well as scaffolding proteins linking receptors to effectors and internal Ca^{2+} stores (Sala and Segal, 2014). For several decades, it has been suggested that actin polymerization plays a critical role in mediating synaptic plasticity (Fifkova and Delay, 1982). Dendritic spines exist in various morphological states and are generally classified into four

main categories; filopodia, thin, stubby, and mushroom, with the latter forming stable and mature synapses (Bellot et al., 2014). In the adult cortex, filopodia, which are generally thought to be immature protrusions but are required for initial spinogenesis (formation of new spines), are low in density (Zuo et al., 2005). Moreover, others have suggested that filopodia are indeed not dendritic spines due to their overall lack of a defined spine head (Dailey and Smith, 1996).

Furthermore, the pruning and formation of new dendritic spines, as well as the stabilization of existing spines (i.e. structural plasticity), is thought to underlie several components of plasticity mediating learning and memory (Fu and Zuo, 2011). Indeed, several studies have demonstrated changes in the morphology of dendritic spine heads following LTP induction, such as the enlargement of spine heads and shortening/widening of the spine neck (Tonnesen et al., 2014), are highly correlated with the potentiation of glutamatergic excitatory neurotransmission (Kasai et al., 2003). Thus, synaptic plasticity at excitatory synapses mediating learning and memory in various brain regions is reflected in alterations in dendritic spine morphology, and such changes may be an index of the activity state of neurons.

Role of AMPA receptor subunit conformation and transmission in dendritic spine morphology

Ionotropic glutamate receptors subserve the majority of excitatory neurotransmission within the brain (Hollmann and Heinemann, 1994). Physiologically, NMDA receptor activation produces a rise in intracellular Ca^{2+} which is important for enlargement of dendritic spine heads during the induction of long-term potentiation. This series of events is dependent on calmodulin, actin

polymerization, and an increase in AMPA receptor-mediated glutamate currents (Matsuzaki et al., 2004). Studies *in vitro* have shown that, in particular, the GluA2 subunit of AMPA receptors is important for dendritic spine head enlargement (Passafaro et al., 2003).

The GluA1 subunit of AMPA receptors is critical for glutamatergic plasticity, and phosphorylation of several key C-terminal residues of GluA1 potentiates AMPA receptor-mediated excitatory transmission. Specifically, phosphorylation of GluA1^{S845} through a cAMP-dependent protein kinase A (PKA)-mediated mechanism enhances glutamate currents (Roche et al., 1996). Interestingly, AMPA receptors are extremely abundant in mature, mushroom-type dendritic spines, but display low abundance in thin and filopodia-type dendritic spines, subtypes which are thought to be more malleable in response to differential excitatory input and may be the site of so-called silent synapses (Matsuzaki et al., 2001). Collectively, these findings indicate that AMPA receptor phosphorylation, and trafficking to synapses, is a critical event mediating synaptic potentiation; which requires actin polymerization and enlargement of dendritic spine heads. Regarding the effect of short access cocaine SA on AMPA receptor phosphorylation in the PrL cortex, our lab has found no such alterations during early withdrawal. However, in contrast to early withdrawal, one week of abstinence (i.e. early abstinence) results in profound alterations in AMPA receptor phosphorylation due to elevated PKA activity.

Prelimbic cortex and early abstinence

As discussed above, the PrL cortex shows a state of diminished glutamatergic neurotransmission during early withdrawal which is reversed by BDNF. However, additional data collected in our laboratory suggest that plasticity occurring over one week of abstinence renders the PrL cortex hypersensitive to inputs encoding cocaine-conditioned stimuli. Specifically, following one week of forced abstinence there is enhanced phosphorylation of CREB with no alteration in ERK2 phosphorylation. Furthermore, the PKA target GluA1^{S845} is also elevated after one week of forced abstinence (Sun et al., 2014b). Importantly, an intra-PrL infusion of the PKA inhibitor, Rp-cAMPS, prior to context-induced relapse after abstinence normalizes the hyperphosphorylation of GluA1 and CREB, suppressing context-induced relapse.

PKA phosphorylation of GluA1^{S845} has been shown to enhance plasma membrane insertion of AMPA receptors, augmenting excitatory neurotransmission (Banke et al., 2000; Oh et al., 2006). Apart from the upstream kinase ERK2, PKA is also an important regulator of CREB phosphorylation and CREB-mediated gene transcription in the cortex (Kelly, 2018). Several experiments have implicated dopamine receptor D1-PKA signaling in both the PrL cortex (Boudreau et al., 2009) as well as the NAc core (Hope et al., 2005) in neuroplasticity following chronic cocaine administration. In a cocaine SA paradigm, infusion of dopamine into the NAc core or the PrL cortex is sufficient to induce reinstatement following extinction (Cornish and Kalivas, 2000; McFarland and Kalivas, 2001).

The finding that the PrL cortex shows a hyperphosphorylation of PKA targets, GluA1 and CREB, indicates the potential for hyperactivity within the PrL cortex following one week of abstinence. This is not without precedent, as a recent experiment showed elevated AMPA:NMDA ratio, an index of synaptic potentiation, following withdrawal from cocaine-induced conditioned place preference (Otis and Mueller, 2017). Noncontingent cocaine administration has also been shown to increase excitability of PrL neurons by inhibiting G protein-gated inwardly rectifying K^+ (GIRK) channels (Dong et al., 2005; Hearing et al., 2013). Interestingly, a deletion of GIRK channel-encoding genes in forebrain neurons of knockout mice is sufficient to augment cocaine-induced locomotion, which is associated with increased PrL-NAc core glutamate transmission (Marron Fernandez de Velasco et al., 2017). Finally, a cocaine-induced behavioral sensitization paradigm augments extracellular glutamate levels in the PrL cortex after 7 days of withdrawal, suggesting elevated glutamate tone on PrL pyramidal neurons (Williams and Steketee, 2004).

A recent study found that after extinction from cocaine SA, there is an increase in intrinsic excitability of PrL neurons (Sepulveda-Orengo et al., 2017). This induction of PrL hyperexcitability is likely not an epiphenomenon, as drugs that impair cocaine reinstatement show a normalization of this hyperexcitability (Sepulveda-Orengo et al., 2017). Recent evidence also indicates a role for sensitized PrL D1-PKA signaling following chronic cocaine injections in decreasing the threshold for the induction of spike-timing-dependent LTP in layer V pyramidal neurons, perhaps priming synapses for potentiation following subsequent cue

exposure (Ruan and Yao, 2017). Moreover, elevated BDNF expression in the PrL cortex following 8 days of cocaine withdrawal facilitates LTP induction in layer V pyramidal neurons, which mediates locomotor sensitization (Lu et al., 2010).

Taken together, these findings indicate that the PrL cortex likely transitions from a state of glutamatergic hypoactivity to one of glutamatergic hypersensitivity as a function of abstinence duration. This hypersensitive state may be dependent on elevated sensitivity to dopaminergic inputs, perhaps priming synapses for an augmented response to incoming glutamatergic inputs. This is supported by the finding that there is increased activation of prefrontal cortical regions following presentation of cocaine-conditioned cues in human cocaine abusers (Pulipparacharuvil et al., 2008) as well as increased immediate early gene expression, a proxy for elevated neuronal activity (Dragunow and Faull, 1989), during presentation of cocaine-conditioned cues (James et al., 2018) or contexts (Hearing et al., 2008) in rodents. Although it is unclear whether cocaine SA alters the electrophysiological properties of PrL neurons after one week of abstinence, *ex vivo* and *in vivo* electrophysiology have been used to address cocaine-induced alterations in such properties of neurons in the PrL cortex and the NAc core at other timepoints.

Cocaine-induced alterations in physiology and structural plasticity in cortico-accumbens circuitry

Although several studies have investigated how chronic cocaine exposure alters excitatory neurotransmission within the NAc core, fewer experiments have investigated alterations in physiology induced by chronic cocaine exposure in the PrL cortex. In the NAc core, basal AMPA:NMDA ratio is elevated following

extinction from cocaine SA, which is augmented by 15 minutes of cue-induced reinstatement, representing a period of transient synaptic potentiation (tSP). The elevated AMPA:NMDA ratio is associated with increased dendritic spine head diameters following extinction that undergo further potentiation during cue-induced reinstatement (Gipson et al., 2013; Smith et al., 2014). Importantly, these transient adaptations rely on glutamate release arising from the PrL cortex (Stefanik et al., 2016). Further, it has been shown that chronic cocaine SA and withdrawal produce a marked inability to induce LTP or LTD in NAc core neurons following stimulation of the prefrontal cortex *in vivo* (Moussawi et al., 2009). Moreover, animals undergoing 30 days of abstinence from cocaine SA show a higher proportion of 'phasically active' NAc core neurons during resumption of cocaine SA relative to one day of abstinence, suggesting prolonged abstinence elevates cocaine-cue encoding and responsiveness in NAc core neurons (Hollander and Carelli, 2005). Thus, cocaine SA induces dysfunctional glutamatergic transmission in PrL afferents within the NAc core, which are likely important for craving and relapse to cocaine seeking following re-exposure to cocaine-conditioned stimuli.

As discussed above, few experiments have investigated cocaine-induced alterations in physiology or structural plasticity within the PrL cortex, which is surprising given its critical role in behavioral activation and subsequent relapse. A key study found that, relative to baseline, the firing rate of mPFC neurons is suppressed following cocaine infusions in a SA paradigm. However, this effect was normalized after 10 days of SA. Interestingly, this was associated with decreased basal firing rate following the first cocaine infusion during each day of SA (Sun and

Rebec, 2006). Furthermore, the authors found enhanced burst firing and numbers of spikes per burst relative to baseline in cocaine-experienced animals. The authors conclude that although cocaine dampens basal PFC firing rates, the encoding of cocaine-conditioned stimuli is enhanced following chronic cocaine SA. Data from our lab indicate that daily cocaine experience produces a dampening of PrL firing rates, with subsequent daily sessions recruiting a larger percentage of suppressed neurons (Dennis et al., 2018). Moreover, it has been shown that 30 days of abstinence from cocaine SA increases the percentage of 'phasically active' PrL, but not IL, cortical neurons during extinction day 1, relative to one day of abstinence (West et al., 2014). A similar effect was shown following resumption of cocaine SA after one month of abstinence.

Following long-access cocaine SA and extinction training, a subset of rats who show compulsive cocaine-seeking behavior have decreased intrinsic excitability in deep-layer pyramidal neurons of the PrL cortex (Chen et al., 2013). Rescuing this hypoexcitability with optogenetic stimulation reduced compulsive cocaine seeking (Chen et al., 2013). In concert, these findings indicate that, in general, cocaine experience increases the encoding of cocaine-associated stimuli by PrL neurons. However, this may be associated with suppressed activity of these neurons at baseline.

Cocaine-induced alterations in PrL structural plasticity

Although well-documented adaptations in dendritic spine morphology or density have been demonstrated in the NAc core, fewer experiments have been done investigating such adaptations in the PrL cortex. The few studies that have been

performed have provided mixed results regarding the effect of cocaine SA and various lengths of abstinence on PrL structural adaptations. This discrepancy appears to be due to different techniques to label dendritic spines, different abstinence timepoints, different pyramidal neurons (i.e. layer II/III versus V), as well as different regions of the dendrite analyzed (basal versus apical). Using Golgi staining, experiments have generally reported increased spine density on apical dendrites after one month of abstinence (Robinson et al., 2001) and basal dendrites after one week of abstinence (Rasakham et al., 2014). This agrees with the finding that MDMA behavioral sensitization produces increases in spine density of distal apical dendrites of layer V PrL neurons (Ball et al., 2009). However, Golgi staining typically uses 2D photomicrographs to trace dendrites, neglecting dendritic spines that protrude axially. Additionally, relative to labeling of neurons with the lipophilic dye DiI, Golgi staining severely underestimates the number of spines, particularly thin spines (Shen et al., 2008). In contrast, more recent experiments using advanced techniques have found reduced layer II/III apical spine density after two weeks of abstinence (Radley et al., 2015) and reduced layer V apical spine density specifically in neurons innervating D1-, but not D2,-expressing MSN's in the NAc core after 14 days of withdrawal from daily noncontingent cocaine injections (Barrientos et al., 2018).

Although these experiments have provided valuable insight into how cocaine SA alters the structure and function of PrL neurons, only recently have they revealed pathway-specific structural adaptations. This is important given the heterogeneity of PrL efferents. For example, layer II/III pyramidal neurons project

to several downstream structures including the BLA (Gabbott et al., 2005; Little and Carter, 2013). This well-defined projection likely contributes to prefrontal cortical modulation of cognition as well as emotional drive. However, layer II/III pyramidal neurons also project to the contralateral mPFC (Little and Carter, 2013), as well as dorsal striatal regions regulating motor control (Gabbott et al., 2005). In contrast, layer V pyramidal neurons provide robust innervation of the NAc core (Gabbott et al., 2005), a pathway that has been shown to be a key projection in cocaine-induced plasticity underlying relapse (discussed in detail above). Layer V pyramidal neurons also innervate the dorsomedial striatum, as well as the BLA. Additionally, these neurons project to other subcortical structures implicated in prefrontal cortical regulation of motivation, such as the lateral hypothalamus (Gabbott et al., 2005).

Thus, experiments investigating PrL structural adaptations resulting from cocaine SA should provide additional information regarding how these adaptations might occur in a pathway-specific manner. These observations would provide critical information regarding projection-defined adaptations. Importantly, no studies to date have investigated not only how cocaine SA alters PrL structural plasticity during early withdrawal, but also whether this occurs in neurons projecting from the PrL cortex to the NAc core. Assuming cocaine-induced plasticity is altered in a pathway-specific manner, it is therefore imperative to possess tools to interrogate the effect of pathway-specific manipulations of PrL neurons on subsequent behavioral responses to cocaine-conditioned stimuli.

Designer Receptors Exclusively Activated by Designer Drugs (DREADDs): A chemogenetic toolkit for altering neuronal activity in a pathway-specific manner

DREADDs are mutated human muscarinic receptors that lack the binding site for the endogenous ligand, acetylcholine, but have gained affinity for the exogenous ligand clozapine-N-oxide (CNO) (Pei et al., 2008). Specifically, DREADDs take advantage of endogenous signaling cascades coupled to $G\alpha_i$ (hM4Di), $G\alpha_q$ (hM3Dq), and $G\alpha_s$ (rM3Ds) signaling which decrease, increase, and modulate neuronal excitability, respectively (Rogan and Roth, 2011). DREADDs are typically introduced into neuronal populations through adeno-associated viral vectors containing DNA encoding for DREADD receptors (Smith et al., 2016). Initially, DREADD expression was exclusively driven by a cell-type specific promoter (i.e. CaMKIIα) or a pan-neuronal promoter (i.e. Synapsin). More recently, the advent of intersectional viral approaches has allowed for the manipulation of specific neuronal pathways using DREADDs. This requires the use of viral vectors injected in terminal regions of interest which show preferential retrograde transport and express Cre-recombinase in all neurons projecting to said region (Junyent and Kremer, 2015; Tervo et al., 2016). This is combined with infusions of viral vectors containing Cre-dependent DNA in given brain regions innervating the area where retrograde viruses were infused. Ultimately, this allows for Cre-dependent DREADD expression in a defined pathway of interest (Garcia et al., 2017).

In the last several years, the use of pathway-specific DREADDs has been applied to the interrogation of prefrontal cortical efferents implicated in relapse to cocaine seeking. For example, Augur and colleagues recently found that

chemogenetic activation of the ventromedial prefrontal cortex (vmPFC), including the IL cortex, immediately prior to cue-induced reinstatement was sufficient to suppress relapse. Moreover, they found that preferentially activating vmPFC projections to the NAc shell was sufficient to reproduce this effect (Augur et al., 2016). This finding suggests that the primary mechanism of action of hM3Dq activation of this pathway was to reactivate IL cortical neurons projecting to the NAc shell encoding the updated contingency of cocaine availability inherent in extinction training.

Using Gi-coupled DREADDs, Kerstetter and colleagues found that inhibition of PrL projections to the NAc core during daily cocaine SA sessions resulted in enhanced responding on the formerly active lever during extinction, and increased responding on the active lever during cocaine prime-induced reinstatement. However, inhibiting this pathway immediately prior to reinstatement was sufficient to suppress cocaine prime-induced reinstatement (Kerstetter et al., 2016). This finding is consistent with a role for elevated PrL glutamate release in the NAc core mediating cocaine prime-induced reinstatement (McFarland et al., 2003).

Data from our lab indicate that Gi-DREADD inhibition of all PrL outputs using a CaMKIIα promoter immediately after the final SA session suppresses relapse to contexts, cues, as well as a priming injection of cocaine. Specifically inhibiting the PrL projection the NAc core at the same timepoint was without effect on relapse behavior. However, the suppressive effect of global PrL Gi-DREADD inhibition on relapse behavior was recapitulated when specifically inhibiting the PrL projection to the paraventricular nucleus of the thalamus (PVT). One interpretation

of these data is that there exist parallel, dichotomous glutamatergic pathways arising from the PrL cortex during early withdrawal from cocaine SA. Thus, PrL-NAc core may exist in a hypoactive state, whereas PrL-PVT may exist in a hyperactive state following cocaine SA. This is not without precedent, as a recent study found that these two pathways differentially encode reward-predictive cues (Otis et al., 2017).

Collectively, these findings indicate that pathway-specific DREADD modulation of PrL outputs can differentially affect various aspects of relapse to cocaine seeking depending on the specific pathway being manipulated.

Purpose of studies and overall hypothesis

The data collected in our lab and others clearly show that the PrL cortex undergoes profound alterations in glutamatergic plasticity during early withdrawal which, in some instances, is opposite relative to one week of abstinence. This chain of events has been shown to be critical for subsequent relapse. Because early withdrawal represents a critical timepoint for relapse prevention due to the dephosphorylation events that occur in the PrL cortex, it was imperative to examine whether preventing these dephosphorylation events from occurring through targeting STEP activity is sufficient to suppress relapse (Aim1). Moreover, because the dephosphorylation events occurring in the PrL cortex during early withdrawal are reflective of a hypoactive glutamatergic state, it is reasonable that artificially increasing glutamatergic neuronal activity in the PrL cortex during early withdrawal would be sufficient to suppress relapse after abstinence (Aim 2). Further, the dephosphorylation events occurring in the PrL during early withdrawal,

as well as the hyperphosphorylation of PKA targets after one week of abstinence, have previously been shown to be associated with altered AMPA receptor transmission and spine morphology. Thus, we hypothesized that spine morphology and AMPA receptor immunoreactivity in dendritic spines might also be altered in an analogous manner at these various timepoints (Aim 3). Finally, because the PrL projection to the NAc core is involved in the suppressive effect of BDNF on relapse when infused into the PrL cortex immediately after SA, it is likely that elevating neuronal activity preferentially in this pathway is sufficient to suppress relapse after abstinence. Additionally, cocaine-induced alterations in structural plasticity might be occurring in this pathway, which we hypothesized to be bidirectionally regulated during early withdrawal and one week of abstinence.

Therefore, we investigated whether 1) cocaine SA-induced alterations in the PrL cortex during early withdrawal are mediated by the activation of STEP, resulting in dysfunctional glutamate transmission in the PrL to NAc core pathway, 2) artificially elevating corticostriatal glutamatergic transmission during early withdrawal would suppress relapse after abstinence, and 3) these dephosphorylation events during withdrawal and the hyperphosphorylation of PKA targets following one week of abstinence are associated with changes in the activation state of PrL-NAc neurons and altered dendritic spine morphology associated with AMPA receptor immunoreactivity in dendritic spines (Figure 1.2).

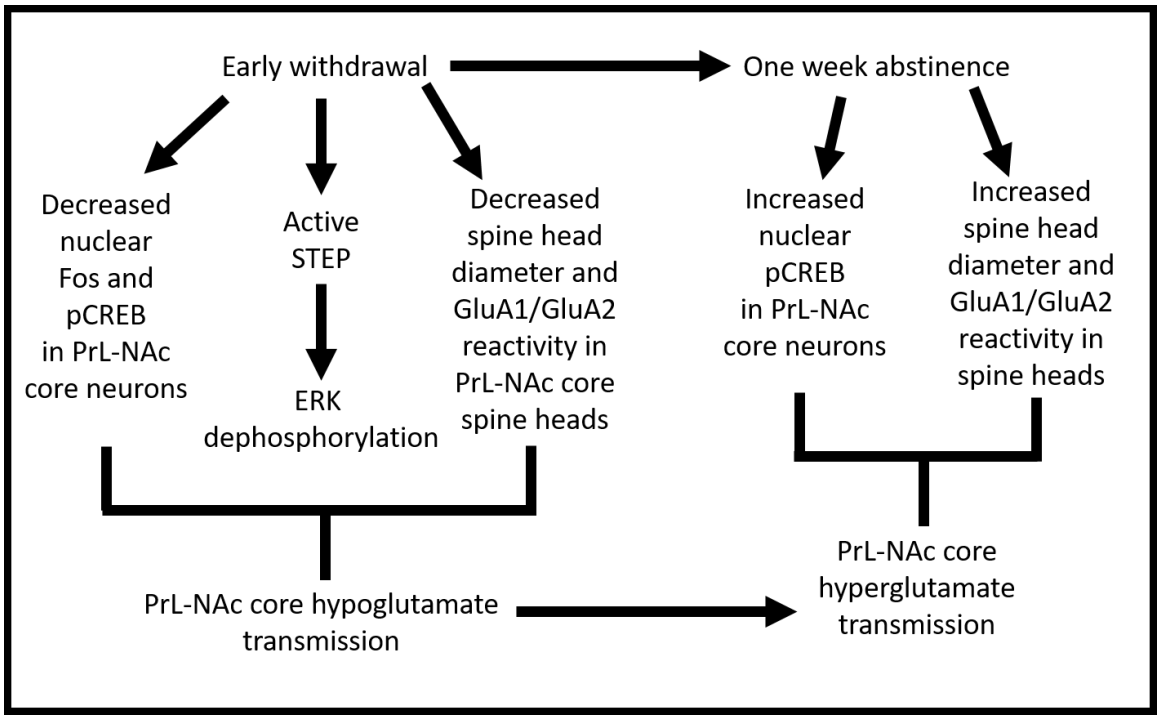

Figure 1.3. Hypothesized alterations in glutamate signaling, gene transcription regulators, and structural plasticity during early withdrawal and after one week of abstinence from cocaine SA.

Chapter 2. STEP activation in the PrL cortex mediates cocaine-induced ERK dephosphorylation during early withdrawal and plays a role in relapse after abstinence

Data presented in Chapter 2 have been published in *Addiction Biology* (23(1):219-229, 2018). Minor changes to the original article have been made for appropriate integration into this dissertation.

Introduction

Cocaine SA causes a transient dephosphorylation of critical neuronal plasticity-related proteins in the PrL cortex of rats that leads to subsequent relapse to cocaine seeking, as discussed in detail in Chapter one. The dephosphorylation of ERK is a critical component of the cocaine-induced alterations in PrL plasticity occurring during early withdrawal. BDNF-mediated inhibition of cocaine seeking after abstinence when infused into the PrL cortex immediately after SA is blocked by a prior infusion of the mitogen-activated extracellular signal-regulated kinase inhibitor U0126 (Whitfield et al., 2011). Thus, the suppressive effect of BDNF on relapse is dependent on normalizing ERK dephosphorylation in the PrL cortex during early withdrawal.

A major question is how cocaine SA causes ERK dephosphorylation in the PrL cortex. Of several phosphatases that dephosphorylate ERK, STEP has emerged as a fundamental regulator of the ERK cascade in response to dopamine and glutamate interactions in the striatum triggered by psychostimulants (Lombroso et al., 1993; Valjent et al., 2005). STEP is a CNS-specific tyrosine phosphatase localized to dopaminoceptive neurons with high expression in the striatum (Lombroso et al., 1993) and moderate expression in the medial prefrontal

cortex (Boulanger et al., 1995). Canonically, STEP is activated by Ca^{2+} influx through GluN2B-containing NMDA receptors (Paul et al., 2003), leading to a calcineurin-dependent phosphatase cascade that culminates in the dephosphorylation and activation of STEP (Boulanger et al., 1995; Paul et al., 2003; Goebel-Goody et al., 2012). Following activation, STEP dephosphorylates regulatory tyrosine residues on various substrates implicated in neuronal plasticity, including ERK (Paul et al., 2003; Paul and Connor, 2010), the Src family kinase, Fyn (Nguyen et al., 2002), GluN2A (Tian et al., 2016), and GluN2B (Braithwaite et al., 2006).

STEP activity is augmented in several neuropsychiatric and neurodegenerative disorders. For example, STEP activity is elevated in human postmortem samples and in animal models of Alzheimer's Disease (AD) (Snyder et al., 2005; Kurup et al., 2010), Parkinson's Disease (Kurup et al., 2015), and schizophrenia (Xu et al., 2018). Moreover, inhibition of STEP with systemic injections of the novel, relatively selective inhibitor, TC-2153, significantly improves memory deficits in a mouse model of AD (Xu et al., 2014) as well as PCP-induced hyperlocomotion in mice (Xu et al., 2016). TC-2153 treatment reverses the biochemical, electrophysiological, and cognitive deficits in mouse models of schizophrenia and in glutamatergic neurons derived from human-induced pluripotent stem cells from schizophrenic patients (Xu et al., 2018). As expected, TC-2153 acutely increases ERK phosphorylation *in vivo* (Xu et al., 2016; Xu et al., 2018).

Regarding preclinical models of addiction, dephosphorylation events within the PrL cortex during early withdrawal from cocaine SA are accompanied by decreased phosphorylation, and thus increased activation, of STEP (Sun et al., 2013), suggesting STEP is a likely mediator of the ERK dephosphorylation in the PrL cortex during early withdrawal from cocaine SA. Therefore, we investigated whether inhibition of STEP with an intra-PrL microinfusion of TC-2153 immediately following the final SA session would prevent ERK dephosphorylation in the PrL cortex during early withdrawal and decrease relapse to cocaine seeking. We also tested whether systemic injections of TC-2153 at the same time point would reduce relapse. Our results indicate that intra-PrL administration of TC-2153 immediately following the final SA session suppressed context-induced relapse and cue-, but not cocaine prime-, induced reinstatement. Intra-PrL TC-2153 also prevented the cocaine-induced ERK dephosphorylation within the PrL cortex during early withdrawal. However, systemic TC-2153 injections at the same time point had the opposite effects on cocaine-seeking. Overall, our results indicate that the cocaine-induced activation of STEP is an important regulator of neuroadaptations occurring within the PrL cortex during early withdrawal that lead to subsequent cocaine seeking.

Materials and Methods

Animal subjects and surgery

Adult male Sprague Dawley rats (*n*=166) Charles Rivers Laboratories; Wilmington, MA) were individually housed on a twelve-hour reverse light/dark cycle (lights on at 6AM). Upon arrival, rats were allowed at least 3 days of acclimation to the

vivarium. During this time, they were provided standard rat chow (Harlan; Indianapolis, IN) and water ad libitum. All animal use protocols were approved by the Institutional Animal Care and Use Committee of the Medical University of South Carolina and were performed according to the National Institutes of Health Guide for the Care and Use of Laboratory Animals (8th ed., 2011). All rats weighed 275-325g at the time of surgery. On the day of surgery, rats were injected i.p. with a ketamine (66 mg/kg) and xylazine (1.33 mg/kg) mixture for anesthesia and ketorolac (2.0 mg/kg) for analgesia. Rats that underwent SA were implanted in the right jugular vein with chronic indwelling i.v. silastic catheters (Fisher Scientific; Hampton, NH). Catheters were attached by subcutaneous tubing to a backmount which exited from an incision in the back. Following catheterization, rats were either secured in a stereotaxic apparatus (Kopf Instruments, Tujunga, CA) or underwent post-operative recovery care (specified below). Following securement in the stereotaxic apparatus, 26-gauge bilateral stainless-steel guide cannulae (Plastics One, Roanoke, VA) were aimed 1 mm above the PrL cortex (+2.8mm anteroposterior, +/- 0.6mm mediolateral, -3.0mm dorsoventral relative to bregma). Guide cannulae were fixed to the skull with cranioplastic cement and anchored with steel screws. Following surgery, a bilateral 10 mm stylet was inserted into the guide cannula to prevent blockage, and rats were infused i.v. with 0.1 ml of cefazolin and 0.05 ml of Taurolidine-Citrate Solution (TCS; Access Technologies, Skokie, IL). Post-operative care was conducted for 5 days, during which rats were inspected for abnormalities, and catheters were flushed with 0.05 ml TCS.

Self-administration

Rats were trained to self-administer cocaine on a fixed-ratio 1 schedule of reinforcement for 12-14 days (2 hr/day; criterion of ≥ 10 infusions/day), during which rats were food restricted to 20g of chow to motivate learning. SA was conducted in standard MedPC operant chambers which contained two retractable levers (Fairfax, VT), and were housed within sound-attenuating cubicles fitted with a fan for airflow and masking noise. Active lever presses elicited a light and tone cue complex followed by a 0.2 mg/50 µl infusion of cocaine hydrochloride (NIDA, Research Triangle Park, NC), followed by a 20 second timeout period. Yoked-saline controls received a non-contingent infusion of 0.9% saline (with light and tone cues) when their cocaine partner received a contingent cocaine infusion. For all experiments, inactive lever presses had no programmed consequence. Sucrose SA was conducted in the same manner as cocaine SA experiments, except active lever presses were reinforced with a single 45 mg chocolate flavored sucrose pellet (BioServe-F07256; Flemington, NJ).

Intracranial microinfusions

Prior to intracranial microinfusions, rats were habituated to a different behavioral room equipped with an infusion pump (Harvard Apparatus) containing two gas-tight Hamilton syringes for at least 2 days immediately following their SA sessions. The day prior to their microinfusions, a stylet extending 1 mm past the tip of the guide cannula was inserted. Immediately following their final SA session, rats were infused (0.5 µl/hemisphere, 0.25 µl/minute) with either vehicle (0.01% DMSO in filtered 0.1M PBS) or a 1 µM concentration of TC-2153. Injectors (33 gauge) were

left in place for 1 minute after infusions to facilitate diffusion. Following microinfusions, rats were either returned to the vivarium for 6 days of homecage abstinence or were rapidly decapitated two hours later for phospho-protein analysis.

Systemic injections

TC-2153 (2.0 mg/ml) was dissolved in 18% DMSO/2% Tween-20 in filtered 0.1M PBS, and rats were injected (i.p.) 2.5X body weight to achieve a final dose of 5 mg/kg, immediately after the final SA session. Six and 10 mg/kg have been shown to increase p-ERK in mice *in vivo* (Xu et al., 2014; Xu et al., 2016). However, due to solubility restrictions (4 mg/ml did not stay in solution in our hands), we tested only 5 mg/kg. Following injections, rats were returned to the vivarium for 6 days of homecage abstinence.

Post-abstinence relapse test, extinction, cue- and cocaine prime-induced reinstatement

Following abstinence, rats underwent a post-abstinence (PA) relapse test under extinction conditions (active lever presses had no programmed consequence). After at least 6 days (no more than 21 days) of further extinction training to a criterion of an average of ≤15 presses on the active lever over the last 3 days, rats underwent a 2-hour cue-induced reinstatement test. During this test, active lever presses elicited the cocaine-associated cue complex, but no infusion. Following further extinction, rats underwent a 2-hour cocaine prime-induced reinstatement test (10 mg/kg, i.p.) under extinction conditions. Following the cocaine prime test, rats were decapitated with anesthesia to confirm accuracy of cannula placements.

Histology

Following decapitation, brains were extracted, rapidly frozen in isopentane, and stored at -80°C. Brains were either coronally sectioned (40 µM) with a cryostat and Nissl-stained to confirm cannula placements, or a single 3mm wide X 2mm deep tissue punch through the dorsomedial PFC (AP +~4.68–2.76) was taken using a modified biopsy punch (Braintree Scientific; Braintree, MA), and stored at -80°C until processing. Cannula placements were confirmed during dissection.

Tissue processing

Tissue processing was performed as previously described (Sun et al. 2013). Briefly, 115 µl of ice-cold RIPA buffer (in mM: 50 Tris-HCL, pH 7.4, 150 NaCl, 2 EDTA, pH 7.4, and 10% Glycerol, 1% Triton X, 1% NP-40, and 1% Sodium Deoxycholate) with a complete set of protease and phosphatase inhibitors, was added to each punch. Punches were briefly sonicated, incubated in ice-cold buffer for 30 minutes, centrifuged at 10,000 x g for 20 minutes at 4°C, and the supernatant was used for all analyses. Protein concentrations were determined using a standard BCA assay. Lysates were then diluted to 2 µg/µl in 0.1X Sample Buffer (Protein Simple; San Jose, CA) and individually aliquoted.

Wes™ immunoassay

The Wes™ capillary electrophoresis system (Protein Simple, Bio-Techne, San Jose, CA) was used for protein quantification. Aliquots of lysates (2 µg/µl) were thawed and further diluted in 0.1X Sample Buffer to 0.8 µg/µl for analysis of p-ERK and 0.4 µg/µl for analysis of t-ERK using a combination of ¾ 0.1x Sample Buffer and ¼ 4X Master Mix (1:1 mix of 40 mM DTT and 10X Sample Buffer, Protein

Simple, San Jose, CA) according to the manufacturer's instructions. Samples were denatured at 95°C for 5 minutes. A rabbit primary antibody against p-ERK1/2 (1:50, Cell Signaling Technology-9101S RRID:AB_331646) was multiplexed with a primary antibody against calnexin (Enzo life sciences-ADI-SPA-860-F RRID:AB_11178981) at a concentration of 1:2000. A rabbit primary antibody against t-ERK1/2 (1:100, Cell Signaling Technology-9102S RRID:AB_10695746) was multiplexed with 1:1000 calnexin. Supplier anti-rabbit secondary antibodies were used as instructed (Protein Simple, San Jose, CA).

Each plate contained samples from all experimental groups, and both p-ERK2 and t-ERK2 were analyzed for each sample from the same aliquot. Analysis of electropherogram peaks was performed using Compass™ software (Protein Simple) using the Gaussian distribution of the Area Under the Curve (AUC) of the peak luminol-peroxidase signal in the capillaries. Analysis was done by dividing the AUC of p-ERK2 by t-ERK2. Data are expressed as a fold change relative to the respective controls.

Experimental design

Figure 2.1 shows the timeline for all experimental procedures conducted. Experiment 1 was conducted to determine the optimum concentration of TC-2153 that increased p-ERK when microinfused into the PrL cortex. Rats received a single intra-PrL microinfusion of vehicle or TC-2153 (0.5, 1, or 5 μM) and were rapidly decapitated two hours later. These concentrations were chosen based on previous work showing that treatment of cortical cultures with concentrations of TC-2153 ranging from 1-5 μM increased p-ERK (Xu et al., 2014). The time point

was chosen because the cocaine-induced dephosphorylation of ERK in the PrL cortex occurring two hours after the end of SA is necessary for subsequent cocaine seeking because normalizing ERK dephosphorylation with a single intra-PrL BDNF infusion suppresses cocaine seeking (Whitfield et al., 2011).

Experiment 2 was designed to determine whether an intra-PrL microinfusion of TC-2153 immediately following the final SA session would suppress relapse after abstinence and extinction. Rats were either microinfused with vehicle or the optimal concentration of TC-2153 (1 μM) from Experiment 1 immediately following the final of 12-14 cocaine SA sessions. Following 6 days of forced abstinence, rats underwent a PA context-induced relapse test, further extinction, a cue-induced reinstatement test, further extinction, and a cocaine prime-induced reinstatement test. In Experiment 3, rats either underwent cocaine SA or received yoked-saline infusions and received either an intra-PrL microinfusion of TC-2153 (1 μM) or vehicle immediately after the final SA session. Rats were rapidly decapitated two hours later to determine the effect of TC-2153 on the cocaine-induced ERK dephosphorylation within the PrL cortex during early withdrawal. Experiment 4 was conducted in the same manner as Experiment 2, except active lever presses were reinforced with chocolate sucrose pellets instead of cocaine infusions and there was no sucrose-primed test. The design of Experiment 5 was similar to Experiment 2, except rats received a systemic injection of TC-2153 (5 mg/kg, ip) or vehicle immediately following the final cocaine SA session.

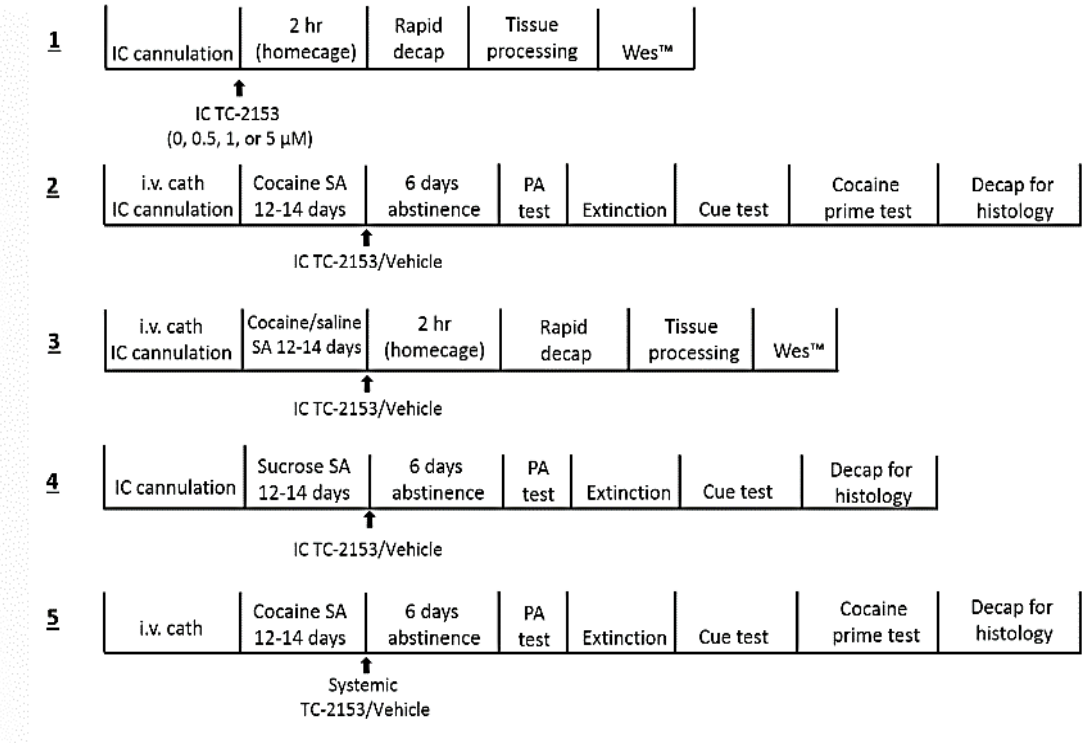

Figure 2.1. Schematic of the experimental timelines for all experiments. Final sample sizes: Experiment 1-(0 µM: n=5, 0.5 µM: n=7, 1 µM: n=6, 5 µM: n=7); Experiment 2- (TC-2153 (1µM): n=9, vehicle: n=13); Experiment 3- (Saline+Vehicle: n=10, Saline+TC-2153: n=7, Cocaine+Vehicle: n=8, Cocaine+TC-2153: n=9); Experiment 4- (TC-2153 (1 µM): n=7, Vehicle: n=4); Experiment 5- (TC-2153 (5 mg/kg): n=10, Vehicle: n=11).

Statistical analysis

All analyses were performed using GraphPad Prism 7 software (La Jolla, CA). All behavioral data were analyzed with a mixed-model ANOVA with time (SA/extinction versus PA/Cue/cocaine prime test) as the within-subject variable and treatment (TC-2153 versus Vehicle) as the between-subject variable. If significant main effects or an interaction was observed, Bonferroni-corrected pairwise comparisons were used to compare groups during and across time points. Grubbs' test was used to determine statistical outliers and these were removed

from final analyses (n=4). Data in Experiment 1 were analyzed with a one-way ANOVA followed by Dunnett's multiple comparison test to compare all TC-2153 concentrations to the vehicle control group. Data in Experiment 3 were analyzed with a two-way ANOVA followed by Student-Neuman-Keuls pairwise comparison tests. All data are expressed as the mean +/- SEM, and statistically significant differences were determined at $p<0.05$.

Results

Histology

Cannula placements for experiments 2 and 4 are shown in Figure 2.2. Circles indicate the region of the PrL cortex dissected for subsequent phospho-protein analyses in experiments 1 and 3. Cannula placements were deemed suitable if the tip of the cannula was located within the ventral tier of the anterior cingulate cortex or within the PrL cortex, but not in the infralimbic cortex. Additionally, the most ventral portion of the cannula had to be between AP +4.20 – AP +2.76 mm from Bregma. As shown in Figure 2.2, most cannula placements were tightly focused around AP +3.00 – AP +3.24 mm from Bregma.

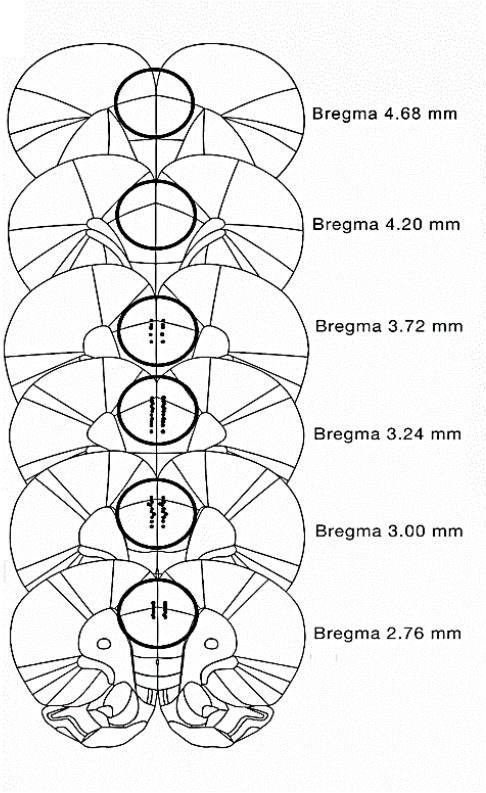

Figure 2.2. Map of coronal sections through the PFC showing all cannula placements for experiments 2 and 4. The circled regions correspond to areas where tissue punches were taken for experiments 1 and 3 (AP ~+4.68mm-+2.76mm relative to bregma).

Experiment 1. Intra-PrL microinfusion of TC-2153 increased p-ERK in naïve rats

Naïve rats (n=32; n=8/group) received a bilateral intra-PrL microinfusion of vehicle or one of three concentrations of TC-2153 (0.5, 1, or 5 μM). Rats were rapidly decapitated two hours after the infusion to determine the optimal concentration of TC-2153 that increased p-ERK in the PrL cortex *in vivo*. Of the 32 rats initially used, 2 died after surgery and 4 brain samples were incorrectly punched. One sample was not analyzed due to lysate discoloration.

A one-way ANOVA indicated a significant effect of intra-PrL TC-2153 on p-ERK ($F_{(3,21)}$=3.21, $p<0.05$). Dunnett's multiple comparison test indicated that only

the 1 μM concentration of TC-2153 significantly increased p-ERK relative to vehicle controls (p=0.04; Fig. 2.3A,C). There was no effect of TC-2153 on t-ERK normalized to calnexin ($F_{(3,21)}$=0.08, p>0.05; Fig. 2.3B,D). Thus, for all future microinfusion experiments, we used a 1 μM concentration of TC-2153.

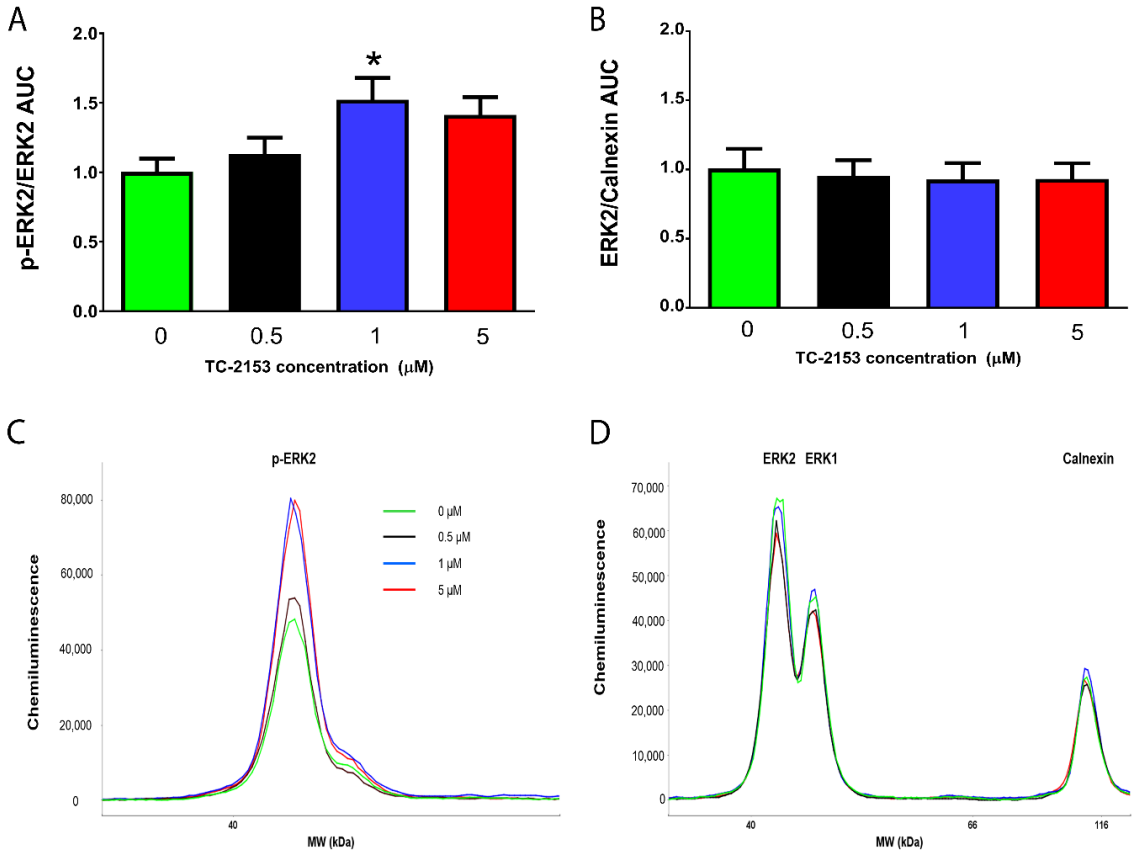

Figure 2.3. A single intra-PrL microinfusion of TC-2153 (1 μM) increased p-ERK in naïve rats. Rats were infused with vehicle (0) or 0.5, 1, or 5 μM of TC-2153 and rapidly decapitated two hours later to determine the optimal concentration of TC-2153 that increased p-ERK when microinfused into the PrL cortex. **A.** Only 1 μM TC-2153 increased p-ERK relative to vehicle-infused rats (*p<0.05). **B.** There was no difference in t-ERK/calnexin. Representative chemiluminescent peaks for p-ERK **(C)** and t-ERK multiplexed with calnexin **(D)** for groups in experiment 1.

Experiment 2. Intra-PrL microinfusion of TC-2153 suppressed context-induced relapse and cue-, but not cocaine prime-, induced reinstatement.

We next investigated the effect of a bilateral intra-PrL microinfusion of TC-2153 (1 μM) immediately following SA on context-induced relapse following abstinence, cue-, and cocaine prime-, induced reinstatement following extinction. Two rats died during surgery, 5 rats died before finishing SA, 11 rats were removed from the final analysis due to cannula placements outside of the PrL cortex, and 2 rats were outliers according to Grubbs' test during the cue and cocaine prime test in the TC-2153 and vehicle group, respectively. Final group sizes were: n=13 (vehicle) and n=9 (TC-2153). Figure 2.4A shows SA data for both groups. When analyzing active lever presses during the final 10 days of SA, results revealed a significant main effect of time ($F_{(9,180)}$=2.37, $p<0.05$). However, there was no significant main effect of treatment ($F_{(1,20)}$=0.46, $p>0.05$) nor a significant treatment by time interaction ($F_{(9,180)}$=0.74, $p>0.05$). When analyzing inactive lever presses, results revealed there was no significant main effect of time ($F_{(9,180)}$=0.69, $p>0.05$), treatment ($F_{(1,20)}$=0.00008, $p>0.05$), nor a significant treatment by time interaction ($F_{(9,180)}$=1.35, $p>0.05$). When analyzing infusions, results revealed a significant main effect of time ($F_{(9,180)}$=4.48 $p<0.0001$), but no significant main effect of treatment ($F_{(9,180)}$=2.78, $p>0.05$), nor a significant treatment by time interaction ($F_{(9,180)}$=0.39, $p>0.05$). Thus, there was no difference between groups regarding active lever presses, inactive lever presses, or infusions during the final 10 days of SA. However, both groups showed elevated responding on the active, but not inactive, lever as well as increased infusions earned over the course of SA.

After their respective intracranial infusions, rats were exposed to 6 days of abstinence followed by a PA test. Results revealed a significant main effect of time ($F_{(1,20)}$=6.09, $p<0.05$) and treatment ($F_{(1,20)}$=8.53, $p<0.01$), but no treatment by time interaction ($F_{(1,20)}$=3.30, $p>0.05$) for active lever presses. Bonferroni-corrected pairwise comparisons indicated that active lever presses were similar between groups during the last 3 days of SA before microinfusions ($p>0.05$). Rats infused with vehicle ($p<0.01$), but not TC-2153 ($p>0.05$), pressed the active lever significantly more during the PA test than during the last 3 days of SA and rats infused with TC-2153 pressed the active lever during the PA test significantly less than vehicle-infused controls ($p<0.01$; Fig. 2.4B). For inactive lever presses, there was a significant main effect of time ($F_{(1,20)}$=23.17, $p<0.0001$), but no significant main effect of treatment ($F_{(1,20)}$=3.62, $p>0.05$), nor a significant treatment by time

interaction ($F_{(1,20)}$=1.77, p>0.05). Thus, both groups showed elevated inactive lever pressing during the PA test relative to the last 3 days of SA.

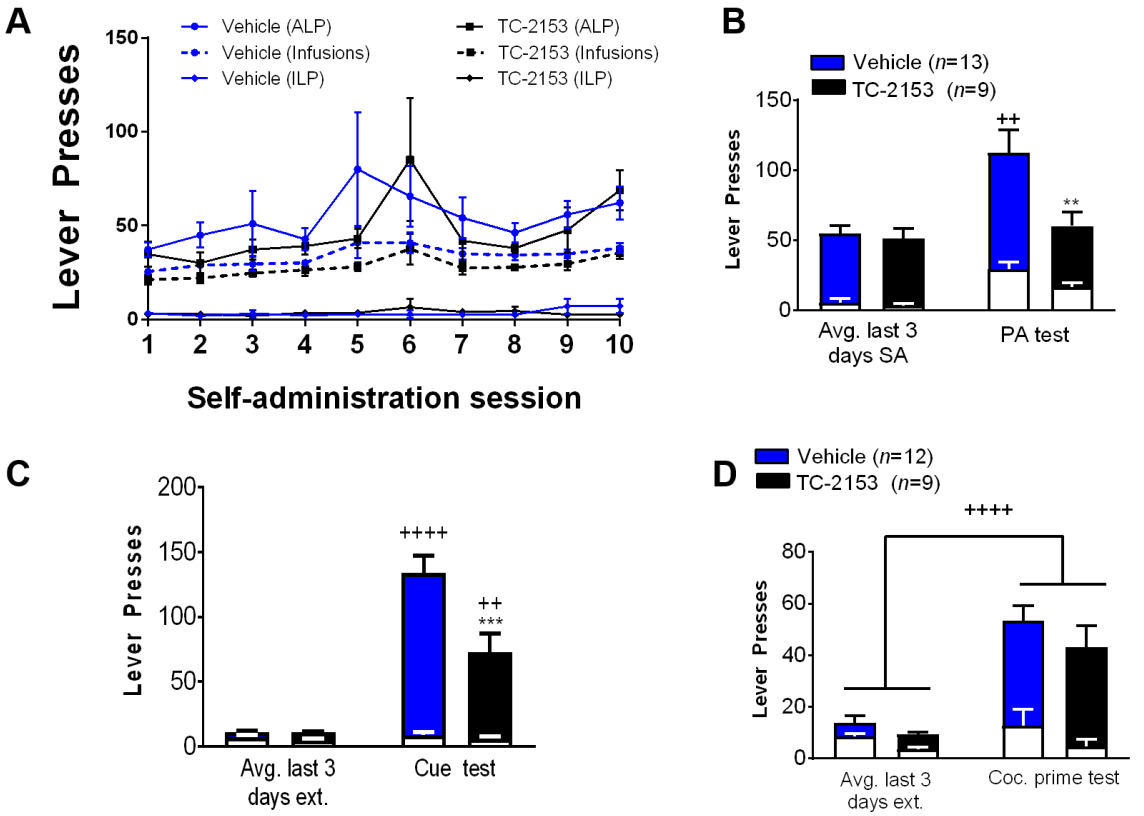

Figure 2.4. A single intra-PrL TC-2153 microinfusion immediately following the final SA session suppressed cocaine seeking following abstinence and extinction training. Rats were either infused in the PrL cortex with TC-2153 (1 μM) or vehicle immediately following the final SA session. **A.** SA data for rats in experiment 2. **B-D.** TC-2153 suppressed active lever pressing during **(B)** the PA test following abstinence as well as **(C)** during the cue-induced reinstatement test after extinction, but not **(D)** the cocaine prime-induced reinstatement test (++p<0.01, ++++p<0.0001 compared to the last 3 days of SA/extinction; **p<0.01, ***p<0.001 compared to vehicle).

After completion of extinction, rats underwent a cue-induced reinstatement test. For active lever presses, there was a significant main effect of time ($F_{(1,20)}$=88.67, p<0.0001) and treatment ($F_{(1,20)}$=8.82, p<0.01), as well as a significant treatment by time interaction ($F_{(1,20)}$=9.80, p<0.01; Fig. 2.4C). Bonferroni-corrected pairwise comparisons indicated that active lever pressing

over the last 3 days of extinction did not differ between groups ($p>0.05$). Both vehicle- ($p<0.0001$) and TC-2153- ($p<0.01$) infused rats pressed the active lever significantly more during the cue test than during the last 3 days of extinction and rats infused with TC -2153 pressed the active lever significantly less than vehicle-infused rats ($p<0.001$). For inactive lever presses, there was no significant main effect of treatment ($F_{(1,20)}=1.56$, $p>0.05$), time ($F_{(1,20)}=1.47$, $p>0.05$), not a significant treatment by time interaction ($F_{(1,20)}=0.007$, $p>0.05$).

Following re-extinction to criterion, rats underwent a cocaine prime-induced reinstatement test (Fig. 2.4D). One rat removed its headcap prior to the cocaine prime test and was excluded from the analysis. For active lever presses, there was a significant main effect of time ($F_{(1,19)}=54.86$, $p<0.0001$), indicating that both groups had increased active lever pressing during the cocaine prime-induced reinstatement test relative to the last 3 days of extinction. However there was no significant main effect of treatment ($F_{(1,19)}=1.857$, $p>0.05$) or a significant treatment by time interaction ($F_{(1,19)}=0.33$, $p>0.05$). For inactive lever presses, there was no significant main effect of treatment ($F_{(1,19)}=2.20$, $p>0.05$), time ($F_{(1,19)}=0.51$, $p>0.05$), nor a significant treatment by time interaction ($F_{(1,19)}=0.16$, $p>0.05$). These results show that a single intra-PrL microinfusion of TC-2153 immediately following SA suppresses cocaine seeking in the PA and cue-, but not cocaine prime-, induced reinstatement tests.

Experiment 3. Intra-PrL microinfusion of TC-2153 prevented the cocaine-induced ERK dephosphorylation within the PrL cortex during early withdrawal

To determine the effect of STEP inhibition on the cocaine-induced ERK dephosphorylation within the PrL cortex during early withdrawal, rats (n=48) were randomly assigned to either cocaine SA or yoked-saline groups following surgery. One rat was removed prior to the end of SA after a catheter failure. Immediately following the final of 12-14 cocaine/yoked saline SA sessions, the PrL cortex of rats was microinfused bilaterally with TC-2153 or vehicle and rapidly decapitated two hours after the infusion. Of the remaining 47 rats, 13 were excluded from analyses for the following reasons: cannula placements that were outside of the PrL cortex (n=6), catheter failure on the final day of SA (n=1), or tissue samples were punched incorrectly (n=6). Following exclusion, final group sizes were as follows: Saline+Vehicle (n=10), Saline+TC-2153 (n=7), Cocaine+Vehicle (n=8), Cocaine+TC-2153 (n=9).

Figure 2.5A shows the SA data for cocaine self-administering rats and yoked saline controls. A two-way repeated measures ANOVA revealed a significant main effect of SA (cocaine versus yoked saline) for active lever presses ($F_{(1,32)}=92.34$, $p<0.05$). Bonferroni-corrected pairwise comparison test indicates that cocaine self-administering animals pressed the active lever significantly more than yoked saline controls during sessions 1-10 ($p<0.0001$). Moreover, cocaine SA rats receiving vehicle microinfusions were not significantly different than cocaine SA rats receiving TC-2153 microinfusions when analyzing average active lever presses during the last 3 days of SA ($t_{(15)}=0.006$, $p>0.05$) or average infusions

earned over the last 3 days of SA ($t_{(15)}$=0.11, p>0.05; Fig. 2.5B). A two-way ANOVA revealed a significant main effect of treatment (TC-2153 versus vehicle) as well as SA (cocaine versus saline) on p-ERK (Treatment: $F_{(1,30)}$=14.84, p<0.001, SA: $F_{(1,30)}$=10.28, p<0.01), but no significant treatment by SA interaction ($F_{(1,30)}$=0.08, p>0.05). Student-Neuman-Keuls tests revealed that p-ERK levels were significantly lower in the cocaine + vehicle group versus the yoked-saline + vehicle group. TC-2153 significantly increased p-ERK in yoked-saline rats (p<0.05; Fig. 2.5C,E) and prevented the cocaine SA-induced decrease. There was no effect of treatment, SA, or a significant treatment by SA interaction on t-ERK/calnexin (Treatment: $F_{(1,30)}$=2.28, p>0.05, SA: $F_{(1,30)}$=2.43, p>0.05, treatment by SA: $F_{(1,30)}$=3.12, p>0.05; Fig. 2.5D,F). These results indicate that intra-PrL TC-2153 infused immediately following the final SA session prevented the cocaine-induced ERK dephosphorylation within the PrL cortex during early withdrawal.

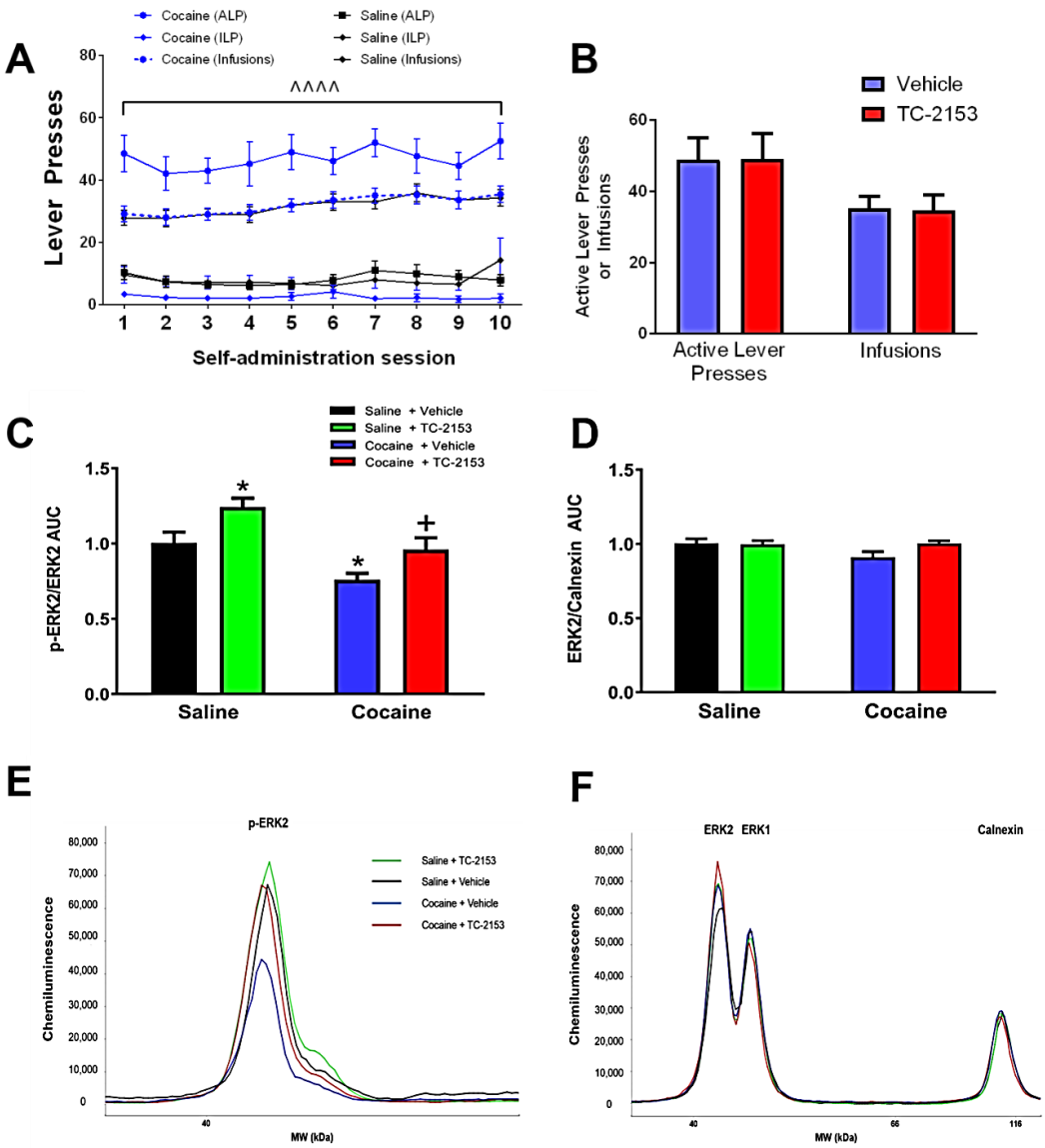

Figure 2.5. Intra-PrL TC-2153 normalizes the cocaine-induced decrease in p-ERK2 within the PrL cortex during early withdrawal. **A.** SA data for cocaine (n=17) and yoked saline (n=17) rats. Cocaine SA rats pressed the active lever significantly more than yoked saline controls (^^^^p<0.0001) **B.** Cocaine self-administering rats infused with vehicle or TC-2153 were equal regarding active lever presses over the last 3 days of SA as well as average infusions earned. **C.** Rats microinfused with vehicle immediately following the final cocaine SA session show decreased p-ERK relative to yoked-saline rats infused with vehicle. This decrease is prevented in rats that received a TC-2153 microinfusion immediately following cocaine SA. Additionally, yoked-saline rats microinfused with TC-2153 showed augmented p-ERK compared to saline-vehicle rats (*p<0.05 compared to Saline-Vehicle, +p<0.05 compared to Cocaine-Vehicle). **D.** There were no differences between groups in t-ERK/calnexin. **E-F.** Representative chemiluminescent peaks for p-ERK **(E)** and t-ERK multiplexed with calnexin **(F)** for groups in experiment 3.

Experiment 4. Intra-PrL microinfusion of TC-2153 did not affect context-induced relapse or cue-induced reinstatement of sucrose seeking

To determine whether the suppressive effect of intra-PrL infusion of TC-2153 on relapse was cocaine-specific, rats (n=16) underwent 12-14 days of sucrose SA and were microinfused with either TC-2153 or vehicle immediately following the final SA session. One rat died after surgery and 3 rats removed their headcaps prior to the PA test. Of the remaining 12 rats, one was removed from analysis because its cannula placement was outside of the PrL cortex. Figure 2.6A shows sucrose SA data for all final rats included in this experiment. When active lever presses were analyzed, a two-way repeated-measures ANOVA revealed a significant main effect of time ($F_{(9,81)}$=4.26, p<0.0001), but no significant main effect of treatment ($F_{(1,9)}$=0.63, p>0.05), nor a significant treatment by time interaction ($F_{(9,81)}$=0.89, p>0.05). For pellets earned, a two-way repeated-measures ANOVA indicated a significant main effect of time ($F_{(9,81)}$=6.24, p<0.05), but no significant main effect of treatment ($F_{(1,9)}$=0.99, p>0.05) nor a significant treatment by time interaction ($F_{(9,81)}$=0.89, p>0.05). Following infusions, rats underwent 6 days of forced abstinence followed by a PA test. For active lever presses, a two-way ANOVA revealed a significant main effect of time ($F_{(1,9)}$=35.69, p<0.001; Fig. 2.6B), but no main effect of treatment ($F_{(1,9)}$=0.00005, p>0.05) or a significant treatment by time interaction ($F_{(1,9)}$=0.01, p>0.05), indicating that both groups had reduced active lever pressing during the PA test relative to the last 3 days of sucrose SA. For inactive lever presses, there was no significant main effect of treatment ($F_{(1,9)}$=1.09, p>0.05), time ($F_{(1,9)}$=1.14, p>0.05), nor a significant treatment by time interaction ($F_{(1,9)}$=2.44, p>0.05). Following further extinction to criterion, rats

underwent a cue-induced reinstatement test. When analyzing active lever presses, results indicated a significant main effect of time ($F_{(1,9)}$=37.79, p<0.001; Fig. 2.6C), but not treatment ($F_{(1,9)}$=0.31, p>0.05) or a significant treatment by time interaction ($F_{(1,9)}$=1.08, p>0.05). For inactive lever presses, there was no significant main effect of treatment ($F_{(1,9)}$=0.79, p>0.05), time ($F_{(1,9)}$=0.51, p>0.05), nor a significant treatment by time interaction ($F_{(1,9)}$=0.47, p>0.05). These data indicate that both groups had increased active lever pressing during the cue-induced reinstatement test relative to the last 3 days of extinction, which was not altered by a prior TC-2153 microinfusion.

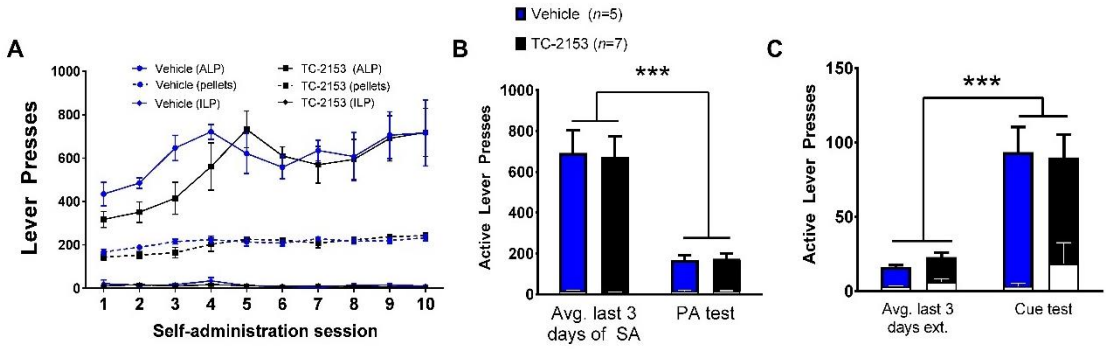

Figure 2.6. A single intra-PrL microinfusion of TC-2153 fails to suppress sucrose seeking after abstinence and extinction. **A.** Sucrose SA data for all rats in experiment 4. **B-C,** Animals microinfused with TC-2153 or vehicle show equal responding on the active lever during the PA test **(B)** as well as **(C)** during the cue-induced reinstatement test, but both groups had reduced responding during the PA test relative to the last 3 days of SA and increased responding during the cue test relative to the last 3 days of extinction (***p<0.001 compared to the last 3 days of SA or extinction, two-way ANOVA).

Experiment 5. A systemic injection of TC-2153 preferentially suppressed cocaine prime-induced reinstatement

Previous findings indicate systemic TC-2153 is able to alter ERK2 phosphorylation in the mPFC *in vivo* (Xu et al., 2014). To test the ability of TC-2153 to induce p-ERK2 in the PrL cortex two hours after injection, naïve rats were either injected with vehicle or TC-2153 (5 mg/kg, i.p., n=4/group) and rapidly decapitated two

hours later. A two-tailed t-test showed that rats injected with TC-2153 had significantly higher p-ERK2 relative to tERK2 in the PrL cortex two hours after injection ($t_{(6)=}$2.81, $p<0.05$, Fig. 2.7A). There was no difference in tERK2 normalized to Calnexin between groups ($t_{(6)}$=0.62, $p>0.05$, Fig. 2.7B). To determine the effect of systemic administration of TC-2153 on relapse, rats (n=28) underwent cocaine SA for 12-14 days as above. Three rats became ill and were euthanized prior to the end of SA. Two rats were removed for catheter failure prior to finishing SA. One rat per group was an outlier according to Grubbs' test in the cocaine prime test and was removed from all analyses. The remaining rats were injected i.p. with TC-2153 (5 mg/kg, n=10) or vehicle (n=11) immediately following the last of 12-14 cocaine SA sessions. Figure 2.7C shows SA data for all rats in this experiment. When comparing active lever presses between vehicle versus TC-2153 injected rats, a two-way repeated-measures ANOVA indicated there was no significant main effect of time ($F_{(9,171)}$=1.27, $p>0.05$), treatment ($F_{(1,19)}$=0.33, $p>0.05$), nor a significant treatment by time interaction ($F_{(9,171)}$=1.61, $p>0.05$). For inactive lever presses, there was no significant main effect of time ($F_{(9,171)}$=0.92, $p>0.05$), treatment ($F_{(1,19)}$=3.75, $p>0.05$), nor a significant treatment by time interaction ($F_{(9,171)}$=0.82, $p>0.05$). For infusions, there was a significant main effect of time ($F_{(9,171)}$=7.64, $p<0.0001$), but not treatment ($F_{(1,19)}$=0.13, $p>0.05$), nor a significant treatment by time interaction ($F_{(9,11)}$=1.41, $p>0.05$). Thus, there was no difference between groups for active lever presses, inactive lever presses, nor infusions earned during SA. However, both groups had increased infusions as a function of SA time. Following 6 days of abstinence, rats were returned to their SA

chambers for the PA test. For active lever presses, a two-way ANOVA revealed a significant main effect of time ($F_{(1,19)}$=23.10, p<0.001; Fig. 2.7D), indicating that both groups had increased active lever pressing in the PA test relative to the last 3 days of SA, but there was no significant main effect of treatment ($F_{(1,19)}$=0.18, p>0.05) or a significant treatment by time interaction ($F_{(1,19)}$=0.003, p>0.05). There was a significant main effect of time ($F_{(1,19)}$=51.78, p<0.05), but no significant main effect of treatment ($F_{(1,19)}$=3.82, p>0.05), nor a significant treatment by time interaction ($F_{(1,19)}$=2.15, p>0.05) when analyzing inactive lever presses.

Following completion of extinction, rats underwent a cue-induced reinstatement test. For active lever presses, results showed a significant main effect of time ($F_{(1,19)}$=110.50, p<0.0001; Fig. 2.7E), indicating that both groups pressed the active lever significantly more during the cue-induced reinstatement test compared to the last 3 days of extinction, but there was no main effect of treatment ($F_{(1,19)}$=2.50, p=0.13) or a treatment by time interaction ($F_{(1,19)}$=2.38, p>0.05). When analyzing inactive lever presses, there was no significant main effect of treatment ($F_{(1,19)}$=2.21, p>0.05), time ($F_{(1,19)}$=1.59, p>0.05), nor a significant treatment by time interaction ($F_{(1,19)}$=0.11, p>0.05).

Following re-extinction to criterion, rats underwent a cocaine prime-induced reinstatement test. When analyzing active lever presses, there were significant main effects of time ($F_{(1,19)}$=42.66, p<0.0001), treatment ($F_{(1,19)}$=7.065, p<0.05), as well as a significant treatment by time interaction ($F_{(1,19)}$=8.26, p<0.01; Fig. 2.7F). Bonferroni-corrected pairwise comparisons indicated that active lever presses were equal between groups over the last 3 days of extinction (p>0.05), but rats

injected with TC-2153 pressed the active lever significantly less than vehicle-injected rats during the cocaine prime test ($p<0.001$). For inactive lever presses, there was no significant main effect of time ($F_{(1,19)}=0.0005$, $p>0.05$), treatment ($F_{(1,19)}=0.74$, $p>0.05$), nor a significant treatment by time interaction ($F_{(1,19)}=3.22$, $p>0.05$). Collectively, these data indicate that injections of TC-2153 immediately following SA preferentially suppress cocaine prime-induced reinstatement.

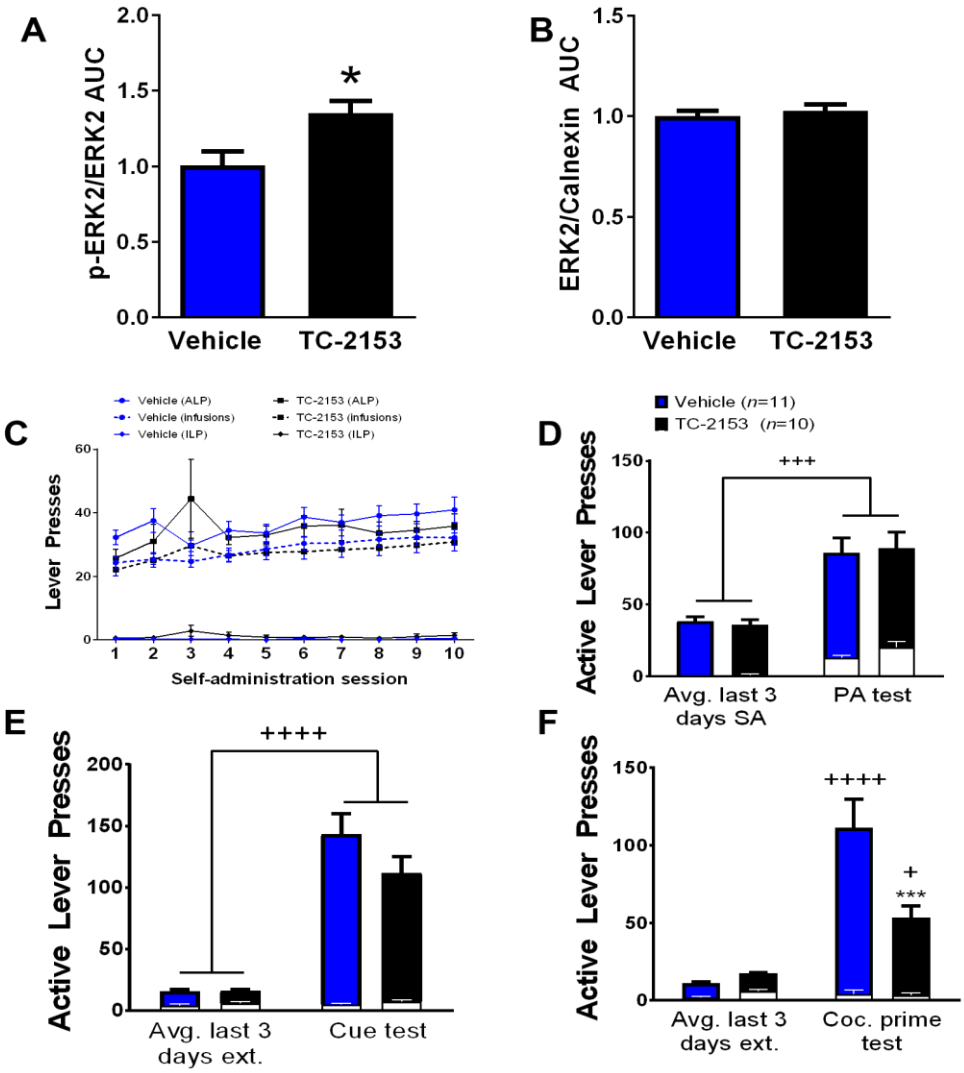

Figure 2.7. Systemic injection of TC-2153 suppressed cocaine prime-induced reinstatement but not post-abstinence context-induced relapse or cue-induced reinstatement. **A-B.** A single systemic injection of TC-2153 (5 mg/kg, i.p.) increased PrL cortical p-ERK2 **(A)** two hours after injection in naïve rats, without affecting tERK2 **(B)** (n=4/group). **C.** SA data for all rats in experiment 5. **D-F.** Rats

were either injected with TC-2153 (5 mg/kg, i.p.) or vehicle immediately following the final cocaine SA session. Both groups had increased active lever pressing during **(D)** the PA test following 6 days of forced abstinence as well as **(E)** during the cue-induced reinstatement test following extinction. There was no effect of TC-2153 on active lever pressing in either test. However, TC-2153 injections suppressed **(F)** cocaine prime-induced reinstatement (++++$p<0.0001$, +++$p<0.001$, +$p<0.05$ compared to the last 3 days of SA/extinction, *$p<0.05$, ***$p<0.001$ compared to vehicle).

Discussion

Summary of findings

The results of the current experiments are the first to show that the cocaine-induced activation of STEP in the PrL cortex during early withdrawal from cocaine SA (Sun et al., 2013) plays a significant role in relapse. Interestingly, we found that an intra-PrL TC-2153 microinfusion immediately after SA suppressed context-induced relapse and cue-, but not cocaine prime-, induced reinstatement. However, systemic TC-2153 injections had the opposite effect. Additionally, intra-PrL TC-2153 prevented the cocaine-induced ERK dephosphorylation in the PrL cortex during early withdrawal. These results corroborate previous findings that early withdrawal from cocaine SA is a critical time point whereby an intervention, like an infusion of BDNF or TC-2153, that normalizes ERK and/or GluN2 signaling in the PrL cortex produces an enduring suppression of relapse (Whitfield et al., 2011; Go et al., 2016). This finding coupled with the finding that BDNF does not alter food seeking (Berglind et al., 2007), and TC-2153 does not alter sucrose seeking, indicates that intra-PrL interventions during early withdrawal selectively attenuate cocaine seeking without affecting the motivation to seek natural rewards.

Differential effect of systemic vs. intra-PrL TC-2153 on cocaine seeking

Recent studies indicate that systemic delivery of TC-2153 normalizes cognitive/behavioral dysfunction in animal models of disorders with augmented STEP activity (Xu et al., 2014; Xu et al., 2016; Xu et al., 2018). However, our experiments are the first to microinfuse TC-2153 and we found that systemic versus intra-PrL TC-2153 differentially suppressed cocaine seeking. Several potential explanations exist for these observed differences.

The lack of effect of systemic TC-2153 on context-induced relapse and cue-induced reinstatement could be due to the inability of 5 mg/kg TC-2153 to prevent the dephosphorylation of ERK within the PrL cortex during early withdrawal from cocaine SA. However, this is unlikely because 5 mg/kg TC-2153 increased p-ERK within the PrL cortex two hours after an injection in naïve rats. STEP is heavily-enriched in other regions, such as the striatum and hippocampus (Boulanger et al., 1995) thus it is likely that systemic TC-2153 also increases p-ERK in these regions, as previously reported for the hippocampus (Xu et al., 2014). Furthermore, intra-PrL TC-2153 also increased p-ERK acutely in naïve rats, but, unlike systemic TC-2153, prevented context-induced relapse as well as cue-induced reinstatement after extinction when infused immediately after SA. Thus, we hypothesize that the inability of systemic TC-2153 to suppress context- and cue-induced cocaine seeking is likely due to the inhibition of STEP in other brain regions, in addition to the PrL cortex, during early withdrawal, and that one or more of these regions may underlie the preferential inhibition of cocaine prime-induced reinstatement.

The striatum, including the NAc core, is heavily-enriched in both major isoforms of STEP, STEP46 and STEP61 (Lombroso et al., 1993; Sharma et al., 1995). However, only STEP61 is expressed in the PFC. Furthermore, STEP46 has greater enzymatic activity than STEP61 (Boulanger et al., 1995), and TC-2153 has ~1.75 higher affinity for STEP46 than STEP61 (Xu et al., 2014). Acute cocaine has been shown to increase p-ERK in the NAc core by inactivating STEP46, which requires concomitant activation of dopamine D1 and NMDA receptors (Paul et al., 2000; Valjent et al., 2005; Girault et al., 2007). By extension, cocaine prime-induced reinstatement is thought to require the integration of dopamine and glutamate inputs in the NAc core from the VTA and PrL cortex, respectively (Shen et al., 2014a), and is associated with increased extracellular dopamine and glutamate in the NAc core (McFarland et al., 2003), suggesting that a priming injection of cocaine likely increases p-ERK by inactivating STEP46 in the NAc core. The differential expression pattern and function of STEP46 and STEP61 in the PrL cortex and NAc core, and the role of dopamine and glutamate interactions in the NAc core in regulating STEP and cocaine prime-induced reinstatement, suggest that systemic TC-2153 may preferentially suppress cocaine prime-induced reinstatement by inhibiting STEP in the NAc core during early withdrawal, which future experiments should investigate.

Intra-PrL TC-2153 prevented the cocaine-induced ERK dephosphorylation during early withdrawal

The results of the current study agree with previous studies indicating that cocaine SA decreases p-ERK in the PrL cortex during early withdrawal (Whitfield et al., 2011; Go et al., 2016). Consistent with our hypothesis, we show here that this

effect was prevented by intra-PrL microinfusions of TC-2153. ERK is central to neuroadaptations occurring within neural circuits that mediate drug seeking (Lu et al., 2006; Zhai et al., 2008). Therefore, it is not surprising that time-course experiments indicate that p-ERK changes dynamically within the PFC during various stages of abstinence from cocaine SA (Whitfield et al., 2011; Miszkiel et al., 2014). For example, cocaine-mediated decreases in p-ERK in the PrL cortex two hours after SA normalize by 22 hours and remain unaltered after six days of abstinence (Whitfield et al., 2011). Importantly, intra-PrL infusion of BDNF is unable to suppress relapse when microinfused after six days of forced abstinence (Berglind et al., 2007). However, the suppressive effect of BDNF on cocaine seeking when it is microinfused immediately after SA depends on normalizing p-ERK during early withdrawal (Whitfield et al., 2011).

Potential mechanism of STEP activation during early withdrawal

STEP has been shown to be dephosphorylated and activated by Ca^{2+} influx through GluN2B-containing NMDA receptors via a PP2B-PP1 dependent mechanism in corticostriatal cultures (Paul et al., 2003). Moreover, extrasynaptic NMDA receptor stimulation inactivates ERK in cultured hippocampal and cortical neurons (Kim et al., 2005; Ivanov et al., 2006; Leveille et al., 2008) whereas synaptic NMDA receptor stimulation leads to STEP ubiquitination, facilitating sustained ERK activation (Hardingham et al., 2001; Hardingham et al., 2002; Xu et al., 2009). Thus, an attractive hypothesis is that a hyperglutamatergic tone arises in the PrL cortex after chronic SA which facilitates extrasynaptic NMDA receptor stimulation, and subsequent activation of STEP, inhibiting NMDA function

and associated ERK signaling during early withdrawal. In support, not only does cocaine SA lead to the dephosphorylation of ERK and CREB, but also GluN2A^{Y1325} and GluN2B^{Y1472} (Go et al., 2016), and STEP dephosphorylates GluN2B^{Y1472} (Braithwaite et al., 2006).

TC-2153 also enhances GluN2A pan-tyrosine phosphorylation in hippocampal cultures. Interestingly, STEP$^{-/-}$ mice have increased GluN2A pan-tyrosine, but not GluN2A^{Y1325}, phosphorylation (Tian et al., 2016) suggesting a different tyrosine site in GluN2A may be dephosphorylated by STEP. However, STEP may indirectly dephosphorylate GluN2A^{Y1325} via dephosphorylation and inactivation of Fyn as demonstrated *in vitro* (Nguyen et al., 2002). Thus, future experiments should investigate whether TC-2153 prevents the cocaine-induced GluN2A/B dephosphorylation. Furthermore, an intra-PrL microinfusion of Ro-25-6981, a selective GluN2B antagonist, immediately after SA does not reduce relapse (Go et al., 2016). However, treatment of cortical cultures with memantine, a non-selective NMDA antagonist, preferentially blocks extrasynaptic NMDA receptors (Leveille et al., 2008), suggesting that preferential inhibition of extrasynaptic GluN2B-containing NMDA receptors may prevent the cocaine-

induced activation of STEP, ERK dephosphorylation, and subsequent cocaine seeking (Figure 2.8).

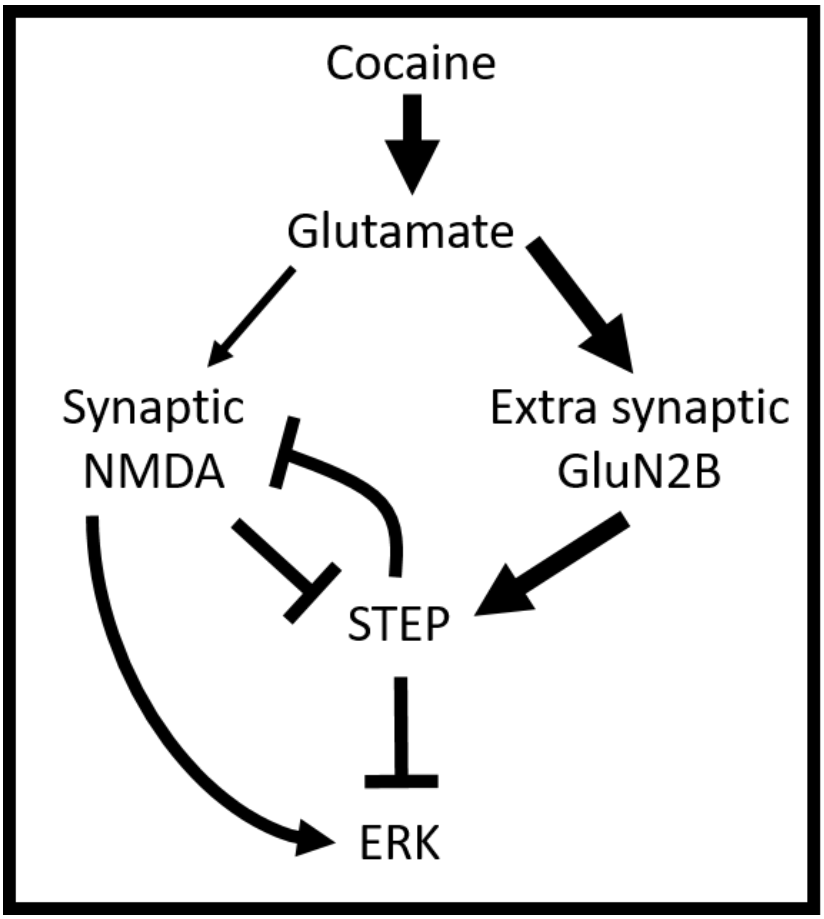

Figure 2.8 Cocaine SA-induced activation of STEP in the PrL cortex during early withdrawal may rely on increased activation of extrasynaptic NMDA receptors due to glutamate overflow.

Conclusions

ERK dephosphorylation in the PrL cortex during early withdrawal represents a critical neuroadaptation that promotes relapse. Normalizing p-ERK with a single intra-PrL BDNF (Whitfield et al., 2011) or TC-2153 microinfusion immediately after cocaine SA suppresses cocaine seeking. Although BDNF and TC-2153 have a similar effect on cocaine seeking, they are likely producing this effect in different

ways. Intra-PrL BDNF immediately after SA is likely acting upstream of STEP by directly increasing activity of MEK signaling during early withdrawal (Whitfield et al., 2011), as well as potentially inducing the degradation of STEP (Saavedra et al., 2016). However, TC-2153 acts only at the level of STEP to prevent the catalytic activity of STEP following activation (Xu et al., 2014). Both interventions culminate in normalized p-ERK, highlighting the importance of ERK dephosphorylation as a neuroadaptation occurring in the PrL cortex during early withdrawal that leads to cocaine seeking. In conclusion, our results reveal a key role of STEP activation in the PrL cortex in regulating cocaine seeking, as well as associated adaptations in p-ERK that occur during early withdrawal from cocaine SA.

Chapter 3: The effect of chemogenetic activation of the PrL cortex and PrL-NAc core pathway on relapse to cocaine seeking after abstinence

Introduction

Relapse is thought to arise from dysfunctional medial prefrontal cortex-dependent regulation of subcortical basal ganglia structures (Quintero, 2013). Specifically, cocaine-induced alterations in the glutamatergic projection arising from the PrL cortex innervating the NAc core has been implicated in the initiation of drug seeking following presentation of cocaine-conditioned contexts, cues, or a priming injection after abstinence or extinction (Kalivas, 2009). Moreover, the development of cocaine addiction is thought to occur through distinct stages of altered neuroplasticity, which are differentially regulated by drug-taking, abstinence, and re-exposure to cocaine-conditioned stimuli (Kalivas and O'Brien, 2008). Thus, pharmacological agents targeting specific adaptations mediating relapse may be beneficial at one stage of addiction relative to other stages.

Previous work from our lab indicates that the suppressive effect of PrL cortical BDNF on cocaine seeking when infused immediately after SA can be blocked by antagonizing GluN2A/B-containing NMDA receptors prior to BDNF. Thus, preventing BDNF-TrkB signaling from elevating glutamatergic neurotransmission by antagonizing NMDA receptors prior to BDNF during early withdrawal prevents the long-term suppressive effect of BDNF on cocaine seeking (Go et al., 2016). These findings indicate that BDNF is likely augmenting glutamate transmission in the PrL-NAc core pathway during early withdrawal. Although intra-PrL BDNF likely exerts its effects by normalizing corticostriatal glutamate

transmission through increased synaptic activity during early withdrawal, it is unknown whether simply elevating synaptic activity in the PrL cortex during early withdrawal is sufficient to suppress cocaine seeking after abstinence and extinction training.

A plethora of literature indicates that the PrL-NAc core pathway is the primary glutamatergic projection mediating the initiation of cocaine seeking (McFarland et al., 2003; Reissner et al., 2015; McGlinchey et al., 2016). However, recent data indicate that divergent pathways arising from the PrL cortex differentially encode reward-predictive cues. PrL-NAc, relative to PrL-PVT, neurons differentially encode cue-elicited reinforcement learning of appetitive behaviors, and their coordinated activity permits plasticity relevant for cue-encoding (Otis et al., 2017). Moreover, during the acquisition of cocaine SA, some PrL cortical neurons show decreased activity relative to baseline (i.e. prior to beginning daily SA sessions), with a larger percentage showing hypoactivity on the last day of SA relative to the first. However, a certain percentage of pyramidal neurons show elevated firing rates relative to baseline, although the percentage does not change from the first to the last day of SA (Dennis et al., 2018). Therefore, it could be postulated that these neurons may differentially encode cocaine cue salience through divergent outputs during the critical early withdrawal period. With the advent of optogenetics and chemogenetics, it has only recently been possible to definitively show the relationship between the PrL cortex and its downstream targets in drug seeking following various periods of abstinence.

Apart from transiently elevating the firing rates of neurons, Gq-coupled DREADDs also engage cell-signaling pathways associated with Gq-signaling, including the MAPK pathway (Bellocchio et al., 2016). In the last decade, DREADDs have been used extensively to probe the role of the medial prefrontal cortex in working memory (Liu et al., 2014), fear memory prediction (Yau and McNally, 2015), as well as behavioral activation elicited by cocaine conditioned cue exposure (Augur et al., 2016), among other prefrontal-dependent behaviors. Apart from being utilized as a tool to potentiate, or inhibit, general populations of neurons in various brain regions, DREADDs have also been combined with intersectional viral approaches which allow for modulation of specific PrL cortical projections (Garcia et al., 2017). These experiments rely on injections of retrograde-transported viruses, such as canine-adeno virus type 2 (CAV2) or AAVrg, which express Cre-recombinase (Junyent and Kremer, 2015; Tervo et al., 2016) in combination with Cre-dependent viral vectors expressing DREADDs.

Using this intersectional viral approach, Kerstetter and colleagues found that suppressing PrL-NAc core neurons during progressive ratio (PR) cocaine SA augments responding on the formerly active lever during the first extinction session, as well as cocaine prime-induced reinstatement. However, inhibition of PrL-NAc core neurons immediately prior to drug-prime reinstatement suppressed drug seeking (Kerstetter et al., 2016). This is consistent with optogenetic evidence that inhibiting PrL-NAc core neurons prior to reinstatement prevented cocaine seeking (Stefanik et al., 2013). Thus, PrL-NAc core manipulations have opposing effects depending on the timepoint of intervention. Moreover, augmenting activity

in the IL-NAc shell pathway prior to reinstatement following extinction training suppresses cocaine seeking (Augur et al., 2016). Thus, intersectional viral approaches can be utilized to gain a better understanding of corticostriatal pathways that mediate, or suppress, cocaine seeking. However, to date, no studies have applied this technique to alter PrL cortical activity, specifically that of NAc core efferents, immediately after cocaine SA.

The data discussed above suggest that BDNF elevates synaptic activity in the PrL cortex during early withdrawal, which may provide a long-term normalization of corticostriatal glutamate transmission. We therefore hypothesized that chemogenetic-mediated activation of the PrL cortex immediately after the final SA session would suppress relapse after abstinence, an effect mediated by PrL-NAc core activation. To investigate this hypothesis, we used either CaMKIIα-driven hM3Dq, or hSyn-DIO-hM3Dq, DREADDs in combination with NAc core CAV2-Cre-eGFP or rgAAV-pmSyn1-Cre-eBFP viral vectors to activate PrL cortical glutamatergic neurons, or preferentially activate the PrL-NAc core output, respectively. Although we did not find any effects that persisted during an entire two-hour relapse test in either experiment, we did see trends in some of the relapse tests as well as specific timepoints during relapse wherein hM3Dq activation was effective. Thus, global chemogenetic activation of the PrL cortex as well as the PrL-NAc core pathway is insufficient to suppress relapse to the same degree as BDNF during early withdrawal. This difference may be due to the transient nature of hM3Dq activation as opposed to the more-sustained nature of BDNF-TrkB signaling.

Materials and Methods

Animal subjects

Sixty-seven adult male Sprague Dawley rats were used for this study (Charles Rivers Laboratories, Wilmington, MA). Rats were maintained in the vivarium under the same conditions as experiments described in Chapter two.

Surgery

Rats were anesthetized, and chronic indwelling catheters were implanted into the jugular vein as described in Chapter two. All viral procedures and constructs used in this study were approved by the Medical University of South Carolina Institutional Biosafety Committee. For intra-cranial viral microinjections, rats were fixed into a stereotaxic apparatus and glass micropipettes were used to inject either an AAV5-CaMKIIα-hM3Dq-mCherry (UNC vector core, Chapel Hill, NC or Addgene, Cambridge, MA), AAV5-CaMKIIα-mCherry (UNC vector core, Chapel Hill, NC or Addgene, Cambridge, MA), AAV5-CaMKIIα-eGFP (UNC vector core), AAV5-hSyn-DIO-hM3Dq-mCherry (Addgene), or AAV5-hSyn-DIO-mCherry (Addgene) into the PrL cortex (AP +2.8 mm, ML +/- 0.6 mm, DV -3.8mm from bregma). All viruses injected into the PrL cortex had a titer of ~3 X 10^{12} viral genomes/ml and 0.75 µl/hemisphere was injected. In Experiment 3, rats also received microinjections of either CAV2 vector expressing a Cre-eGFP fusion protein under control of a CMV promoter (CAV2-Cre-eGFP; 3.6 X 10^{12} viral genomes/ml, Montpellier vector core, 0.75 ul/hem) or AAVrg pmSyn1-EBFP-Cre (~3 X 10^{12} viral genomes/ml Addgene, 0.75 ul/hem) into the NAc core (+ 1.6 mm AP, +/- 2.8 mm ML, - 7.1 mm DV from bregma, 10º angle). These viruses are

retrogradely transported, expressing Cre-recombinase in neurons expressing Cre-dependent viral vectors that innervate the injected brain region (Junyent and Kremer, 2015; Tervo et al., 2016). All microinjections were delivered over a course of 5 minutes and glass micropipettes were left in place for 10 minutes to facilitate diffusion away from the injection site.

Behavior

Cocaine SA was performed identical to that which was used in Chapter two. Rats received 10-14 days of SA. Immediately following the final cocaine SA session, all rats were injected with CNO (3 mg/kg i.p., NIDA chemical synthesis and drug supply program). Subsequent forced abstinence (i.e. 6 days), post-abstinence context-induced relapse, extinction, cue-induced reinstatement, extinction, and cocaine prime-induced reinstatement were performed identical to Chapter two.

Approximately one week following the cocaine prime test, rats received another injection of CNO (3 mg/kg, i.p.), were anesthetized (ketamine/xylazine), then transcardially perfused with 150 ml of 0.1M phosphate-buffered saline (PBS) followed by 200 ml of 4% paraformaldehyde (PFA, pH 7.4) two hours after the injection because this timepoint has been shown to be when maximal Fos induction occurs following acute cocaine (Graybiel et al., 1990). Brains were immersed in the same fixative for 1 hour and were then processed for immunohistochemical detection of the mCherry or eGFP tag/reporter and the activity protein, Fos.

Immunohistochemistry

Fifty µm sections containing the medial prefrontal cortex (mPFC) and NAc core were sliced on a cryostat (Leica Biosystems, Mannheim, Germany). The collected sections were stored in 0.1 M PBS containing 0.2% sodium azide and stored at 4ºC until immunohistochemical processing.

Three to four sections from AP +2.76 to AP +4.2 mm from bregma were used for mCherry and Fos detection. First, sections were blocked in PBS with 0.3% Triton X-100 (PBST) and 2% normal goat serum (NGS) for two hours. Next, tissue was incubated at 4ºC in PBST containing primary antisera with NGS (2%) overnight. Primary antisera consisted of a chicken anti-mCherry (1:2000; LS Biosciences #LS-C204825, Seattle, WA RRID:AB_2716246), chicken anti-GFP (1:1000; Abcam #ab13970, Cambridge, MA RRID:AB_300798) and either rabbit anti-cFos (1:250, Santa Cruz Biotechnology, sc-52 RRID:AB_2106783) or mouse anti-cFos (1:100, Santa Cruz Biotechnology, sc-166940). Sections were then rinsed in PBST (3 X 10 minutes), then incubated in species-specific secondary antisera conjugated to either Alexa Fluor®594 (1:1,000; Abcam #ab150172) for mCherry detection or Alexa Fluor®647 (1:1,000; Abcam #ab150115) for detection of Fos. In experiment 2, mCherry/eGFP and Fos colocalization was not performed due to diffuse virus expression when hM3Dq was driven by a CaMKIIα promoter. Thus, sections were immunoprocessed for only Fos (1:250, Santa Cruz Biotechnology, sc-52 RRID:AB_2106783) followed by Alexa Fluor®594-conjugated secondary antisera (1:1,000; Cell-signaling technologies, #8889). Sections were incubated in secondary antisera for two hours at room temperature

protected from light. Sections were then rinsed in PBST (3 X 10 minutes), then mounted on superfrost-plus glass slides using ProLong gold anti-fade (Thermo Fisher Scientific; Waltham, MA). Slides were stored at 4ºC until imaging was performed.

Epifluorescent and confocal imaging

Epifluorescent photomicrographs of mCherry and eGFP expression in the PrL cortex and NAc core, respectively, were acquired using a 2.5X air objective with an Olympus brightfield microscope equipped with appropriate wavelength filters. These images were used for verification of virus placement in the PrL cortex and NAc core. Animals were excluded from analyses if significant virus expression was observed in the infralimbic cortex (see results) or if virus expression was significantly different between hemispheres. ImageJ was used to manually draw regions of interest for Cg1, IL, and PrL cortex on each photomicrograph. The percent of total integrated density in each region was calculated for each section. Three to four sections were analyzed per animal, and then averaged to obtain a single integrated density data point for each region for each animal. In Experiment 2, Fos immunoreactivity was detected using a Leica SP5 laser-scanning confocal microscope. Images were acquired with a He-Ne 543 laser line, 10X air objective, a 1024x1024 frame size, and a 1 µm Z-step size. In experiment 3, a Leica SP5 laser-scanning confocal microscope was used. Images were acquired with a 20X air objective with 1024x1024 frame size and a 1 µm Z-step size. Alexa Fluor® 594 (mCherry) was detected using a He-Ne 543 laser line and Alexa Fluor® 647 (Fos) was detected using a He-NE 633 laser line. In some instances, a Leica SP8 laser-

scanning confocal microscope was used, but imaging parameters were similar. Laser power, pinhole size, and gain was initially optimized and then held constant for the remainder of the experiment.

In Experiment 2, FIJI (NIH) was used to quantify the extent of Fos expression in acquired images. Un-deconvolved Z-stacks were exported to FIJI and automatic thresholds were applied. In experiment 3, un-deconvolved confocal Z-stacks (~35 µm) were exported to Imaris software (Bitplane, Zurich, Switzerland) for analysis. First, background was subtracted from images. Next, the spots module was used to identify mCherry$^+$ soma and Fos$^+$ nuclei. Spot-detection size was held constant throughout the experiment. However, in instances where Imaris did not detect clear mCherry$^+$ soma or Fos$^+$ nuclei, these were manually added. Finally, the number of mCherry$^+$ somas expressing Fos$^+$ nuclei was normalized to the total number of mCherry$^+$ soma and compared between mCherry- and hM3Dq-expressing rats.

Tissue processing and Wes™ immunoassay

Tissue processing and the Wes™ immunoassay were performed in an identical manner as in Chapter 2. However, in this experiment we observed subtle, albeit significant, differences in the AUC of calnexin multi-plexed with p-ERK2 between groups. Thus, p-ERK2 AUC was normalized to calnexin, which was then normalized to the ratio of the AUC of tERK2/calnexin. Like Chapter 2, samples were normalized to control.

Statistical Analyses

All behavioral data were analyzed with a mixed-model two-way ANOVA utilizing Bonferroni-corrected pairwise comparison tests when comparing two or more timepoints between groups. When comparing several bins to the first bin for each virus group independently, Dunnett's multiple comparison test was used. Fos data and neurochemical data were analyzed with a two-tailed t-test with or without Welch's correction when appropriate. Statistical outliers were detected using Grubbs' test (extreme studentized deviate method) and were excluded from all analyses. All data are expressed as the mean +/- standard error of the mean (SEM).

Results

Experiment 1. CNO increased p-ERK2 two hours after injection in naïve rats

Figure 3.1A shows the timeline for Experiment 1. Experiment 1 was designed to determine whether acute activation of CaMKIIα-hM3Dq with CNO (3 mg/kg, i.p.) increased ERK2 phosphorylation (p-ERK2) in the PrL cortex two hours after injection, similar to the effect of BDNF (Whitfield et al., 2011) or STEP inhibition (Chapter 2). Naïve rats (n=9) were either injected with CNO (n=5, 3 mg/kg, i.p.) or vehicle (n=4, 5% DMSO in sterile saline) and rapidly decapitated two hours after the injection. Using a Wes™-based immunoassay, results showed a significant elevation in p-ERK2/tERK2 in hM3Dq rats injected with CNO relative to vehicle ($t_{(7)}$=2.38, $p<0.05$, Fig. 3.1B). There was no difference in tERK2/calnexin ($t_{(7)}$=0.51, $p>0.05$, Fig. 3.1C). Representative chemiluminescent peaks of p-ERK2 for CNO-

injected animals (blue) and vehicle-injected animals (green) are shown in Figure 3.1D.

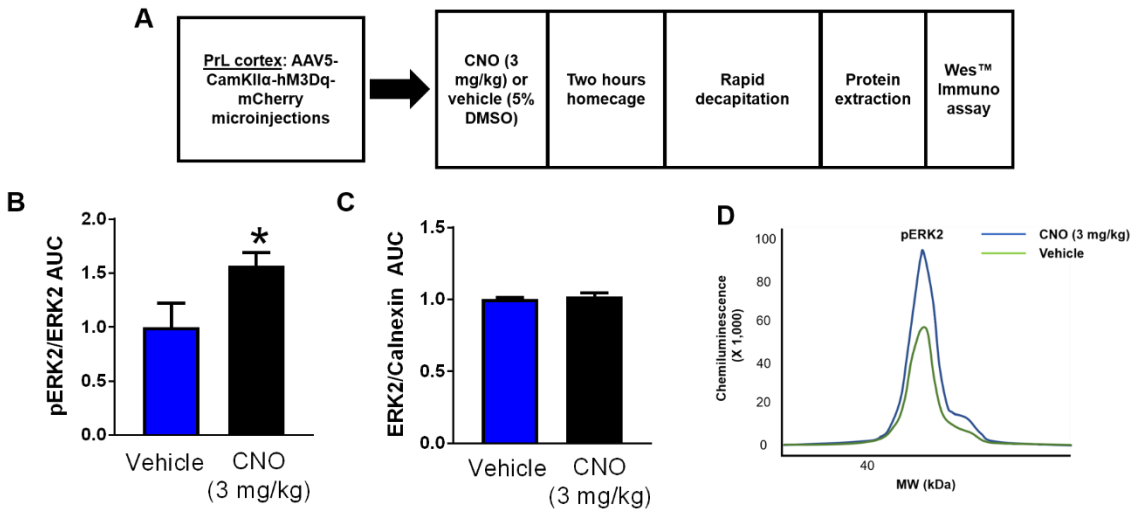

Figure 3.1. CNO (3 mg/kg, i.p.) acutely elevates p-ERK2 in CaMKIIα-hM3Dq-expressing rats. **A.** Experimental timeline. **B.** Naïve rats infused with AAV5-CaMKIIα-hM3Dq injected with CNO (3 mg/kg, i.p.) show elevated ERK2 phosphorylation in the PrL cortex two hours after the injection relative to vehicle-injected controls. **C.** There was no difference in ERK2 between groups. **D.** Representative chemiluminescent peaks for CNO-injected rats (blue) and vehicle-injected rats (green) *p<0.05 compared to vehicle.

Experiment 2. The effect of hM3Dq activation of the PrL cortex immediately after SA on post-abstinence context-induced relapse, cue-, and cocaine prime-, induced reinstatement after extinction

Of the initial 13 rats infused with the eGFP control virus, 3 were removed. One rat was removed for significant virus expression in the IL cortex. One rat was removed for lack of reinstatement in all three tests, and one rat never acquired SA. Of the 13 rats initially infused with hM3Dq virus, 3 were removed. One rat never acquired SA, and two rats were removed for having significant virus expression in the IL cortex. Figure 3.2A shows the experimental timeline for experiment 2. Representative virus expression for CaMKIIα-hM3Dq-expressing rats is shown in

Figure 3.2B. The quantitation of virus expression in three regions of the mPFC is shown in Figure 3.2C. Figure 3.2D shows the last 10 days of SA for eGFP (blue) and hM3Dq (black) rats. Active lever presses (ALP), inactive lever presses (ILP), and infusions were analyzed with a mixed-model two-way ANOVA with virus as the between-subjects factor and SA session as the within-subjects factor. For active lever presses, analyses revealed there was no significant virus by SA session interaction ($F_{(9,162)}$=0.36, p>0.5), main effect of virus ($F_{(1,18)}$=0.08, p>0.05), nor a significant main effect of SA session ($F_{(9,162)}$=0.58, p>0.05). Thus, there was no difference between groups in active lever presses over the last 10 days of SA and both groups showed stable responding on the active lever during this time. For inactive lever presses, there was no significant virus by SA session interaction ($F_{(9,162)}$=0.58, p>0.05), main effect of virus ($F_{(1,18)}$=0.74, p>0.05), or main effect of SA session ($F_{(9,162)}$=1.24, p>0.05). Thus, there was no difference between groups regarding inactive lever presses. For infusions, there was no significant virus by SA session interaction ($F_{(9,162)}$=0.23, p>0.05), nor a main effect of virus ($F_{(1,18)}$=0.33, p>0.05). However, there was a main effect of SA session ($F_{(9,162)}$=4.98, p<0.0001). Thus, there was no difference between groups for infusions earned over the last 10 days of SA, but both groups increased infusions over time.

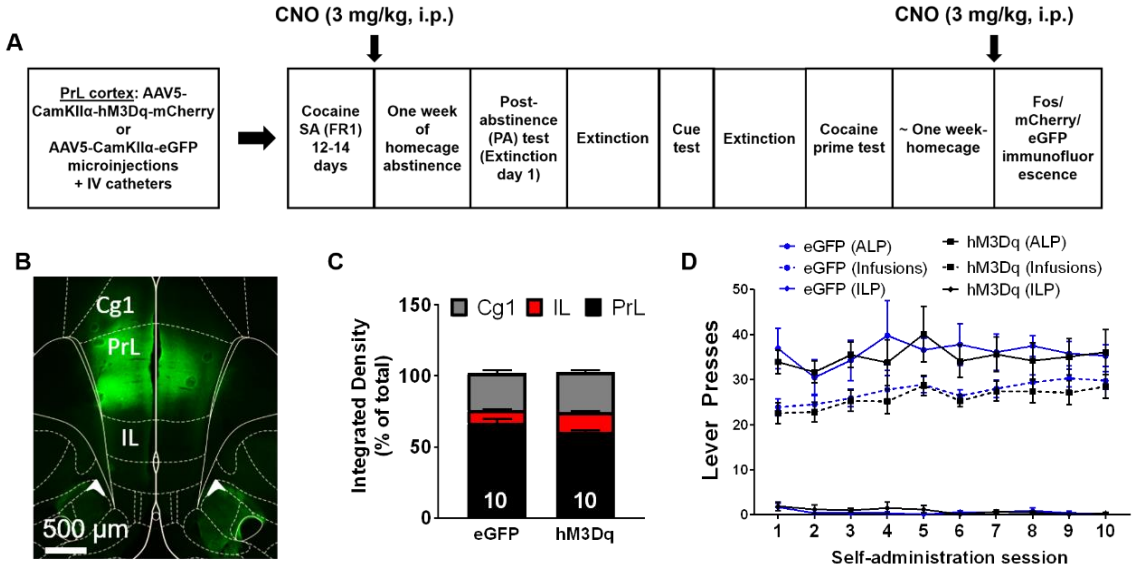

Figure 3.2. PrL cortical CaMKIIα-hM3Dq-mCherry virus expression quantitation and SA data. **A.** Experimental timeline. **B.** Representative virus expression for hM3Dq-expressing rats. **C.** Quantitation of the extent of virus expression in eGFP (left) and hM3Dq (right) rats. The percentage of total virus expression (as shown by fluorescent integrated density) is shown for Cg1 (grey), IL (red), and PrL (black) cortex. **D.** SA data comparing active lever presses (ALP), inactive lever presses (ILP), and infusions between groups over the last 10 days of SA.

hM3Dq activation of the PrL cortex immediately after SA did not suppress context-induced relapse after abstinence

Immediately following the final SA session, all rats were injected with CNO (3 mg/kg, i.p.) and returned to the vivarium for one week of forced home-cage abstinence. Rats then underwent a single two-hour post-abstinence context-induced relapse test under extinction conditions. Figure 3.3A shows the results of the post-abstinence relapse test. A mixed-model two-way ANOVA revealed there was no significant virus by timepoint interaction ($F_{(1,18)}$=2.70, $p>0.05$), nor a significant main effect of virus ($F_{(1,18)}$=3.99, $p>0.05$), but there was a significant main effect of timepoint ($F_{(1,18)}$=47.33, $p<0.0001$). Thus, there was no difference between groups regarding active lever presses during both the last 3 days of SA and the PA test. However, both groups showed elevated responding on the

formerly active lever during the PA test relative to the last 3 days of SA. For inactive lever presses, there was no significant virus by timepoint interaction ($F_{(1,18)}$=0.17, p>0.05), nor a significant main effect of virus ($F_{(1,18)}$=0.22, p>0.05), but there was a significant main effect of time ($F_{(1,18)}$=35.81, p<0.0001). Thus, there was no difference between groups regarding inactive lever presses during the last 3 days of SA or during the PA test. However, both groups showed elevated responding on the formerly inactive lever during the PA test relative to the last 3 days of SA.

Because the results revealed a trend towards reduced active lever pressing in hM3Dq-expressing rats when the entire two-hour PA test data set was analyzed, we performed a follow-up analysis investigating individual timepoints during the PA test in 10-minute bins using a two-way RM ANOVA (Fig. 3.3B). There was no significant virus by time point interaction ($F_{(11,198)}$=1.49, p>0.05) nor a significant main effect of virus ($F_{(1,18)}$=3.67, p>0.05). However, there was a significant main effect of time ($F_{(11,198)}$=9.54, p<0.0001). Thus, akin to the entire two-hour test, there was no significant difference between groups when examining individual timepoints within the PA test, but both groups reduced their responding during the PA test.

hM3Dq activation of the PrL cortex immediately after SA reduced active lever pressing only during the first 10 minutes of cue-induced reinstatement

Following the PA test, rats underwent further extinction training until they reached criterion, then underwent a cue-induced reinstatement test. Figure 3.3C shows the results of the entire two hours of cue-induced reinstatement. For active lever presses, a two-way mixed model ANOVA revealed that there was no significant virus by time point interaction ($F_{(1,18)}$=1.53, p>0.05), nor a significant main effect of

virus ($F_{(1,18)}$=1.58, p>0.05). However, there was a significant main effect of time ($F_{(1,18)}$=78.14, p<0.0001). Thus, there was no overall effect of hM3Dq activation of the PrL cortex immediately after SA on cue-induced reinstatement. However, both groups increased their responding on the formerly active lever during cue-induced reinstatement relative to the last 3 days of SA, as expected. For inactive lever presses, there was no significant virus by timepoint interaction ($F_{(1,18)}$=0.1, p>0.05) nor a significant main effect of virus ($F_{(1,18)}$=0.01, p>0.05). However, there was a significant main effect of time ($F_{(1,18)}$=6.09, p<0.05). Thus, there was no difference between groups during the last 3 days of extinction or during the entire two-hour duration of the cue-induced reinstatement test. However, both groups showed elevated active and inactive lever pressing during reinstatement relative to the last 3 days of extinction.

As in the PA test, we also analyzed individual 10-minute bins during the cue-induced reinstatement test using a two-way RM ANOVA, as shown in Figure 3.3D. In contrast to the PA test, a two-way ANOVA revealed a significant virus by timepoint interaction ($F_{(11,198)}$=2.01, p<0.05). There was also a significant main effect of timepoint ($F_{(11,198)}$=3.86, p<0.0001), but no significant main effect of virus ($F_{(1,18)}$=0.57, p>0.05). Bonferroni-corrected pairwise comparison tests indicated that hM3Dq rats had significantly lower active lever presses during the first 10 minutes of cue-induced reinstatement relative to eGFP rats (p<0.05). Moreover, when comparing each 10-minute bin to the first 10-minute bin in eGFP rats with a Dunnett's multiple comparison test, each timepoint was significantly lower than the first 10 minutes (all p<0.05), except when comparing 20-30 minutes to 0-10

minutes ($p>0.05$). However, when comparing each 10-minute bin to the first 10-minute bin in hM3Dq rats, there was no timepoint that was significantly different from the first 10-minute bin. Thus, there was no significant difference between groups when analyzing active or inactive lever presses during the entire two-hour reinstatement test. However, hM3Dq activation of the PrL cortex immediately after SA suppressed active lever pressing during the first 10 minutes of reinstatement, when lever pressing was highest in eGFP rats.

hM3Dq activation of the PrL cortex immediately after SA did not suppress cocaine prime-induced reinstatement after extinction

Following the cue-induced reinstatement test, rats were re-extinguished until criterion. Rats then underwent a two-hour cocaine prime-induced reinstatement test under extinction conditions (Fig. 3.3E). When analyzing active lever presses, a two-way mixed model ANOVA revealed that there was no significant virus by timepoint interaction ($F_{(1,18)}=0.54$, $p>0.05$), nor a significant main effect of virus ($F_{(1,18)}=1.39$, $p>0.05$). However, there was a significant main effect of time ($F_{(1,18)}=103.8$, $p<0.0001$). For inactive lever presses, there was no significant virus by timepoint interaction ($F_{(1,18)}=0.21$, $p>0.05$), main effect of virus ($F_{(1,18)}=2.08$, $p>0.05$), or main effect of time ($F_{(1,18)}=0.02$, $p>0.05$). Thus, there was no effect of hM3Dq activation of the PrL cortex immediately after SA on active or inactive lever presses during the entire two-hour cocaine prime-induced reinstatement following extinction.

As for the PA test and cue-induced reinstatement test, we also extended this analysis to the individual 10-minute bins within the cocaine prime-induced reinstatement test (Fig. 3.3F). A two-way RM ANOVA revealed that there was no

significant virus by timepoint interaction ($F_{(11,198)}$=0.57, p>0.05), nor a significant main effect of virus ($F_{(1,18)}$=1.0, p>0.05). However, there was a significant main effect of time ($F_{(11,198)}$=15.74, p<0.0001). Thus, there was no difference between groups regarding active lever pressing during individual timepoints within the cocaine prime-induced reinstatement test, and both groups showed reduced active lever pressing during cocaine prime-induced reinstatement.

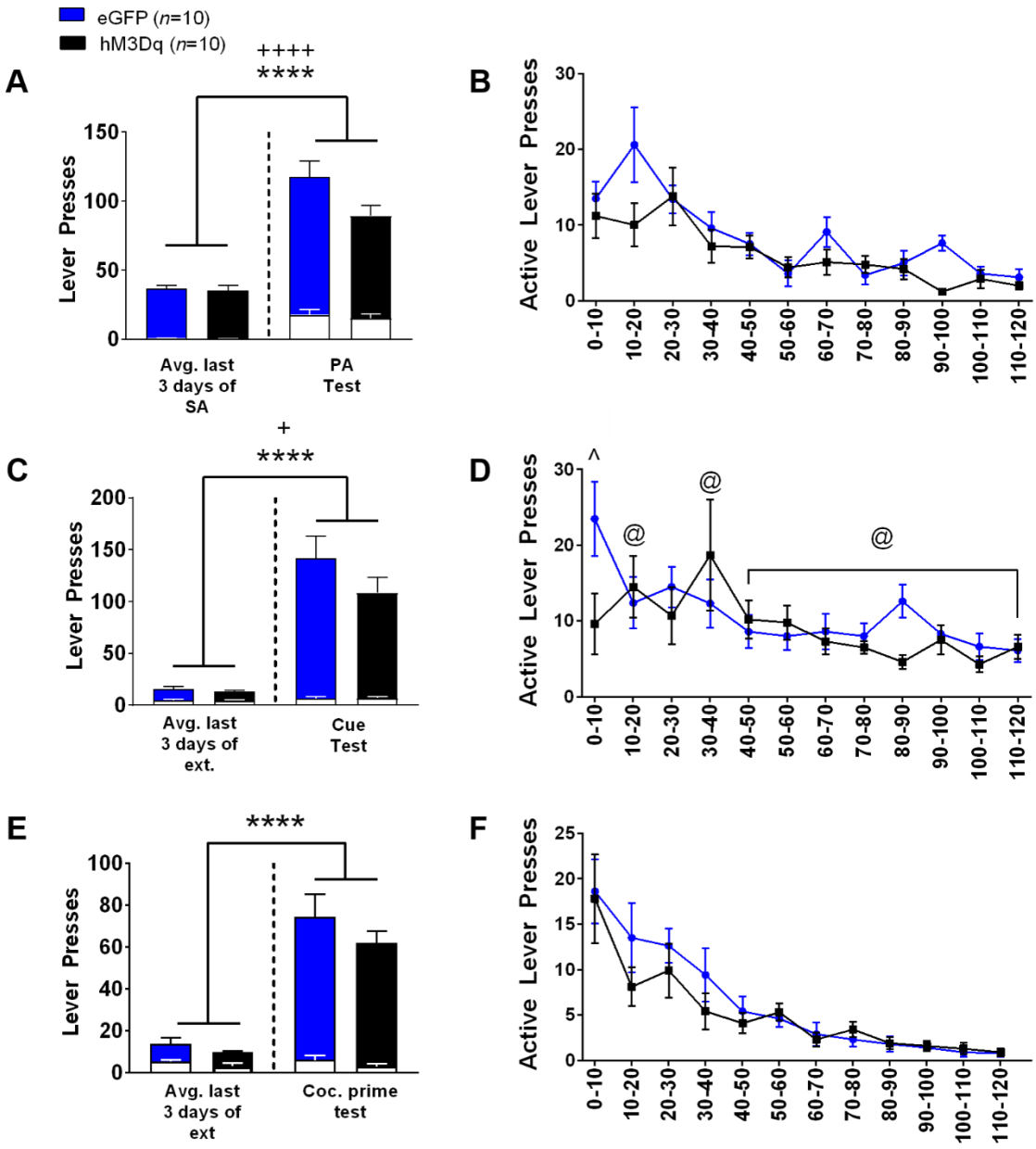

Figure 3.3. Global chemogenetic activation of PrL cortical neurons immediately after SA is without an overall effect on post-abstinence context-induced relapse and cue- and cocaine prime- induced reinstatement after extinction during the two-hour tests but did selectively reduce lever pressing during the first 10 minutes of cue-induced reinstatement. **A.** hM3Dq-mediated activation of the PrL cortex immediately after SA failed to suppress post-abstinence context-induced relapse after abstinence. **B.** There was no effect of hM3Dq activation immediately after SA at any timepoint analyzed during the PA test. **C.** There was also no effect of hM3Dq activation of the PrL cortex on cue-induced reinstatement after extinction when analyzing the entire two-hour session. **D.** There was a specific reduction in lever pressing during the first 10 minutes of cue-induced reinstatement when lever pressing was highest in eGFP control rats. **E.** There was no effect of hM3Dq activation on cocaine prime-induced reinstatement. **F.** There was no effect of hM3Dq activation immediately after SA at any timepoint analyzed during the cocaine prime-induced reinstatement test. White bars indicate inactive lever presses, and colored bars indicate active lever presses. ****p<0.0001 compared to last 3 days of SA (ALP), +p<0.05, ++++p<0.0001 compared to last 3 days of SA (ILP), ^p<0.05 compared to eGFP, @p<0.05 compared to first 10-minute bin.

CNO increased Fos expression in the PrL cortex of hM3Dq rats

Following the cocaine prime-induced reinstatement test, all rats were returned to the vivarium for ~one week. A subset of rats was then given a challenge injection of CNO (3 mg/kg, i.p.) and transcardially perfused two hours later for Fos analysis (Fig. 3.4). A Welch's-corrected t-test showed that hM3Dq-expressing rats showed robust Fos activation relative to eGFP controls ($t_{(6.05)}$=2.92, p<0.05, Fig. 3.4A). Representative Fos induction is shown for eGFP- (Fig. 3.4B), and hM3Dq-expressing (Fig. 3.4C) rats.

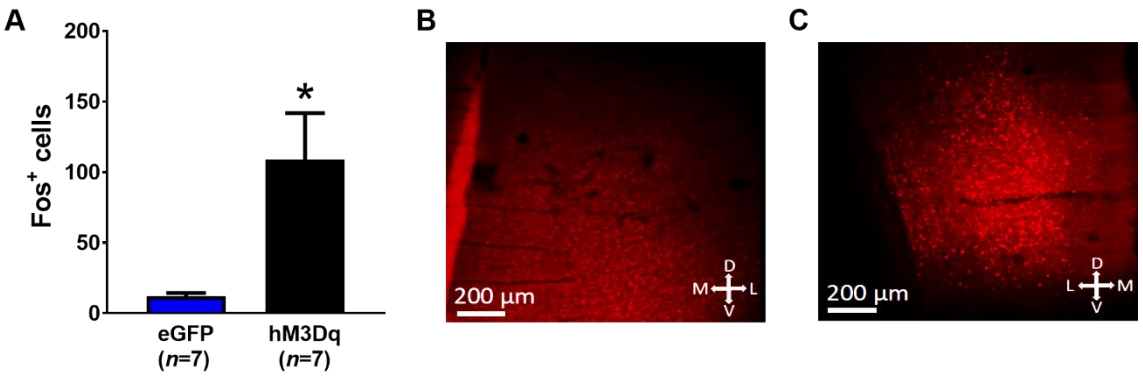

Figure 3.4. Post-experiment CNO challenge increased Fos immunoreactivity in hM3Dq-expressing rats. **A.** Fos+ cells were significantly higher in hM3Dq rats relative to eGFP controls two hours after CNO injection. **B.** Representative Fos (red) immunoreactivity in eGFP rats. **C.** Representative Fos immunoreactivity in hM3Dq rats. *p<0.05 compared to eGFP.

Experiment 3. The effect of hM3Dq activation of PrL cortical neurons projecting to the NAc core immediately after SA on post-abstinence context-induced relapse, cue-, and cocaine prime-, induced reinstatement after extinction

Of the 16 mCherry rats, 4 were removed. One rat was removed for lack of SA acquisition, one rat was removed as a statistical outlier during cue-induced reinstatement, and two rats were removed for virus expression outside of the PrL cortex. Of the 16 hM3Dq rats, 5 were removed. Three rats were removed for significant virus expression outside of the PrL cortex. One rat never acquired SA, and one rat became ill and was removed from the study. Figure 3.5A shows the experimental timeline including surgery, behavioral experiments, time of CNO injections as well as post-experiment CNO-induced Fos quantitation in mCherry- and hM3Dq-expressing rats. Figure 3.5B shows a schematic for dual-viral injections which result in preferential infection of PrL cortical neurons projecting to the NAc core. Figure 3.5C shows representative Cre-dependent expression of the mCherry tag in the hM3Dq construct. Note that virus expression was largely confined to the PrL cortex, particularly layer V. Figure 3.5D shows representative

CAV2-Cre-eGFP expression in the NAc core. Figure 3.5E shows SA data for mCherry and hM3Dq rats. For statistical purposes, only the last 10 days of SA are shown. However, all rats received a minimum of 10 days and a maximum of 14 days of SA.

For active lever presses, a two-way RM ANOVA showed no significant virus by SA session interaction ($F_{(9,189)}$ = 0.8266, $p>0.05$) nor significant main effects of SA session ($F_{(9,189)}$=0.8858, $p>0.05$) or virus ($F_{(1,21)}$=1.51, $p>0.05$). For inactive lever presses, there was no significant virus by SA session interaction ($F_{(9,189)}$=1.35, $p>0.05$) or main effect of virus ($F_{(1,21)}$=1.78, $p>0.05$). However, there was a significant main effect of time ($F_{(9,189)}$=2.58, $p<0.05$). For infusions earned, a two-way RM ANOVA showed no significant virus by SA session interaction ($F_{(9,189)}$=1.47, $p>0.05$) nor a significant main effect of SA session ($F_{(9,189)}$=1.40, $p>0.05$) or virus ($F_{(1,21)}$=1.08, $p>0.05$). Collectively, these results indicate that there was no difference between mCherry and hM3Dq rats regarding active lever presses, inactive lever presses, or infusions over the last 10 days of SA. Immediately following the last SA session, all rats received a single injection of CNO (3 mg/kg, i.p.) and were then returned to the vivarium for one week of forced abstinence.

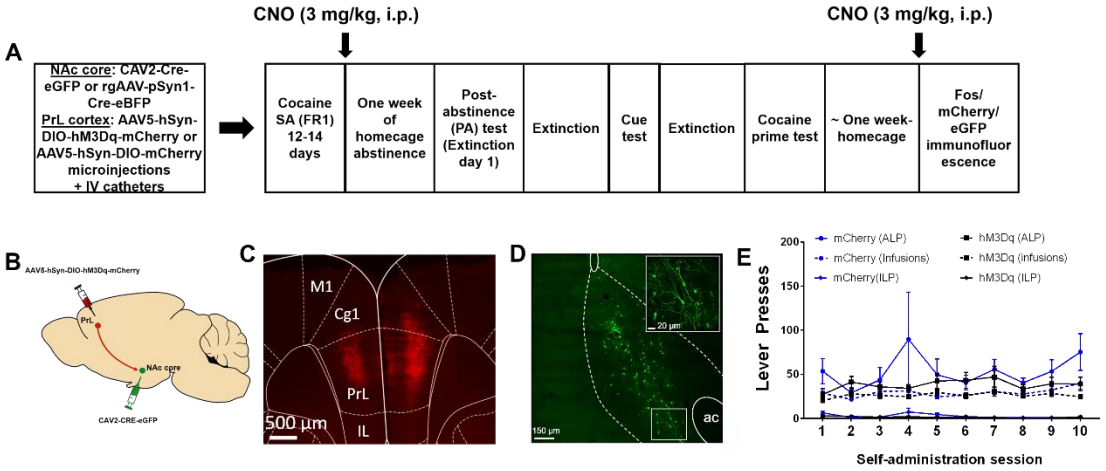

Figure 3.5. Experimental timeline, virus expression, and SA data for experiment 3. **A.** Experimental timeline. **B.** Schematic illustrating use of intersectional viral approach for preferential infection of PrL-NAc core neurons. **C.** Representative AAV5-hSyn-DIO-hM3Dq-mCherry expression in the PrL cortex. Note the majority of virus expression is contained within the PrL cortex, specifically in layer V neurons. **D.** Representative CAV2-Cre-eGFP expression in the NAc core. Circled region denotes anterior commissure (ac), and dotted line indicates NAc core. Inset corresponds to high-magnification view of boxed region. **E.** SA data for experiment 3 showing active lever presses (ALP), inactive lever presses (ILP), and infusions for both groups over the last 10 days of SA.

hM3Dq activation of PrL-NAc core neurons reduced lever pressing only during the first 10 minutes of post abstinence relapse testing

Figure 3.6A shows the average active lever presses for the last 3 days of SA (left) for mCherry (blue) and hM3Dq-expressing (black) rats. A two-way mixed model ANOVA indicated a non-significant virus by timepoint interaction ($F_{(1,21)}$=0.58, p>0.05), but significant main effects of virus ($F_{(1,21)}$=4.78, p<0.05) and time ($F_{(1,21)}$=16.15, p<0.001). There was no significant virus by timepoint interaction ($F_{(1,21)}$=1.88, p>0.05) nor main effect of virus ($F_{(1,21)}$=1.78, p>0.05) on inactive lever presses. However, there was a main effect of time ($F_{(1,21)}$=27.39, p<0.0001). Thus, both groups showed elevated active and inactive lever pressing following one week of forced abstinence, and hM3Dq rats showed reduced active lever pressing

relative to mCherry controls. Bonferroni-corrected pairwise comparison tests indicated that there was no difference between groups over the last 3 days of SA ($p>0.05$), but there was a strong trend towards reduced active lever pressing during the PA test in hM3Dq rats ($p=0.08$).

Because we found a strong trend towards reduced active lever pressing in the overall two-hour PA test, we investigated individual timepoints within the PA test by analyzing lever pressing during 10-minute bins. Figure 3.6B shows the effect of hM3Dq activation immediately after SA on active lever pressing during 10-minute bins. A two-way RM ANOVA showed a significant virus by time interaction ($F_{(11,231)}=2.03$, $p<0.05$) as well as a significant main effect of time ($F_{(11,231)}=11.55$, $p<0.0001$), but not virus ($F_{(1,21)=}2.06$, $p>0.05$). Bonferroni-corrected multiple comparison tests indicated that hM3Dq rats showed reduced active lever pressing during the first 10 minutes of the PA test ($p<0.001$) relative to mCherry controls. Additional analyses comparing each timepoint to this first 10-minute bin only in mCherry control rats indicated that the first 10 minutes of active lever pressing were significantly higher relative to every other 10-minute bin ($p<0.01$ 0-10 vs. 10-20, $p<0.001$ 0-10 vs. 20-30, $p<0.0001$ 0-10 vs. 30-40 and above). Interestingly, only 90-100 minutes was different than 0-10 minutes in hM3Dq rats ($p<0.05$). Thus, hM3Dq activation of PrL-NAc core neurons immediately after SA suppresses relapse during the first 10 minutes of testing, when lever pressing is most-elevated in mCherry control rats.

hM3Dq activation of PrL-NAc core neurons failed to suppress cue-induced reinstatement after extinction

Figure 3.6C shows the average last 3 days of extinction active lever pressing for mCherry and hM3Dq rats as well as active and inactive lever pressing during cue-induced reinstatement. A two-way mixed model ANOVA indicated a non-significant virus by time point interaction ($F_{(1,21)}$=2.92, p>0.05) as well as a non-significant main effect of virus ($F_{(1,21)}$=3.14, p>0.05). However, there was a significant main effect of timepoint ($F_{(1,21)}$=102.9, p<0.0001). There was a no virus by time point interaction ($F_{(1,21)}$=0.23, p>0.05), main effect of treatment ($F_{(1,21)}$=0.27, p>0.05), or main effect of time ($F_{(1,21)}$=1.54, p>0.05) on inactive lever presses. Thus, both groups showed elevated active, but not inactive, lever pressing during cue-induced reinstatement relative to the last 3 days of extinction but there was no difference between groups on active lever presses during extinction or cue-induced reinstatement.

When analyzing 10-minute bins (Fig. 3.6D), a two-way RM ANOVA indicated no virus by time interaction ($F_{(11,31)}$=1.054, p>0.05) or a main effect of virus ($F_{(1,21)}$=3.065, p>0.05). However, there was a significant main effect of time ($F_{(1,21)}$=3.283, p<0.001). Thus, both groups showed reduced active lever pressing as a function of time during cue-induced reinstatement but there was no effect of hM3Dq activation on any timepoint.

hM3Dq activation of PrL-NAc neurons after SA failed to suppress cocaine prime-induced reinstatement after extinction

Figure 3.6E shows the average last 3 days of extinction (left) for mCherry and hM3Dq rats. When analyzing active lever presses, a two-way mixed-model

ANOVA revealed there was no significant virus by timepoint interaction ($F_{(1,21)}$=2.68, p>0.05), nor main effect of virus ($F_{(1,21)}$=2.86, p>0.05). However, there was a significant main effect of time ($F_{(1,21)}$=37.86, p<0.0001). There was no significant virus by timepoint interaction ($F_{(1,21)}$=2.65, p>0.05), main effect of virus ($F_{(1,21)}$=0.91, p>0.05), or a main effect of time ($F_{(1,21)}$=3.40, p>0.05) on inactive lever presses. Thus, both groups showed elevated active, but not inactive, lever pressing during cocaine prime-induced reinstatement relative to the last 3 days of extinction, and hM3Dq activation was without an effect on cocaine prime-induced reinstatement during the 2-hour test. Further analysis of individual 10-minute binned data with a two-way RM ANOVA indicated that there was no significant virus by time interaction ($F_{(11,231)}$=0.849, p>0.05) or main effect of virus ($F_{(1,21)}$=2.893, p>0.05) but there was a significant main effect of time ($F_{(11,231)}$=6.57, p<0.0001). In this analysis, both hM3Dq-activated and control groups showed reduced active lever pressing as a function of time during cocaine prime-induced reinstatement but there was no effect of hM3Dq activation *per se* on active lever pressing (Fig. 3.6F).

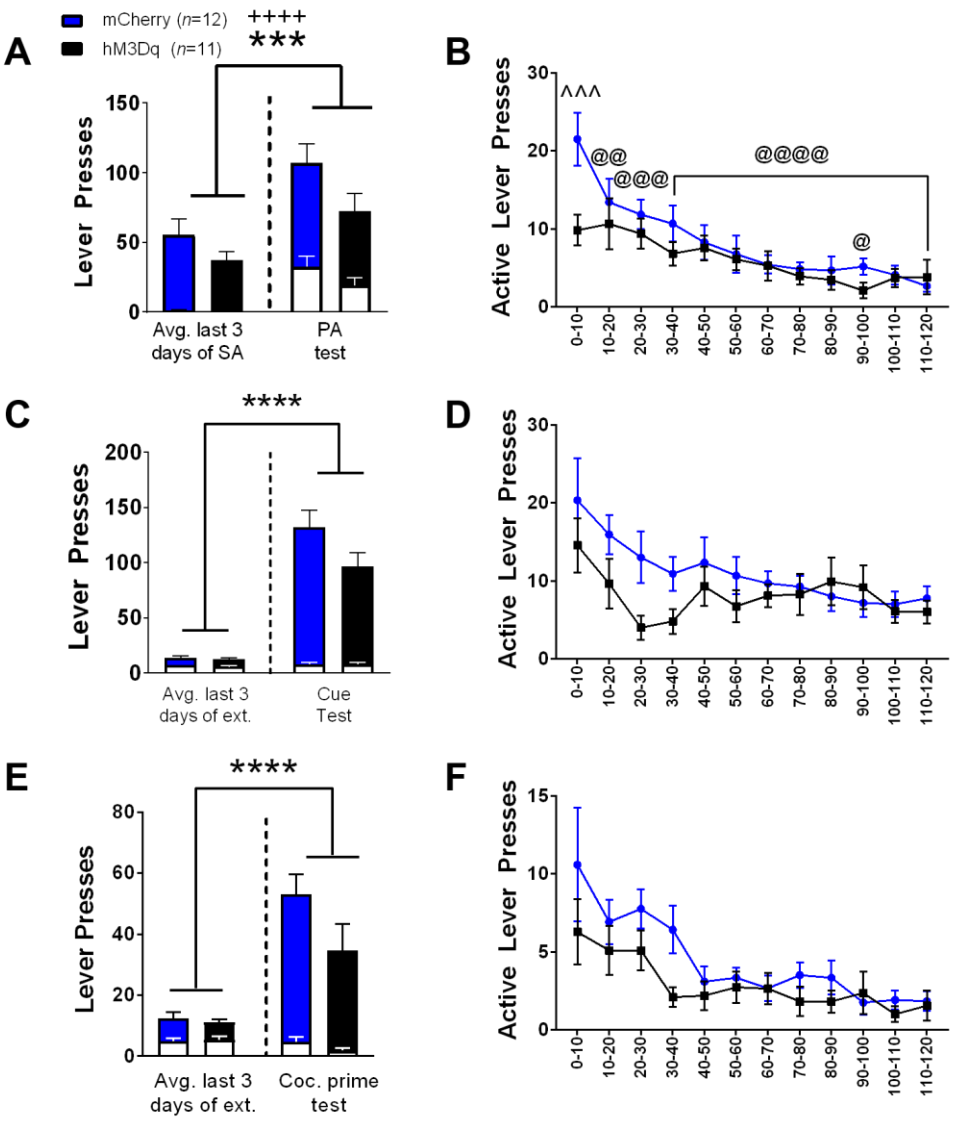

Figure 3.6. Activation of PrL-NAc core neurons immediately after SA failed to suppress post-abstinence context-induced relapse or cue- and cocaine prime-induced reinstatement after extinction during two-hour tests but did reduce lever pressing selectively during the first 10 minutes of post-abstinence context-induced relapse. **A.** PrL-NAc core activation immediately after SA had no effect on lever pressing during two-hour post-abstinence relapse testing. **B.** PrL-NAc core activation suppresses active lever pressing during the first 10 minutes of relapse testing, when mCherry lever pressing was highest. **C.** PrL-NAc core activation was without an effect during two-hour cue-induced reinstatement testing. **D.** There was no effect of PrL-NAc core activation during any timepoint during cue-induced reinstatement. **E.** There was no effect of PrL-NAc core activation on cocaine prime-induced reinstatement. **F.** There was no effect of PrL-NAc core activation during any timepoint during cocaine prime-induced reinstatement. *** $p<0.001$, **** $p<0.0001$ compared to last 3 days of SA or extinction (ALP), ++++ $p<0.0001$ compared to last 3 days of SA (ILP), ^^^ $p<0.001$ compared to mCherry, @ $p<0.05$, @@ $p<0.01$, @@@ $p<0.001$, @@@@ $p<0.0001$ compared to first 10-minute bin.

Post-experimental CNO challenge induced robust Fos expression in mCherry neurons preferentially in hM3Dq rats

Approximately one week following the cocaine prime-induced reinstatement test, a subset of rats received another single injection of CNO (3 mg/kg, i.p.) and were perfused two hours later for Fos immunohistochemistry. Figure 3.7A shows that CNO induced robust Fos activation in mCherry neurons in hM3Dq rats relative to mCherry as shown by Welch's-corrected t-test ($t_{(10.69)}$=13.83, p<0.0001). Representative Fos immunoreactivity in mCherry rats is shown in Figure 3.7B. Representative Fos immunoreactivity in hM3Dq rats is shown in Figure 3.7C.

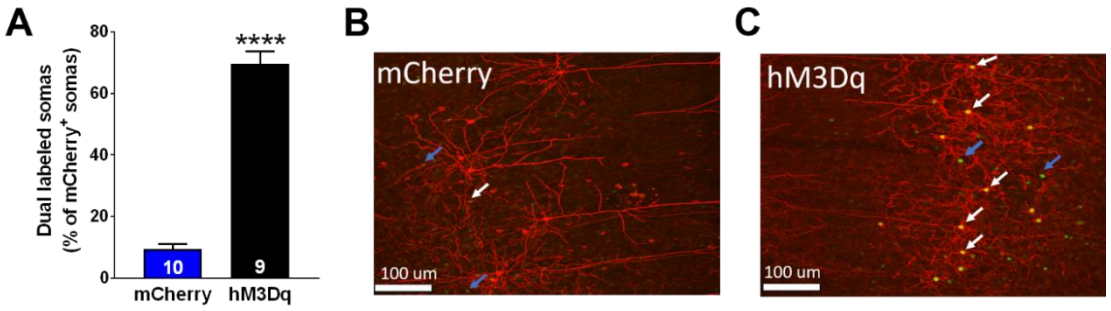

Figure 3.7. Post-experiment CNO challenge increased Fos immunoreactivity in mCherry+ neurons preferentially in hM3Dq-rats. **A.** Approximately 75% of mCherry+ neurons showed robust Fos immunoreactivity in hM3Dq-expressing rats compared to mCherry controls. **B.** Representative Fos immunoreactivity in mCherry control rats. **C.** Representative Fos immunoreactivity in hM3Dq-expressing rats. Blue arrow: $Fos^{+}mCherry^{-}$ soma. White arrow: $Fos^{+}mCherry^{+}$ soma. ****p<0.0001 compared to mCherry.

Discussion

Summary of findings

Here we provide data showing an overall lack of support for the hypothesis that augmenting PrL cortical, and specifically PrL-NAc core, neuronal activity during early withdrawal is sufficient to suppress relapse after abstinence. Although we found that hM3Dq activation increased p-ERK2 two hours after injection in naïve rats (Experiment 1), we did not find an overall behavioral effect of hM3Dq activation of the PrL cortex (Experiment 2), or PrL-NAc core neurons (Experiment 3), immediately after SA. However, we did observe several trends when overall two-hour testing was analyzed. Subsequent analyses of the within-session timecourses indicated that activation of all PrL cortical outputs immediately after SA transiently suppressed cue-induced reinstatement after extinction (i.e. first 10 minutes) when control lever pressing was highest. However, we did not see such an effect during post-abstinence context-induced relapse or cocaine prime-induced reinstatement after extinction. Moreover, when specifically activating PrL-NAc core neurons immediately after SA, there was a transient inhibition of cocaine seeking during the post-abstinence context-induced relapse test, but not during cue- or cocaine prime-induced reinstatement after extinction, again, when control lever pressing was invigorated.

Relevance of early timepoints in relapse testing

Although our previous experiments have typically examined data during the entire two-hour test (Whitfield et al., 2011; Barry and McGinty, 2017), there is precedent for examining early portions of relapse testing. Although context-induced

reinstatement after extinction and context-induced relapse after abstinence are mediated by distinct brain regions (Fuchs et al., 2006), the cocaine-conditioned context represents a shared stimulus which elicits cocaine seeking. Context (Stankeviciute et al., 2014)- and cue (Gipson et al., 2013)-induced reinstatement potentiate dendritic spine head diameter, which tightly correlates with lever pressing behavior, in NAc core medium spiny neurons (MSNs) during the first 15 minutes of reinstatement. During cue-induced reinstatement, this transient synaptic potentiation is associated with an augmented AMPA:NMDA ratio and is dependent on glutamate release from the PrL cortex, which likely holds true for context-induced reinstatement. Moreover, after 45 minutes of reinstatement, spine head size and AMPA:NMDA ratios normalize. At this time lever pressing is diminished, presumably due to within-session extinction learning.

Although we did not see any significant differences when examining overall lever pressing during the two-hour session, the finding that lever pressing was suppressed during early parts of post-abstinence context-induced relapse (Experiment 3) and cue-induced reinstatement (Experiment 2) is likely an important, albeit subtle, effect of hM3Dq activation of PrL cortex, and PrL-NAc core, immediately after SA. Moreover, the overall lack of effect suggests that there are distinct mechanisms in the suppressive effect of BDNF relative to hM3Dq, which could be due to differential signaling and duration of effects induced by these two interventions.

BDNF-TrkB signaling vs. Gq-DREADD signaling: Similarities and differences

Previous data indicate that intra-PrL BDNF suppresses cocaine seeking by normalizing glutamate transmission in the PrL cortex during early withdrawal, leading to a long-term stabilization of glutamate release in the NAc core (Berglind et al., 2007; Berglind et al., 2009; Go et al., 2016). Moreover, there is evidence that intra-PrL BDNF alters neuronal signaling in the NAc core as early as two hours after the infusion (Berglind et al., 2007; Sun et al., 2014a). BDNF is typically recognized as a neurotrophic factor that induces neuronal activity by linking TrkB activation with NMDA receptor tyrosine phosphorylation and glutamate release (Huang and McNamara, 2010; Zhang et al., 2013). Ultimately, this facilitates CREB-mediated gene transcription (Mao et al., 2015) via ERK-MAPK signaling (Tao et al., 1998).

However, there is also a clear role for BDNF acting in a homeostatic manner depending on the activity state of neurons (Rutherford et al., 1998). At the synaptic level, it has been suggested that BDNF may preferentially alter transmission differentially at individual synapses depending on the state of potentiation or depression at these synapses (Nagappan and Lu, 2005). This may be critical for the sustained induction of ERK activity. For example, sequential stimulation of only seven spatially-dispersed dendritic spines by glutamate uncaging *in vitro* is sufficient to induce sustained ERK, and ultimately CREB, activation in the nucleus, effects largely due to NMDA receptor-mediated elevations in intracellular Ca^{2+} (Zhai et al., 2013). In contrast, DREADDs are thought to integrate with endogenous Gq-coupled signaling cascades (Alexander et al., 2009), presumably

lacking specificity regarding the spatial location of their mode of action, specifically at sites of internal Ca^{2+} stores. This is important considering the functional heterogeneity that exits between various internal Ca^{2+} stores (Blaustein and Golovina, 2001). Thus, DREADDs are likely promiscuous regarding their engagement of Gq-coupled signaling cascades to induce neuronal firing.

Interestingly, muscarinic type-1 acetylcholine receptor activation facilitates the activation of STEP through the release of Ca^{2+} from intracellular stores (Tian et al., 2016), opposing the Src-mediated phosphorylation of GluN2A-containing NMDA receptors. Thus, the activation of Gq-coupled DREADDs with CNO may induce STEP activation, which would likely be dependent on the dose of CNO used. However, because we found elevated p-ERK2 two hours after CNO (3 mg/kg, i.p.) injection in naïve rats, and because STEP is a major regulator of the magnitude of ERK signaling (Paul et al., 2003), it is unlikely that the dose of CNO used in our experiments activates STEP two hours after injection.

Furthermore, BDNF super-activates (i.e. above and beyond baseline) ERK signaling in the PrL cortex during early withdrawal (Whitfield et al., 2011; Barry and McGinty, 2017), driving CREB phosphorylation and presumably CREB-mediated gene transcription of plasticity-regulating genes (Whitfield et al., 2011). Although we did not test whether hM3Dq activation is able to normalize the cocaine-induced dephosphorylation of ERK2 or CREB in the PrL cortex during early withdrawal, we hypothesize that hM3Dq activation likely does not elevate ERK2 or CREB phosphorylation to the same degree as BDNF. Moreover, BDNF leads to sustained ERK2 phosphorylation with maximal effects seen at two hours, returning to

baseline by six hours, but CREB phosphorylation remains elevated six hours after a single BDNF infusion in naïve rats (Whitfield et al., 2011). Previous experiments have shown that treatment of striatal cultures with high concentrations of CNO (50 μM) only transiently activates ERK2 phosphorylation, which returns to baseline levels two hours after treatment (Bellocchio et al., 2016). Moreover, activation of striatal projection neurons in mice with CNO (1 mg/kg, i.p.) elevates pERK within 30 minutes which returns to baseline by 140 minutes (Alcacer et al., 2017). One caveat of the latter finding was that this experiment was performed in dopamine denervated mice. These findings are consistent with the hypothesis that hM3Dq activation may not elevate ERK2 and CREB phosphorylation in the PrL cortex for the entire two hours after the end of cocaine SA due to the transient effects of CNO.

BDNF-TrkB signaling elevates ERK-MAPK signaling not only through autophosphorylation of TrkB (Atwal et al., 2000), but also by BDNF-TrkB-GluN2B-mediated activation of ERK (Krapivinsky et al., 2003). Moreover, blockade of NMDA receptors prior to BDNF prevents the suppressive effect of BDNF as well as BDNF-mediated elevations in ERK2 phosphorylation in the PrL cortex during early withdrawal (Go et al., 2016). These findings suggest that the activation of ERK by BDNF is dependent on the source of Ras-MAPK activity (i.e. downstream of TrkB or directly at the level of TrkB). Such fine-tuned regulation of ERK signaling likely does not occur with hM3Dq activation, as previous findings indicate that Gq-DREADDs activate ERK exclusively through a PKC-dependent mechanism, at

least *in vitro* (Kaufmann et al., 2013), and there is no evidence for NMDA-induced elevations in Ca^{2+} following hM3Dq activation.

Considerations for experimental approach

Recent evidence indicates that CNO is back-metabolized to clozapine, which is the direct agonist for DREADD receptors (Gomez et al., 2017). Clozapine shows high-affinity for dopamine D2 receptors, α adrenergic receptors, as well as several serotonin receptor subtypes. Specifically, acute treatment with clozapine (10 mg/kg, i.p.) reduces binding affinity of the 5-HT_{2A} serotonin receptor (Wilmot and Szczepanik, 1989). Moreover, a subthreshold dose of clozapine (0.1 mg/kg, i.p.) alters striatal-dependent locomotor activity in hM4Di-expressing mice, which is comparable in magnitude to 10 mg/kg, i.p. CNO (Gomez et al., 2017). Thus, we cannot exclude the effects of clozapine in our experiments. However, because all animals were injected with CNO at a relatively low dose (3 mg/kg, i.p.), which did not affect the ability of control animals to reinstate, we suggest that off-target effects of clozapine are likely not present. Thus, any effect (or lack thereof) is likely due to clozapine binding to DREADD receptors as opposed to the well-documented actions of clozapine at various other receptors when delivered acutely (Wilmot and Szczepanik, 1989). Moreover, others have suggested that 10 mg/kg, i.p. CNO may be required for sustained activity of DREADD receptors over a two-hour window (Mahler and Aston-Jones, 2018). Because 0.1 mg/kg clozapine is a subthreshold dose for altering behavior in animals that do not express DREADDs, and is equivalent, at least behaviorally, to 10 mg/kg CNO in animals expressing

DREADDs, a 10 mg/kg dose of CNO or 0.1 mg/kg dose of clozapine may provide a more pronounced effect of DREADD receptor activation in our paradigm.

Summary, conclusions, and future directions

In conclusion, the results presented herein do not support the hypothesis that augmented PrL cortical or PrL-NAc core neuronal activity during early withdrawal is sufficient to suppress cocaine seeking after abstinence. However, we found discrete timepoints in the post-abstinence context-induced relapse test as well as cue-induced reinstatement when hM3Dq was effective, particularly when control lever pressing was elevated. Although it is unknown at exactly what point PrL cortical ERK2 phosphorylation normalizes in cocaine self-administering animals, it is likely that BDNF provides an enduring normalization during the critical early withdrawal period. However, we hypothesize that hM3Dq activation transiently elevates neuronal activity in the PrL-NAc core pathway during early withdrawal, culminating in a transient reversal of ERK2 dephosphorylation which is not sustained during the entire timecourse of early withdrawal from cocaine SA. This normalization is likely more transient and not as strong as BDNF, and does not prevent STEP activation as is the case of TC-2153 according to data presented in Chapter two (Fig. 3.8A). We propose that this ultimately leads to a transient attenuation of stimulus-induced drug seeking relative to BDNF or STEP inhibition with TC-2153 (Fig. 3.8B), which is differentially regulated by activating the PrL cortex or specifically activating the PrL-NAc core pathway. Accordingly, future experiments should determine whether hM3Dq activation is sufficient to normalize the cocaine-induced dephosphorylation of ERK2 in the PrL cortex during early

withdrawal, as well as glutamate release in the NAc core after extinction, as previously found for BDNF (Berglind et al., 2009; Whitfield et al., 2011). Additionally, future studies should examine dose-dependent effects of clozapine or CNO on relapse to cocaine seeking.

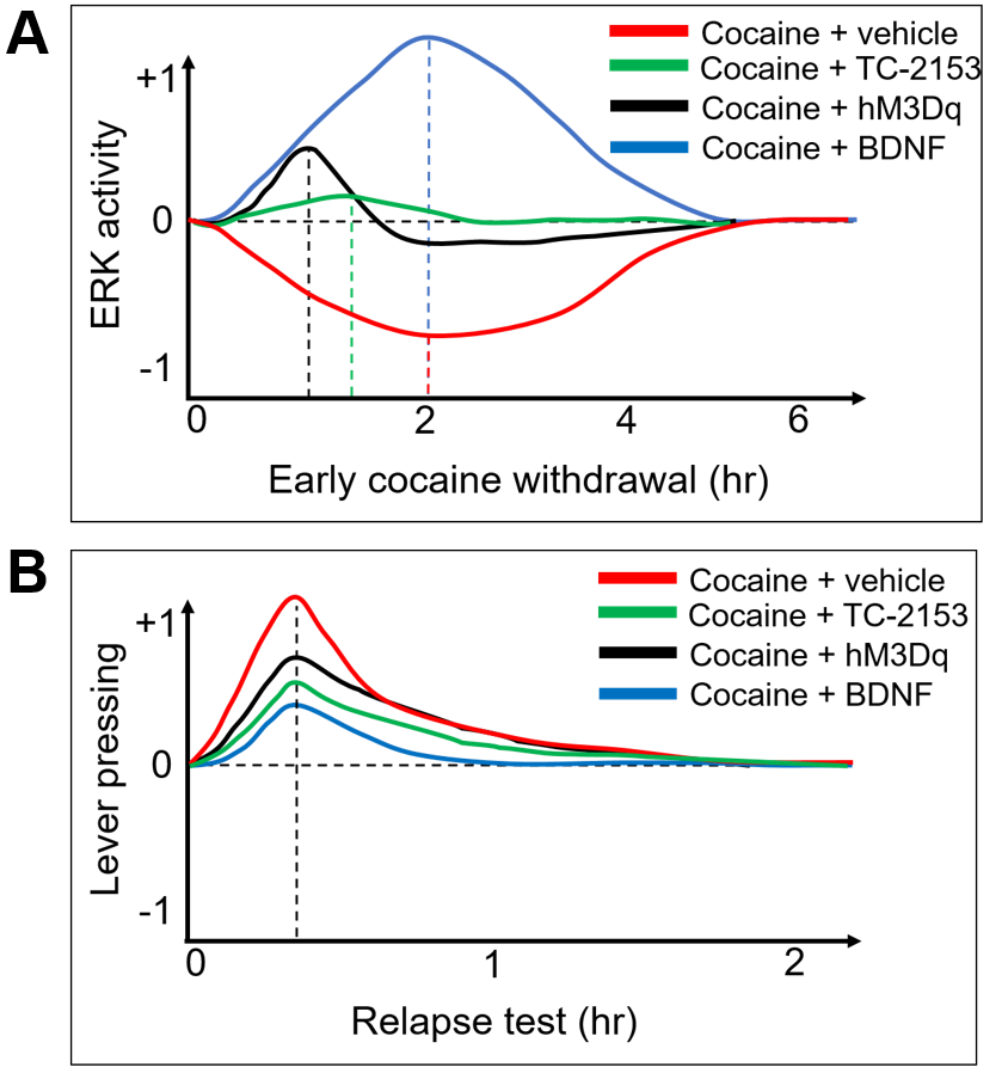

Figure 3.8. Comparison between hM3Dq activation, STEP inhibition, and BDNF on ERK activation during early withdrawal and subsequent lever pressing during relapse testing. **A.** Schematic illustrating the hypothesized temporal difference in modulation of the cocaine-induced ERK dephosphorylation in the PrL cortex during early withdrawal between BDNF, TC-2153, and hM3Dq activation. The horizontal dotted line indicates baseline ERK activity, whereas the vertical dotted lines indicates timepoint of maximal or minimal ERK activity. **B.** Schematic illustrating the hypothesized behavioral consequences of BDNF, TC-2153, and hM3Dq during early withdrawal on relapse testing after abstinence or extinction.

Chapter 4: Biphasic effect of abstinence duration following cocaine SA on corticostriatal structural plasticity and AMPA receptor expression in dendritic spines

Introduction

In contrast to depressed glutamatergic neurotransmission in the PrL cortex during early withdrawal, after one week of abstinence from cocaine SA, hyper-phosphorylation of the PKA targets, CREB^{S133} and GluA1^{S845}, in the PrL cortex and synapsin-1^{S9} in the NAc core emerge (Sun et al., 2014b; Sun et al., 2014a). Inhibition of PKA with intra-PrL Rp-cAMPs normalizes these hyper-phosphorylation events and prevents context-induced relapse to cocaine seeking under extinction conditions (Sun et al., 2014b). GluA1^{S845} phosphorylation by PKA enhances glutamate currents by promoting membrane insertion of AMPA receptors (Banke et al., 2000). Further, learning promotes incorporation of GluA1-containing AMPA receptors in large, mushroom-type dendritic spines (Matsuo et al., 2008). In addition, mushroom-type spines, relative to smaller, less stable spines, show an augmented AMPA receptor-mediated excitatory current in response to glutamate uncaging (Matsuzaki et al., 2001). Thus, cocaine-induced adaptations in glutamate transmission are likely associated with altered dendritic spine morphology and AMPA receptor expression. However, it is unknown how the signaling events occurring in the PrL cortex during these stages of early withdrawal and abstinence translate into alterations in spine morphology and/or density, changes that have been linked to relapse propensity (Russo et al., 2010; Gipson et al., 2013).

Although cocaine-induced alterations in structural plasticity within the NAc core are well-documented (Gipson et al., 2013; Stefanik et al., 2016), conflicting reports have appeared about modifications in structural plasticity in PrL pyramidal neurons after the end of cocaine SA. The earliest report, based on Golgi staining, indicated that cocaine SA followed by one month of abstinence increased layer V apical spine density (Robinson et al., 2001). More recently, it was reported (also with Golgi staining) that synaptic density was significantly reduced, but the density of thin dendritic spines was significantly increased, on layer V pyramidal neurons in the PrL cortex after one week of abstinence (Rasakham et al., 2014). In contrast, using intracellular dye filling, cocaine SA followed by two weeks of abstinence reduced layer II/III distal apical spine density, but remaining spines showed augmented volume (Radley et al., 2015). Thus, changes in structural plasticity in the PrL cortex after cocaine SA may depend on the type of pyramidal neurons analyzed, the duration of cocaine abstinence, and the technological strategy used to reveal dendritic spine morphology.

Various techniques have been used to visualize dendritic spine morphology including Golgi-Cox staining, lipophilic dye (i.e. DiI) labeling, intracellular dye filling (i.e. lucifer yellow iontophoresis), or transgenic animals expressing YFP driven by cell-type specific promoters (i.e. *thy1* promoter-driven YFP transgenic mice). Although Golgi staining provides sparse and complete labeling of deep-layer pyramidal neuron dendritic arbors, it severely underestimates the density of thin spines (Shen et al., 2008). In contrast, lipophilic dyes such as DiI provide sparse and intense labeling of pyramidal neuronal somas but minimize visualization of the

long apical dendrites of deep-layer pyramidal neurons (Trantham-Davidson et al., 2017). Moreover, intracellular dye filling with fluorescent dyes such as Lucifer Yellow allows for investigator-controlled labeling of neurons, but inconsistently labels apical dendritic arbors of deep-layer pyramidal neurons in the PFC (Radley et al., 2015). Finally, *thy1*-YFP transgenic mice have been used extensively for dendritic spine morphometric analyses (Keifer et al., 2015; Swanson et al., 2017). However, their utility is generally restricted to experiments involving mice because only one study has described the use of *thy1*-YFP rats (Magill et al., 2010).

A recent experiment found that intersectional viral approaches using a cell type-specific promoter expressing Cre recombinase in D1 receptor-expressing MSNs in the striatum in conjunction with Cre-dependent fluorescent reporters can be used to label dendritic spines (Dos Santos et al., 2017). In parallel, we recently found that an intersectional viral approach can be used to fully label the dendritic trees of deep-layer pyramidal neurons in the PrL cortex with pathway specificity. Moreover, this approach can be combined with immunohistochemical detection of various proteins of interest in different dendritic subcompartments, allowing for a high-throughput analysis of dendritic spine morphology and associated protein expression in spines of PrL cortical neurons projecting to the NAc core. In the current experiment, we focused our attention specifically on the distal apical tuft of layer V neurons in part because chronic stress produces a selective reduction in distal apical tuft dendrite length as well as spine density in layer V PrL cortical neurons (Liu and Aghajanian, 2008). Additionally, recent evidence indicates a

relationship between abstinence from cocaine SA, stress, and prefrontal pyramidal neuron apical tuft regressive structural plasticity (Radley et al., 2015).

Because PrL cortical glutamatergic transmission switches from a putatively hypoactive to a hyperactive state as a function of abstinence duration from cocaine (Sepulveda-Orengo et al., 2017; Dennis et al., 2018), we hypothesized that activity markers and dendritic spine morphometric features would follow a similar trajectory in PrL-NAc neurons because this pathway is highly implicated in pathological adaptations that promote cocaine seeking (Kalivas et al., 2005). Here we show that cocaine SA causes a biphasic alteration in nuclear markers of neuronal activity (Fos, p-CREB), structural plasticity, as well as AMPA receptor immunoreactivity in dendritic spines of PrL-NAc core neurons after two hours of withdrawal or one week of abstinence, changes which are likely important for subsequent relapse to cocaine seeking.

Materials and Methods

Animal subjects

Thirty-two adult male Sprague Dawley rats were used in this study (Charles Rivers Laboratories; Wilmington, MA). Rats were acclimated to the vivarium and catheter surgery was performed identical to methods in Chapters 2 and 3. Following catheterization, rats were secured in a stereotaxic apparatus (Kopf Instruments, Tujunga, CA) for intra-cranial virus microinjections.

Viral constructs and stereotaxic surgery

All viral procedures and constructs used in this study were approved by the Medical University of South Carolina Institutional Biosafety Committee. All rats

received a single microinjection (0.75 µl/hemisphere) of a canine adeno virus type 2 expressing a Cre-eGFP (CAV2-Cre-eGFP) fusion protein under the control of a CMV promoter ($3.6x10^{12}$ vg/ml) (gift of E. Kremer, Montpellier Molecular Genetic Institute Vector Core, Montpellier, FR) within the NAc core (coordinates: +1.6 mm AP from bregma, +/- 2.8 mm ML from bregma, -7.1 mm DV from skull, 10^{o} angle). Rats were then microinjected within the PrL cortex (coordinates: +2.8 mm AP from bregma, +/- 0.6 mm from bregma, -3.8 DV from skull) with an AAV5-hSyn-DIO-mCherry (~$1.5X10^{12}$ vg/ml) obtained from Addgene (Cambridge, MA). Injections were performed over a period of 5 minutes (0.15 µl/minute) using a Nanoject II (Drummond scientific, Broomall, PA) and injectors were left in place for 10 minutes to facilitate diffusion away from the injection site, then slowly retracted. Following surgery, bore holes were sealed with dental acrylic, and the incision was sutured closed. Rats were allowed at least 5 days of recovery, during which food and water were available ad libitum prior to beginning behavioral training.

Self-administration

SA procedures, including use of yoked saline controls, were conducted in an identical manner to those in Chapter 2.

Abstinence and perfusions

In Experiment 1, rats were returned to their homecage for two hours after the final cocaine SA session, heavily anesthetized with equithesin (~0.5 ml, i.v.), and transcardially perfused with 150 ml of ice-cold 0.1M phosphate buffer (PB) at 60 ml/minute followed by 200 ml of ice-cold 4% paraformaldehyde (PFA, pH 7.4) in 0.1M PB. Brains were rapidly removed and immersed in the same fixative for 1

hour, then transferred to a 20% sucrose solution prior to sectioning. In Experiment 2, rats were perfused one week after the final cocaine SA session following forced homecage abstinence where food and water were provided ad libitum, and brains were post-fixed for 24 hours. To match virus expression duration between experiments, rats in Experiment 1 were given an extra week of recovery after surgery prior to beginning SA.

Immunohistochemistry

Coronal sections (AP +2.52-4.2 mm from bregma) were sliced at 80 µm using a Leica cryostat and collected in 0.1M PBS containing 0.01% sodium azide. Sections were stored at 4ºC until immunohistochemical processing. Immunohistochemistry was performed according to previously published protocols (Scofield et al., 2016b). Briefly, sections were blocked with 0.1M phosphate-buffered saline containing 2% Triton X-100 (PBST) and 2% normal goat serum (NGS) for two hours at RT protected from light. Sections were then incubated in chicken anti-mCherry (1:2000; LS Biosciences #LS-C204825, Seattle, WA RRID:AB_2716246), mouse anti-GluR2 (2.13 ug/ml; Millipore #MAB397, Billerica, MA RRID:AB_2113875), rabbit anti-GluA1 (1:500; Cell Signaling Technology #13185, Danvers, MA), rabbit anti-cFos (1:1000, Santa Cruz Biotechnology #sc-52, Dallas, TX RRID:AB_2106783), or mouse anti-p-CREB (1:200, Cell Signaling Technology, #9196, Danvers, MA RRID:AB_331275) at 4ºC overnight. Sections were washed 3 X 10 minutes in PBST, and then incubated with species-appropriate Alexa Fluor®594 (mCherry), Alexa Fluor®488 (Fos, p-CREB), or Alexa Fluor®647 (GluA1, GluA2)-conjugated secondary antisera (1:1000, Abcam, Cambridge, UK) diluted

in 2% PBST with 2% NGS for 5 hours at room temperature (RT) protected from light. Sections were washed 3 X 10 minutes and then mounted on superfrost plus slides using ProLong® gold Antifade (Thermo Fisher Scientific; Waltham, MA). Slides were stored at 4ºC until imaging.

Confocal microscopy

Fos/p-CREB quantitation. Confocal Z-stack (50 µm) images were captured with a Leica SP8 confocal microscope. Fos or p-CREB immunoreactivity (IR) was excited using an Optically Pumped Semiconductor Laser (OPSL) 488 nm line using a 20X air objective. mCherry IR was excited using an OPSL 552 nm laser line. Z-stacks were then imported to Imaris. The spot tool in Imaris was used and detection threshold and spot size were empirically determined and maintained constant for each measurement. The number of p-CREB-IR or Fos-IR cells was counted automatically for each hemisphere and averaged across 1 section per rat. The spots colocalization extension in Imaris was used to determine coregistry between $mCherry^+$ and $Fos/p\text{-}CREB^+$ somas. The number of mCherry-IR neurons that were p-CREB or Fos-IR was normalized to the number of total mCherry-IR neurons.

Dendritic Spine Imaging. Confocal Z-series data sets were acquired using a Leica SP8 laser-scanning confocal microscope. Dendrites selected for imaging had the following characteristics: the apical dendritic segment was 1) visually connected to the cell body of origin, 2) after the third branch point, 3) >15 µm below the surface of the tissue, and 4) located within 10 µm of the end of the dendrite (i.e. approaching the pial surface). Overall imaging parameters including laser

power, gain, pinhole, and optical section thickness were set empirically prior to imaging and were held constant for the remainder of the experiment. mCherry was excited using an OPSL 552 nm laser line, and GluA1/2 were excited using a Diode 638 nm laser line. Emitted photons were collected using high-sensitivity hybrid detectors (HyD). Images were acquired with a 1024x512 frame size, 3.5X digital zoom, and 0.1 um step size generating a voxel size of 52nm X 52nm X 100nm. Images were acquired using sub-airy unit pinhole sizes. These parameters were selected to obtain optimal deconvolution as recommended by Huygens essential deconvolution software (Hilversum, NL). The resulting set of parameters allows for a minimum resolution of 150nm XY by 300nm Z in our reconstructions. Four to twelve dendritic spine segments were analyzed per animal, each with an accompanying GluA1 or GluA2 channel collected.

Imaris 3D reconstruction, morphological analyses, and colocalization

Following deconvolution, Z-stacks were imported into BitPlane Imaris (version 9.0) for morphological analyses. Z-stacks were cropped in 3D to isolate individual dendrites, and a 3D space-filling model was generated to isolate voxels corresponding to the mCherry-positive dendrite of interest. The filament module was used to semi-manually trace identified dendritic spines as described previously (Trantham-Davidson et al., 2017). Dendritic spine head diameter was calculated using an automated threshold set by Imaris. To calculate dendritic spine density, the number of spines was normalized to the length of the dendrite (in µm). Segments were typically 40-50 µm in length.

The “create channel” filament extension was used to generate a channel defined by the filament built by Imaris, which was used for colocalization analyses. To isolate GluA1/2-IR corresponding to dendritic spine heads relative to total dendrite, the “filament analysis” extension was used to mask all GluA1/2-IR not corresponding to Imaris-defined dendritic spine heads and shafts. Filament analysis uses the predefined boundaries of the spine heads relative to the dendritic shaft to isolate specific channels of interest in dendritic subcompartments.

For colocalization analyses, a region of interest (ROI) containing only the mCherry dendrite was used. The colocalization module of Imaris was used to perform standard intensity-based colocalization analyses between total mCherry signal and total GluA1/2 signal (dendrite shaft and spine heads). The intensity value at which a voxel could be considered coregistered was set empirically by a blinded investigator for both channels as described previously (Scofield et al., 2016b). We recorded the percent of signal above threshold to determine whether differences in the intensity of signal impacted coregistry analyses for GluA1, GluA2, and mCherry. Percent colocalization was calculated by normalizing the total volume of GluA1/2-mCherry coregistry to the total volume of mCherry. The total colocalization channel was then separated into Imaris-defined spine heads and dendritic shaft using the “filament analysis” extension, and a 3D space-filling model was generated corresponding to colocalized voxels for a) spine head-specific colocalization and b) dendritic shaft-specific colocalization. Electron microscopy studies indicate that a significant amount of GluA2 expression is present in both dendritic shafts and spine heads (Vissavajjhala et al., 1996) and *in*

vitro experiments indicate similar patterns for GluA1 (Szepesi et al., 2014). Thus, percent colocalization was determined for total GluA1/2, spine head-specific GluA1/2, and dendritic shaft-specific GluA1/2 by normalizing the volume of colocalized voxels in each compartment to the volume of the mCherry dendrite. To determine specific spine head bins that may account for overall alterations in spine head diameter, the number of spines within each bin was normalized to the total number of spines and compared between groups. To determine spine head bins that show more/less GluA1/2 coregistry in spine heads, the volume of coregistry was manually counted in each spine, then averaged for each bin for each segment, then across segments for each animal. All analyses were performed by an individual blinded to experimental treatment groups.

Statistical analyses

Behavioral data were analyzed with a two-way repeated measures (RM) ANOVA with treatment (cocaine versus saline) as a between-subjects factor and SA session as a within-subjects factor followed by Bonferroni-corrected pairwise comparison's when a significant interaction was observed. A two-tailed t-test with or without Welch's correction was used when two groups were compared for a single dependent variable. Binned dendritic spine head and GluA1/2 colocalization volume data were analyzed with a two-way RM ANOVA with treatment (cocaine versus saline) as a between-subjects factor and bin as a within-subjects factor followed by a Bonferroni-corrected pairwise comparison test when a significant interaction was observed, as previously performed (Ball et al., 2009). Each animal's dendritic spine or colocalization data points were derived from an average

across the analyzed segments. Cumulative frequency distribution data were analyzed to determine general shifts in spine head diameter for each group using a Kolmogorov-Smirnov non-parametric test. When correlating spine head diameter and density with p-CREB-IR, Pearson's correlation test was used. Statistical outliers were detected with Grubbs' test and were excluded from all analyses as discussed in the results. Data are expressed as the mean +/- SEM, and significance was determined at $p<0.05$.

Results

Experimental design and cocaine SA

The timeline for Experiments 1 and 2 are shown in Figure 4.1A. Representative CAV2-Cre-eGFP expression in the NAc core and an mCherry-expressing PrL-NAc core neuron are shown in Figure 4.1B and C, respectively. Figure 4.1D shows a representative PrL-NAc core neuron immunohistochemically processed for GluA2. Figure 4.1E shows cocaine SA data. A two-way RM ANOVA revealed a significant treatment (cocaine versus saline) by session interaction for active lever presses ($F_{(11,264)}=2.01$, $p<0.05$) as well as a significant main effect of treatment ($F_{(1,24)}=38.88$, $p<0.0001$), but not time ($F_{(11,264)}=1.69$, $p>0.05$). Bonferroni-corrected pairwise comparisons indicated a significant difference between cocaine and saline on SA sessions 4-12 (all $p<0.05$). There was no significant treatment by SA session interaction for inactive lever presses ($F_{(11,264)}=1.19$, $p>0.05$), nor was there a significant main effect of time ($F_{(11,264)}=0.60$, $p>0.05$). However, there was a significant main effect of treatment ($F_{(1,24)}=4.31$, $p<0.05$). Thus, yoked saline controls pressed the inactive lever more than cocaine SA rats. Additionally,

cocaine SA rats showed lever discrimination, as evidenced by a significant main effect of lever (active versus inactive) ($F_{(1,24)}$=60.38, p<0.0001).

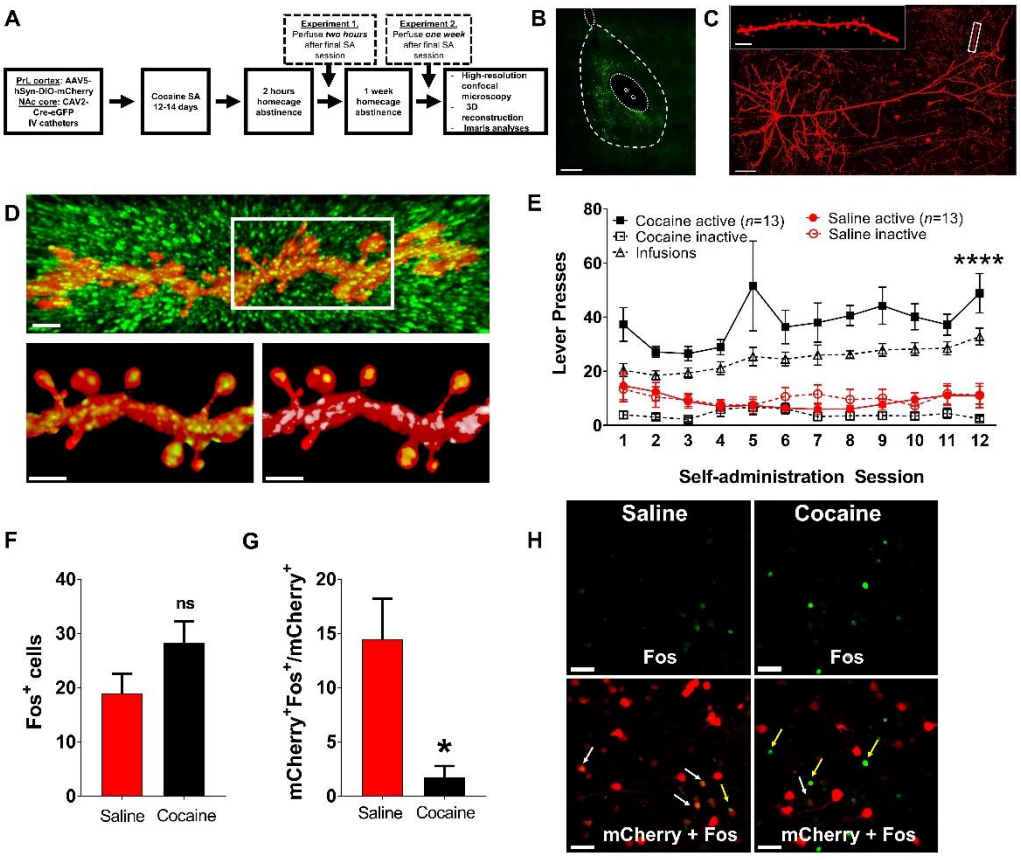

Figure 4.1. Experimental timeline, virus expression, and cocaine-induced alterations in Fos-IR in PrL-NAc core neurons during early withdrawal **A.** Timeline for Experiments 1 and 2. **B.** Representative CAV2-Cre-eGFP virus expression in the NAc core. Dotted lines indicate lateral ventricle (top), anterior commissure (ac, center) and border of NAc core and shell. **C.** Representative mCherry-labeled PrL-NAc core layer V neuron. Inset corresponds to a representative dendritic spine segment taken from the distal apical tuft. **D.** Representative mCherry-labeled spine segment from distal apical tuft of a layer V PrL-NAc core neuron displaying GluA2-IR (top). Bottom left – GluA2 IR corresponding only to mCherry signal within the dendrite. Bottom right – GluA2-mCherry coregistered voxels in dendritic spine heads (yellow) and dendritic shaft (white). **E.** SA data over the last 12 days of SA. Sold lines and closed symbols indicate active lever presses and dotted lines with open signals indicates inactive lever presses. **F-G.** Fos^+ cells in layer V of the PrL cortex **(F)** and $mCherry^+Fos^+$ normalized to total $mCherry^+$ cells **(G)**. **H.** Top - representative images of Fos^+ neurons in saline and cocaine SA rats. Bottom - Representative Fos^+ $mCherry^+$ and Fos^+ $mCherry^-$ neurons in saline and cocaine

SA rats. White arrows indicate Fos^+ $mCherry^+$ neurons, yellow arrows indicate Fos^+ $mCherry^-$ neurons. Scale bars = 200 μm (B), 50 μm (C), 5 μm (Inset, C), 2 μm (D), 40 μm (H). ****p<0.0001 comparing cocaine to saline active lever presses. SA: self-administration. d_H: spine head diameter.

Effect of cocaine SA on PrL-NAc core structural plasticity, Fos-IR, p-CREB-IR, and GluA1/2-IR during early withdrawal.

In Experiment 1, rats (N=16) underwent 12-14 days of cocaine SA or received yoked-saline infusions and were then transcardially perfused two hours after the final SA session. One yoked-saline rat was excluded due to a missed NAc core placement. Two cocaine SA animals were excluded due to failed catheters. The final sample sizes were n=6 for cocaine and n=7 for yoked saline. First, we examined Fos-IR in layer V PrL cortex in a subset of yoked-saline and cocaine SA rats (n=4 per group). One section at approximately the same coronal plane was analyzed per rat. A two-tailed t-test indicated a non-significant effect of cocaine SA on Fos-IR in layer V PrL neurons ($t_{(6)}$=1.70, p>0.05, Fig. 4.1F). When limiting analysis to $mCherry^+$ neurons, a two-tailed t-test revealed a significant reduction in the percent of $mCherry^+$ neurons expressing Fos ($t_{(6)}$=3.31, p<0.05, Fig. 4.1G). Representative images of Fos^+ $mCherry^-$ and Fos^+ $mCherry^+$ neurons for saline and cocaine SA rats are shown in Figure 4.1H.

Next, a subset of animals was used to analyze p-CREB-IR in the PrL cortex (n=5 per group due to limited number of sections available). One section, at approximately the same coronal plane, was analyzed per rat. A two-tailed t-test indicated a non-significant effect of cocaine SA on p-CREB-IR in layer V PrL neurons ($t_{(8)}$=1.16, p>0.05, Fig. 4.2A). However, when limiting analysis only to $mCherry^+$ PrL-NAc core neurons, a Welch's-corrected two-tailed t-test showed a

significant decrease in the percentage of mCherry^{+} neurons displaying p-CREB-IR ($t_{(4.7)}$=2.94, p<0.05, Fig. 4.2B). There was no difference between groups in the average p-CREB signal intensity in all cells that were p-CREB^{+} ($t_{(8)}$=0.87, p>0.05, Fig. 4.2C) or mCherry^{+}p-CREB^{+} neurons ($t_{(8)}$=0.96, p>0.05, Fig. 4.2D). Representative images of mCherry^{-} p-CREB^{+} and mCherry^{+}p-CREB^{+} neurons from yoked-saline and cocaine SA rats are shown in Figure 4.2E.

We next asked whether the alteration in PrL-NAc core activity markers during early withdrawal was associated with altered dendritic spine morphometry and AMPA receptor expression. Adjacent sections from the same rats were immunostained for mCherry and GluA1 or mCherry and GluA2 in two separate runs. Dendritic spine morphometric data from distal tufts of layer V dendrites were pooled from both runs. In a minority of instances when sections from individual animals showed mCherry neurons labeled for GluA1, but not GluA2, and vice versa, due to technical issues, the spine morphometry data for that animal consisted of the run in which mCherry neurons were labeled, but the colocalization data for that animal for the selected protein was not included. A two-tailed t-test indicated that there was a significantly lower spine head diameter average ($t_{(11)}$=3.19, p<0.01, Fig. 4.2F) in cocaine SA rats than in yoked-saline rats but there was no difference in spine density between groups ($t_{(10)}$=1.83, p>0.05, Fig. 4.2G). There was no difference between cocaine and saline groups in the average spine head center intensity ($t_{(11)}$=0.53, p>0.05, Fig. 4.2H), indicating that the mCherry intensity in dendritic spine heads did not contribute to the observed effects. Additional binned analyses revealed that cocaine SA altered the percent of total

spines as a function of spine head diameter (in 0.1 µm bins) as evidenced by a significant two-way RM ANOVA treatment by spine head diameter bin interaction ($F_{(5,55)}$=6.59, p<0.0001). Bonferroni-corrected pairwise comparisons indicated a significant increase in the percent of total spines with head diameters between 0.3-0.4 µm (p<0.01) and a significant decrease in the percent of total spines with head diameters between 0.6-0.7 µm (p<0.05) and above 0.7 µm (p<0.01, Fig. 4.2I) in cocaine SA rats. These changes were associated with a general leftward shift in spine head diameter after all spines in saline (*n*=1651) and cocaine SA (*n*=2159) rats were analyzed as shown by a non-parametric Kolmogorov-Smirnov test (K-S p<0.0001, Fig. 4.2J). Representative dendrites from yoked-saline and cocaine SA rats are shown in Figure 4.2K. Interestingly, there was a positive correlation between spine head diameter and p-CREB-IR (r^2=0.64, p<0.01, Fig. 4.2L) whereas there was a negative correlation between spine density and p-CREB-IR (r^2=0.44, p<0.05, Fig. 4.2M).

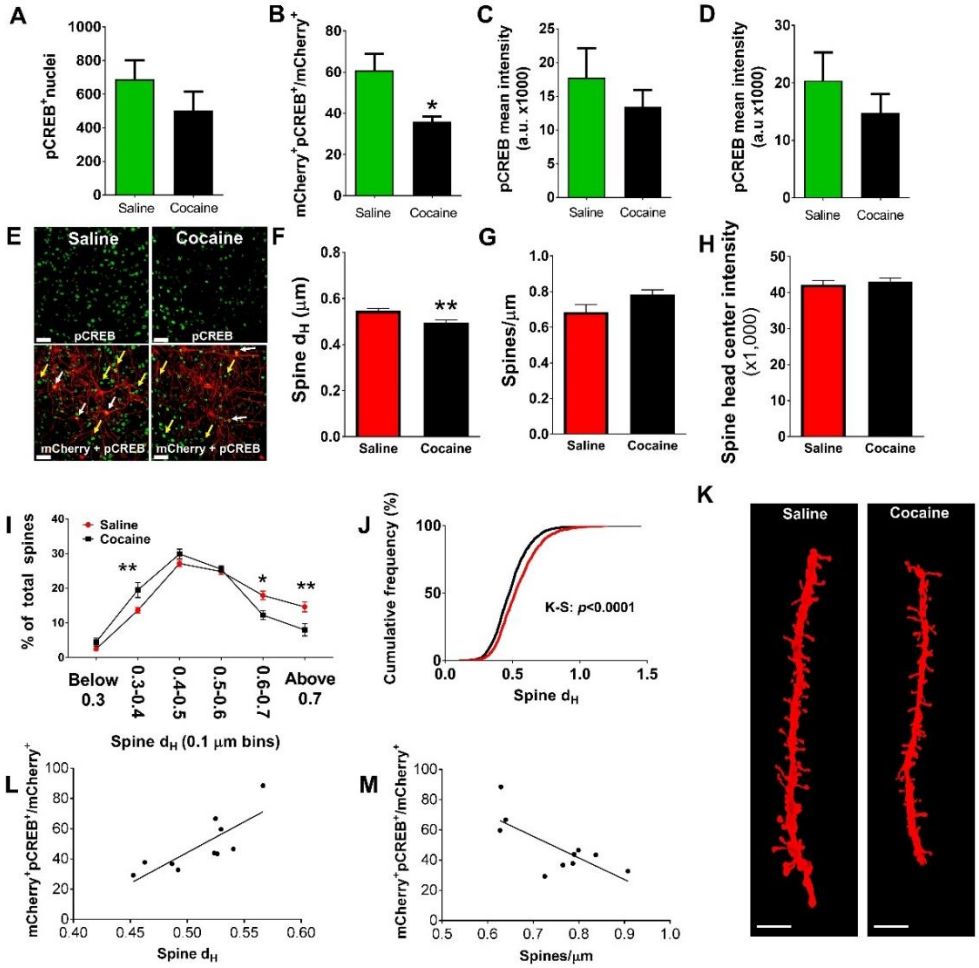

Figure 4.2. Cocaine SA decreased PrL-NAc core p-CREB-IR and dendritic spine head diameter during early withdrawal. **A-B.** p-CREB$^+$ cells in layer V of the PrL cortex **(A)** and mCherry$^+$ p-CREB$^+$ normalized to total mCherry$^+$ cells **(B)**. **C-D.** There was no difference between groups in p-CREB signal intensity in all p-CREB+ neurons **(C)** or mCherry$^+$ p-CREB$^+$ neurons **(D)**. **E.** Top-representative images of p-CREB$^+$ neurons in yoked-saline and cocaine SA rats. Bottom-representative mCherry$^+$ p-CREB$^+$ and mCherry$^+$ p-CREB$^-$ neurons in yoked-saline and cocaine SA rats. White arrows indicate mCherry$^+$p-CREB$^+$ neurons, yellow arrows indicate mCherry$^+$ p-CREB$^-$ neurons. **F.** Cocaine SA decreased spine head diameter compared to yoked-saline controls. **G.** There was no difference in spine density between groups. **H.** The average mCherry signal intensity in the center of the spine head was not different between groups. **I-J.** Cocaine SA rats show a general leftward shift in percent of total spines as a function of spine head diameter **(I)** and cumulative frequency **(J)**. **K.** Representative dendrites from saline and cocaine SA rats. **L-M.** The percentage of mCherry$^+$ neurons that are also p-CREB$^+$ positively correlated with dendritic spine head diameter **(L)**, but negatively correlated with dendritic spine density **(M)**. *p<0.05, **p<0.01 compared to saline. Scale bars = 40 μm (E), 5μm (K).

Next, a subset of the sections was immunostained for mCherry and GluA1, as described above. One saline rat showed no neurons labeled for mCherry in this run and was not included in the analysis. Final sample sizes were n=6 for both groups. Interestingly, analyses revealed a significant reduction in total GluA1-IR in PrL-NAc core dendrites ($t_{(10)}$=2.39, $p<0.05$, Fig. 4.3A). This was accounted for by a decrease in shaft-specific GluA1-IR ($t_{(10)}$=2.45, $p<0.05$, Fig. 4.3B) as well as a decrease in spine head-specific GluA1-IR ($t_{(10)}$=2.30, $p<0.05$, Fig. 4.3C). When analyzing GluA1 volume in spine heads as a function of dendritic spine head diameter, a two-way RM ANOVA revealed a significant treatment by spine head diameter bin interaction ($F_{(5,50)}$=4.18, $p<0.01$). Bonferroni-corrected pairwise comparisons indicated that cocaine SA rats showed a specific decrease in GluA1-IR in spine heads larger than 0.7 μm ($p<0.0001$, Fig. 4.3D). Importantly, these effects are likely not due to differences in empirical thresholds set for GluA1 because the percent of signal above threshold was not different between cocaine and saline groups ($t_{(10)}$=1.10, $p>0.05$, Fig. 4.3E). The percent of mCherry signal above threshold was also not different between groups ($t_{(10)}$=0.73, $p>0.05$, Fig. 4.3F). Furthermore, reduced overall GluA1-IR was not accounted for by reduced average signal intensity of GluA1 in the $mCherry^{+}$ dendrites ($t_{(10)}$=0.29, $p>0.05$, Fig. 4.3G). Representative spine segments are shown in Figure 4.3H.

Next, sections from all animals were immunostained for GluA2. One yoked-saline rat was excluded from analysis due to immunohistochemical detection issues leading to profound saturation in each image. Thus, final sample sizes were n=6 per group. Unlike GluA1, total GluA2-IR was not altered by cocaine ($t_{(10)}$=0.51,

p>0.05, Fig. 4.3I). Moreover, there was no effect of cocaine on shaft-specific GluA2-IR ($t_{(10)}$=0.22, p>0.05, Fig. 4.3J) but there was a trend towards reduced spine head-specific GluA2-IR ($t_{(10)}$=1.74, p=0.11, Fig. 4.3K). However, like GluA1, there was a treatment by spine head diameter bin interaction on GluA2-IR volume as a function of spine head diameter ($F_{(5,50)}$=4.89, p<0.01). A Bonferroni-corrected pairwise comparison test indicated a specific reduction in GluA2-IR in spines larger than 0.7 µm (p<0.0001, Fig. 4.3L) in the cocaine group. These effects are likely not due to differences in the empirical thresholds set for GluA2 because the percent of signal above threshold was not different between groups (GluA2: $t_{(10)}$=0.67, p>0.05, Fig. 4.3M; mCherry: $t_{(10)}$=2.04, p>0.05, Fig. 4.3N). Moreover, there was no difference between groups in the average GluA2-IR intensity in mCherry^{+} dendrites ($t_{(10)}$=0.30, p>0.05, Fig. 4.3O). Representative spine segments are shown in Figure 4.3P.

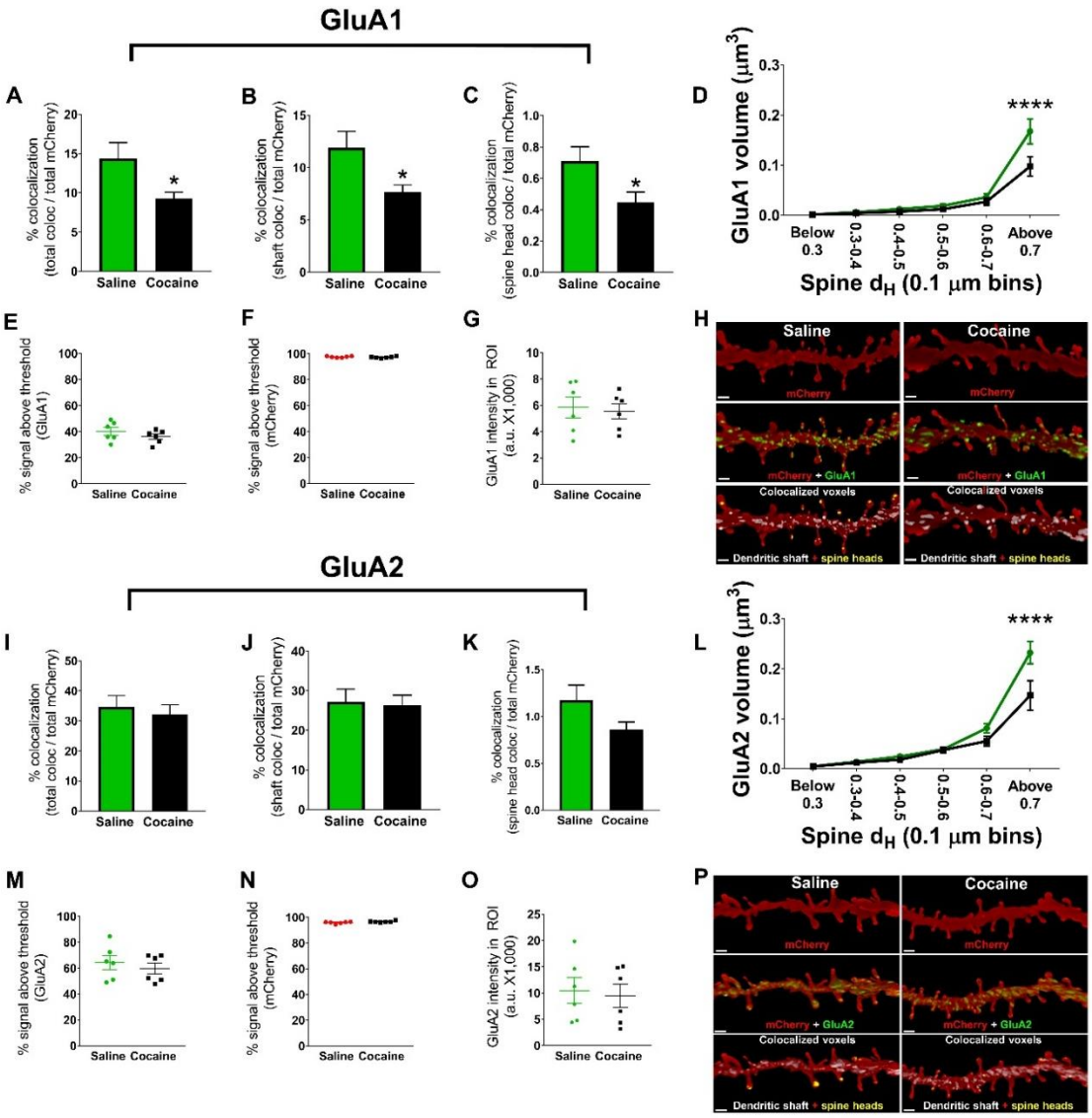

Figure 4.3. Cocaine SA reduced GluA1/2-IR in enlarged mushroom spines of PrL-NAc core neurons during early withdrawal. **A.** Total GluA1-IR was decreased in PrL-NAc core dendrites. **B-C.** The decreased total GluA1-IR was accounted for by **(B)** decreased GluA1 in the dendritic shaft and **(C)** decreased GluA1 in dendritic spine heads. **D.** The decreased GluA1-IR in spine heads was specific to spines with head diameters larger than 0.7 μm. **E-F.** The signal above threshold for GluA1 **(E)** and mCherry **(F)** was not different between groups. **G.** The average GluA1 signal intensity in mCherry$^+$ dendrites was not different between groups. **H.** Representative dendrites from saline (left) and cocaine (right) showing mCherry (top), mCherry + GluA1 (middle), and shaft-specific versus spine head-specific IR (bottom). **I.** There was no difference between cocaine and saline in total GluA2-IR. **J-K.** There was no difference between cocaine and saline in shaft-specific GluA2-IR **(J)**, but a strong trend towards decreased spine head-specific GluA2-IR **(K)**. **L.** Cocaine SA rats showed decreased GluA2-IR only in spines greater than 0.7 μm. **M-N**. The signal above threshold for GluA2 **(M)** and mCherry **(N)** was not different between groups. **O.** The average GluA2 signal intensity in the mCherry$^+$ dendrites

was not different between groups. **P.** Representative dendrites showing decreased spine head-specific GluA2 (bottom) in cocaine (right) relative to saline controls (left). Scale bars = 2 μm. *p<0.05, **p<0.01, ****p<0.0001 compared to saline.

Effect of cocaine SA on PrL-NAc core activity markers, structural plasticity, and GluA1/2-IR after one week of abstinence

In Experiment 2, rats (N=16) underwent 12-14 days of cocaine SA or received yoked-saline infusions. One yoked-saline rat never finished SA due to stress reactions when handled. One yoked-saline rat was removed from analyses because of insufficient virus expression and one cocaine SA rat was removed as a statistical outlier in colocalization analyses. Final sample sizes were n=6 for saline and n=7 for cocaine.

A subset of animals was used to analyze p-CREB-IR in the PrL cortex (n=3 per group). One section, at approximately the same coronal plane, was analyzed per rat. A two-tailed t-test indicated a non-significant effect of cocaine SA on p-CREB-IR, although there was a trend towards elevated p-CREB-IR in cocaine SA rats ($t_{(4)}$=2.04, p=0.11, Fig. 4.4A). However, when limiting analysis only to mCherry$^+$ PrL-NAc core neurons, a two-tailed t-test showed a significant increase in the percentage of mCherry$^+$ neurons displaying p-CREB-IR ($t_{(4)}$=3.41, p<0.05, Fig. 4.4B). There was no difference between groups in the average p-CREB signal intensity in all cells that were p-CREB$^+$ (t(4)=1.02, p>0.05, Fig. 4.4C) or in cells that were mCherry$^+$ p-CREB$^+$ (t(4)=1.18, p>0.05, Fig. 4.4D). Representative images of mCherry$^-$ p-CREB$^+$ and mCherry$^+$ p-CREB$^+$ neurons in yoked-saline and cocaine SA rats are shown in Figure 4.4E.

Next, we asked whether this increase in p-CREB-IR in PrL-NAc core neurons after one week of abstinence was associated with altered spine head

diameter of PrL-NAc core neurons. In contrast to early withdrawal, cocaine SA followed by one week of abstinence produced a profound increase in spine head diameter of PrL-NAc core distal apical tuft dendrites ($t_{(11)}$=7.44, p<0.0001, Fig. 4.4F), but an overall reduction in spine density, in cocaine SA compared to yoked-saline rats ($t_{(11)}$=4.32, p<0.01, Fig. 4.4G). Akin to Experiment 1, there was no difference in the average spine head center intensity between cocaine and saline groups ($t_{(11)}$=1.80, p>0.05, Fig. 4.4H), indicating that the mCherry intensity in dendritic spine heads did not contribute to the observed effects. These effects were associated with a significant treatment by spine head diameter bin interaction ($F_{(5,55)}$=18.86, p<0.0001). Bonferroni-corrected pairwise comparisons indicated that cocaine SA rats showed a reduction in the percent of total spines with head diameters between 0.3-0.4 µm (p<0.001), and 0.4-0.5 µm (p<0.01), but an increase in the percent of total spines with head diameter above 0.7 µm (p<0.0001, Fig. 4.4I). Moreover, these changes were associated with a general rightward shift in spine head diameter when analyzing all spines in yoked-saline (*n*=1907) and cocaine SA (*n*=1642) rats as shown by a Kolmogorov-Smirnov test (K-S p<0.0001, Fig. 4.4J). Representative dendrites from a yoked-saline and cocaine SA rat are shown to the right in Figure 4.4K. Like early withdrawal, we found that spine head diameter and p-CREB-IR showed a positive correlation (r^2=0.82, p<0.01, Fig.

4.4L), whereas spine density and p-CREB-IR showed a non-significant trend towards a negative correlation (r^2=0.58, p=0.07, Fig. 4.4M).

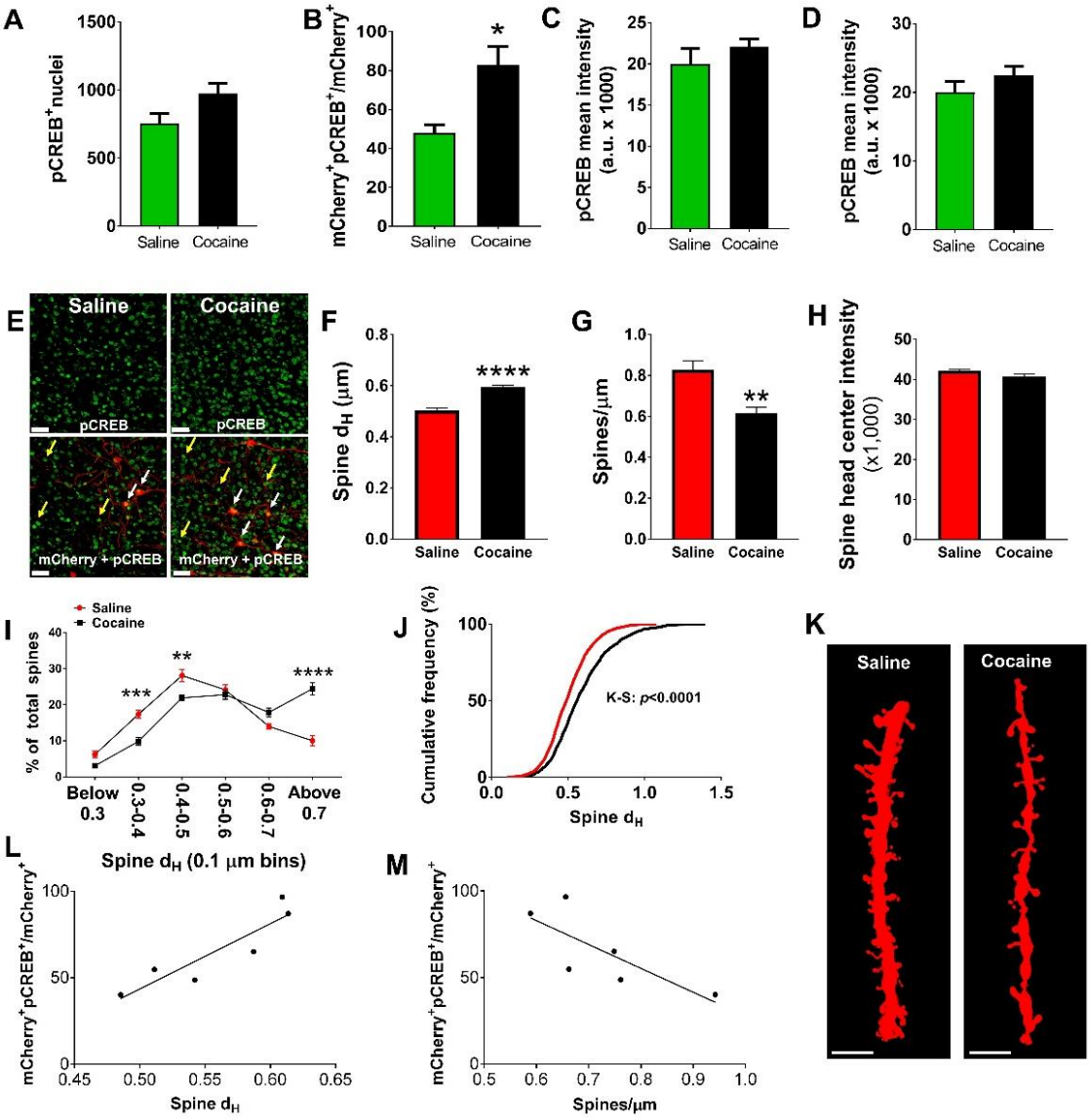

Figure 4.4. Cocaine SA increased PrL-NAc core p-CREB-IR and dendritic spine head diameter following one week of abstinence. **A-B.** p-CREB$^+$ cells in layer V of the PrL cortex **(A)** and mCherry$^+$ p-CREB$^+$ normalized to total mCherry$^+$ cells **(B)**. **C-D.** There was no difference between groups in p-CREB signal intensity in all p-CREB$^+$ neurons **(C)** or mCherry$^+$ p-CREB$^+$ neurons **(D)**. **E.** Top-representative images of p-CREB$^+$ neurons in yoked-saline and cocaine SA rats. Bottom-representative mCherry$^+$ p-CREB$^+$ and mCherry$^+$ p-CREB$^-$ neurons in yoked-saline and cocaine SA rats. White arrows indicate mCherry$^+$ p-CREB$^+$ neurons, yellow arrows indicate mCherry$^+$ p-CREB$^-$ neurons. **F-G.** Cocaine SA increased spine head diameter **(F)**, but decreased spine density **(G)** compared to yoked-saline controls. **H.** The average mCherry signal intensity in the center of the spine head

was not different between groups. **I-J.** Cocaine SA rats showed a general rightward shift in percent of total spines as a function of spine head diameter **(I)** and cumulative frequency **(J)**. **K.** Representative dendrites from saline and cocaine SA rats. **L-M.** The percentage of $mCherry^+$ neurons that are also $p\text{-}CREB^+$ positively correlated with dendritic spine head diameter **(L)** and showed a trend toward negatively correlating with dendritic spine density **(M)**. *p<0.05, **p<0.01, ***p<0.001, ****p<0.0001 compared to saline. Scale bars = 40 μm (E), 5μm (K).

To determine whether this hypertrophic structural alteration in spine head diameter and elevated p-CREB-IR were associated with altered GluA1-IR, we performed the same colocalization analyses as described above. However, sections from one cocaine animal did not show virus expression in the run processed for GluA1 but was included in GluA2 measurements (see below). Interestingly, the elevated spine head diameter was associated with an overall reduction in total GluA1 coregistry with mCherry in the cocaine group ($t_{(10)}$=2.79, p<0.05, Fig. 4.5A). This effect was associated with reduced dendritic shaft-specific GluA1-IR ($t_{(10)}$=3.55, p<0.01, Fig. 4.5B), but increased spine head-specific GluA1-IR ($t_{(10)}$=2.50, p<0.05, Fig. 4.5C). A two-way RM ANOVA revealed a significant treatment by spine head diameter bin interaction of GluA1 volume as a function of spine head diameter ($F_{(5,50)}$=11.87, p<0.0001). Bonferroni-corrected pairwise comparison tests indicated an increase in GluA1-IR in spines larger than 0.7 μm (p<0.0001, Fig. 4.5D) in cocaine SA rats. It is unlikely that differences in empirical thresholds set for GluA1 or mCherry accounted for these differences because the percent of signal above threshold was not different between cocaine and saline groups (GluA1: $t_{(10)}$=0.53, p>0.05, Fig. 4.5E; mCherry: $t_{(10)}$=1.13, p>0.05, Fig. 4.5F). There was also no difference in the average intensity of GluA1-IR in

mCherry^{+} dendrites between groups ($t_{(10)}$=1.54, p>0.05, Fig. 4.5G). Representative spine segments are shown in Figure 4.5H.

Next, sections were immunostained for GluA2 and mCherry and colocalization analyses were performed as described above. All 13 animals showed labeled neurons and thus sample sizes for this experiment were n=6 (saline) and n=7 (cocaine). Interestingly, in contrast to GluA1, total GluA2-IR was unaffected after one week of abstinence from cocaine SA ($t_{(11)}$=0.97, p>0.05, Fig. 4.5I). There was no difference between groups in dendritic shaft-specific GluA2-IR ($t_{(11)}$=0.08, p<0.05, Fig. 4.5J), but cocaine SA rats showed elevated spine head-specific GluA2-IR ($t_{(11)}$=3.47, p<0.01, Fig. 4.5K). A two-way RM ANOVA revealed a significant treatment by spine head diameter bin interaction ($F_{(5,55)}$=5.58, p<0.001). Bonferroni-corrected pairwise comparison tests indicated that the elevated spine head-specific GluA2-IR was specific to spines greater than 0.7 μm (p<0.0001, Fig. 4.5L). Consistent with our previous findings, these effects were not due to differences in thresholds for GluA2 or mCherry because the percent of signal above threshold was not different between groups (GluA2: $t_{(11)}$=0.63, p>0.05, Fig. 4.5M; mCherry: $t_{(11)}$=1.02, p>0.05, Fig. 4.5N). Moreover, the average GluA2 signal intensity in mCherry dendrites was not different between groups ($t_{(11)}$=0.59, p>0.05, Fig. 4.5O). Representative spine segments are shown in Figure 4.5P.

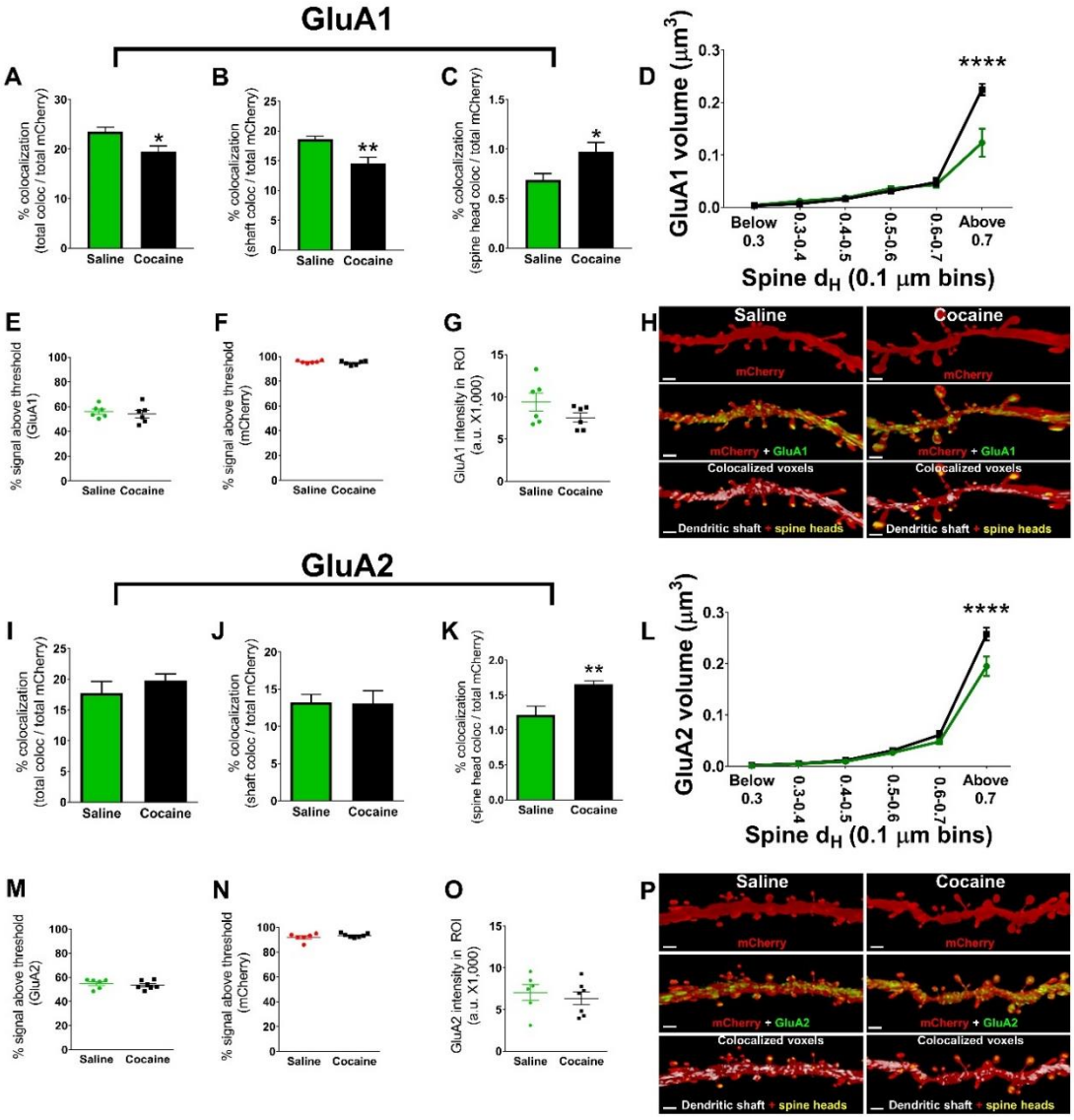

Figure 4.5. Cocaine SA increased GluA1/2-IR in enlarged mushroom spines of PrL-NAc core neurons after one week of abstinence. **A.** Total GluA1-IR was decreased in PrL-NAc core dendrites. **B-C.** This was accounted for by decreased GluA1 in dendritic shafts **(B)**, but increased GluA1 in dendritic spine heads **(C)**. **D.** The increased GluA1-IR in spine heads was specific to spines with head diameters larger than 0.7 μm. **E-F.** The signal above threshold for GluA1 **(E)** and mCherry **(F)** was not different between groups. **G.** The average GluA1 signal intensity in the mCherry-labeled dendrite was not different between groups. **H.** Representative dendrites from saline (left) and cocaine (right) showing mCherry (top), mCherry + GluA1 (middle), and shaft-specific versus spine head-specific IR (bottom). **I.** There was no difference between cocaine and saline in total GluA2 IR. **J-K.** There was no difference between cocaine and saline in shaft-specific GluA2-IR **(J)**, but a significant increase in spine head-specific GluA2-IR **(K)**. **L.** Cocaine SA rats showed increased GluA2-IR only in spines greater than 0.7 μm. **M-N.** The signal above threshold for GluA2 **(M)** and mCherry **(N)** was not different between groups.

O. The average GluA2 signal intensity in the mCherry-labeled dendrite was not different between groups. **P.** Representative dendrites showing decreased spine head-specific GluA2 (bottom) in cocaine SA (right) relative to yoked-saline controls (left). Scale bars = 2 μm. *p<0.05, **p<0.01, ****p<0.0001 compared to saline.

Discussion

Summary of findings

Here we show that cocaine SA biphasically alters nuclear activity markers, structural plasticity, and AMPA receptor expression in dendritic spines of PrL-NAc core neurons depending on the duration of abstinence. We found that two hours after cocaine SA, PrL-NAc core neurons showed decreased Fos-IR and p-CREB-IR, as well as spine head diameter, suggesting diminished neuronal activity in this specific pathway. Further, total GluA1-IR was diminished in PrL-NAc core dendrites, which was accounted for by reduced GluA1-IR in dendritic shafts and spine heads. Interestingly, total GluA2-IR was unaffected by cocaine SA, although both GluA1-IR and GluA2-IR were reduced in enlarged, putative mushroom-type spines (i.e. head diameter greater than 0.7 μm), which make up a minority of overall dendritic spines. In contrast, one week of abstinence was associated with augmented spine head diameter and overall attrition of dendritic spines. Like early withdrawal, one week of abstinence reduced overall GluA1-IR, but not GluA2-IR, in PrL-NAc core neurons; however, both AMPA receptor subunits were elevated in dendritic spine heads of PrL-NAc core neurons, an effect driven by increased IR in enlarged, putative mushroom-type spines. At this timepoint, GluA1-IR was again reduced in the dendritic shaft. Overall, these findings suggest that the PrL-NAc core pathway may be in a hypoactive state during early withdrawal from cocaine and potentiated following one week of abstinence.

Cocaine SA reduced nuclear activity markers in PrL-NAc core neurons during early withdrawal

A previous report indicates that a single session of cocaine SA enhances Fos expression in the PrL cortex, which is normalized after six daily sessions of cocaine SA (Zahm et al., 2010). However, others have found that 10 daily sessions of cocaine SA increased *c-fos* gene expression in the medial prefrontal cortex (including PrL and IL cortices), effects which are maintained following 60 days of cocaine SA (Gao et al., 2017). Previously, we found decreased p-CREB-IR in the PrL cortex during early withdrawal (Whitfield et al., 2011). In our study, we found no effect of cocaine SA on global Fos-IR or p-CREB-IR in layer V PrL cortex. Layer V predominantly contains cortical efferents innervating subcortical structures implicated in motivation, cognition, and motor activation (Gabbott et al., 2005), one of these pathways being the PrL-NAc core pathway, which is well-documented to be involved in drug seeking after abstinence (Kalivas, 2009; Jasinska et al., 2015). Interestingly, when analyzing Fos-IR and p-CREB-IR in this specific pathway during early withdrawal, we found a significant decrease in both markers. Thus, cocaine SA likely leads to a dampening of PrL-NAc core activity during early withdrawal as evidenced by decreased IR of the activity markers, Fos and p-CREB.

Cocaine SA reduced dendritic spine head diameter and GluA1/2 spine head localization in PrL-NAc core neurons

PrL-NAc core apical spine head diameter was decreased during early withdrawal from cocaine SA. This finding positively correlates with reduced global dephosphorylation of GluN2A/B-containing NMDA receptors, ERK, and CREB and

the activation of STEP (Whitfield et al., 2011; Sun et al., 2013; Go et al., 2016; Barry and McGinty, 2017), as well as reduced nuclear Fos-IR and p-CREB-IR, and GluA1/2-IR in dendritic spines of PrL-NAc core neurons in this study. Supporting these observations, a recent study found that following a single injection of cocaine, Fos^{+} neurons relative to random NAc core neurons in cocaine and vehicle-injected controls showed elevated dendritic spine density and spine head volume (Dos Santos et al., 2017). Thus, Fos expression positively correlates with spine morphometric features. Here we found that p-CREB-IR positively correlated with spine head diameter, but negatively correlated with spine density. Thus, animals that showed higher p-CREB-IR in PrL-NAc core neurons tended to have higher average spine head diameter, but lower spine density. In contrast, following CREB overexpression in the amygdala, there is an increase in dendritic spine density (Sargin et al., 2013). This dichotomy likely reflects the difference between CREB overexpression and detection of endogenous p-CREB, as well as different brain regions investigated, and the effects of cocaine SA.

Interestingly, we found distinct and overlapping alterations in AMPA receptor subunit expression in PrL-NAc core dendritic spines. Total GluA1-IR was suppressed in PrL-NAc core neurons but GluA2-IR was only reduced in a specific subset of dendritic spines (i.e. enlarged, mushroom-type spines). GluA1 and GluA2 differentially regulate spine morphology (Prithviraj et al., 2008), with GluA2 playing a key role in spine morphogenesis *in vitro* (Passafaro et al., 2003; Saglietti et al., 2007). Moreover, β3 integrins, which play a critical role in regulating spine morphology (Shi and Ethell, 2006), interact strongly with GluA2-, but not GluA1, -

containing AMPA receptors (Pozo et al., 2012). Although the trafficking of AMPA receptors involves multiple complex interactions with AMPA receptor-interacting proteins through the C-terminal domains of AMPA receptor subunits (Shepherd and Huganir, 2007), there is general consensus that GluA1 and GluA2 differentially undergo trafficking and recycling (reviewed in (Anggono and Huganir, 2012).

Previous data from our lab indicate that short-access cocaine SA has no effect on total GluA1 or GluA2 expression in the PrL cortex two hours after the final SA session (Sun et al., 2013). Others have shown that 16 hours of withdrawal reduces GluA2/3, but not GluA1, protein expression in the mPFC (Hemby et al., 2005). These apparently contrasting findings are likely due to the different timepoints analyzed in the two studies. Moreover, phospho-deficient mutations of p-CREB^{S133} leading to CREB inactivation preferentially alter GluA1 synaptic incorporation in a basal state, without affecting synaptic levels of GluA2/3, in the hippocampus (Middei et al., 2013). Although our findings indicate that cocaine SA differentially regulates total GluA1-IR and GluA2-IR specifically in PrL-NAc core neurons during early withdrawal, the finding that both subunits were reduced in enlarged dendritic spines, which constitute the majority of AMPA receptor expression and function (Matsuzaki et al., 2001), suggests that mature spines undergo AMPA receptor removal during early withdrawal from cocaine. Future studies will address what molecular mechanisms may be responsible for the observed spine morphometric and accompanying GluA1/2 effects.

One week of abstinence from cocaine SA increased the head diameter, but decreased the density, of PrL-NAc core neuron dendritic spines while augmenting GluA1/2 IR in spine heads

Chronic cocaine SA followed by abstinence alters dendritic spine structural plasticity within the PrL cortex (Robinson et al., 2001; Rasakham et al., 2014; Radley et al., 2015). However, the precise induction of PrL cortical structural plasticity is controversial, with some showing hypertrophic spine changes (i.e. increased spine density), whereas others have shown hypotrophic spine alterations (i.e. decreased spine density).

We found that cocaine SA followed by one week of abstinence decreased the density of PrL-NAc core neuron apical dendritic spines but increased the average head diameter. To the best of our knowledge, the only other study investigating layer V PrL cortical structural plasticity after one week of abstinence from cocaine SA found increased layer V basal thin spine density, but decreased synapse number as well as overall dendritic complexity (Rasakham et al., 2014). Our results should not be viewed as contradictory to these findings, rather these differences underline the importance of investigating pathway-specific structural modifications as well as the region of dendrite investigated as inputs to the apical tuft (Liu and Aghajanian, 2008) and basal dendrites (Liu et al., 2015) differ in their origin.

One week of abstinence from cocaine SA leads to increased PKA-mediated phosphorylation of $CREB^{S133}$ as well as $GluA1^{S845}$ in the PrL cortex. Inhibiting PKA activity with an intra-PrL microinfusion of the PKA inhibitor, Rp-cAMPs, suppresses relapse to cocaine seeking when tested in the absence of conditioned cues (i.e.

context-induced relapse) (Sun et al., 2014b). Here we extend these findings by showing that elevated p-CREB^{S133} and GluA1 occurs in PrL-NAc core nuclei and spines, respectively. Although it has not been confirmed that this PKA-mediated induction of AMPA receptor phosphorylation results in a physiological enhancement of PrL cortical glutamate currents, this is not without precedent as it has been recently shown that cocaine conditioned place preference (CPP) training increases evoked AMPA receptor excitatory transmission in layer V PrL cortical neurons (Otis and Mueller, 2017).

Interestingly, we found decreased total GluA1-IR in PrL-NAc core neurons after one week of abstinence which was largely accounted for by decreased dendritic shaft-specific GluA1-IR. However, we found increased spine head-specific GluA1-IR. These findings infer that cocaine SA leads to compartment-specific changes in GluA1-IR in PrL-NAc core neurons one week after abstinence that are distinct from those which occur during early withdrawal. In contrast to early withdrawal, GluA-1IR and GluA2-IR were upregulated in spine heads of PrL-NAc core neurons after one week of abstinence. Although GluA2-lacking AMPA receptors in the NAc play a key role in cocaine seeking after abstinence in long-access SA paradigms (Conrad et al., 2008), we are likely not detecting such receptors in our model because both AMPA receptor subunits were increased in dendritic spines of PrL-NAc core neurons after one week of abstinence. However, we cannot exclude the involvement of GluA3/4-containing AMPA receptors in the effects of cocaine. Thus, it is possible that we are detecting elevated GluA1/3 as well as GluA2/3-containing AMPA receptors in PrL-NAc core spine heads.

Electrophysiological experiments would be needed to further discern the involvement of specific AMPA receptor subunit conformation in the observed effects. Regardless, it is likely that increased AMPA receptor expression in enlarged dendritic spines disposes these dendritic compartments to be hypersensitive to glutamate release because spines with enlarged volume show greater AMPA receptor-mediated excitatory transmission (Matsuzaki et al., 2001; Matsuzaki et al., 2004). Because we found an overall decrease in spine density, but increased spine head diameter, it is intriguing to hypothesize that specific inputs to the distal apical tuft of PrL-NAc core neurons may be potentiated whereas others are depressed, but this remains to be tested. This is supported by previous work showing that spines adjacent to active synapses have an accumulation of AMPA receptors leading to a lack of lateral diffusion (i.e. functional trapping at synapses), but AMPA receptors within spines adjacent to inactive synapses rapidly diffuse away from synaptic sites (Ehlers et al., 2007).

Overexpression of the GluA2 subunit of AMPA receptors is sufficient to increase dendritic spine density and size (Passafaro et al., 2003). Moreover, following learning in a fear conditioning paradigm, newly synthesized GluA1-containing AMPA receptors are incorporated into synapses preferentially in mushroom-type spines (Matsuo et al., 2008). Further, GluA1^{S845} phosphorylation by PKA is critical for the induction of synaptic plasticity governing learning and memory (Huganir and Nicoll, 2013). Stimulation of the PKA-GluA1 pathway by catecholamines lowers the threshold for LTP induction (Hu et al., 2007), indicating that GluA1 phosphorylation by PKA primes AMPA receptors for synaptic

incorporation, as shown previously with D1-PKA-GluA1 in cultured prefrontal cortical neurons (Sun et al., 2005). Thus, the elevated PKA activity and phosphorylation state of the PKA substrates described above that drive relapse after abstinence (Sun et al., 2014b) in conjunction with the results described here suggest that PrL-NAc core neurons likely exist in a hypersensitive glutamate state after one week of abstinence which may be maintained by elevated dopamine tone.

Technical considerations

Although confocal microscopy does not provide adequate resolution to infer surface expression of AMPA receptors or trafficking of AMPA receptors, it does provide the resolution to discern differences in compartmentalization of AMPA receptors (i.e. dendritic shaft versus spine heads). This is important given that previous work shows activity-dependent alterations in AMPA receptor compartmentalization in spines versus dendritic shafts *in vitro* (Shi et al., 1999; Brown et al., 2007). Moreover, conventional techniques to measure receptor surface expression (i.e. immunoblotting) in their current technological state occlude the use of pathway-specific measurements. Interestingly, at both timepoints, we observed differential expression of GluA1 and GluA2 in PrL-NAc core dendrites. It is plausible that this could be due to differential regulation of these AMPA receptor subunits by cocaine experience, which is supported by the finding that at both time points total GluA1-IR was decreased whereas total GluA2-IR was not. However, this interpretation should be viewed with caution because the immunostaining for GluA1 and GluA2 in each experiment was done

independently. Thus, this difference could be due to variations in the affinity of the antibodies for their respective antigens, although both antibodies have been well-validated for the use of immunohistochemistry (Vissavajjhala et al., 1996; Yap et al., 2017). Thus, directly comparing GluA1 and GluA2 findings may not be warranted, whereas the comparison between timepoints for each protein target may be more valid.

Moreover, it could be argued that several variables could account for altered spine morphology and increased, or decreased, GluA1/2 expression in spine heads, including signal intensity. This is extremely unlikely because a) the mCherry intensity in spine heads did not differ between groups in either experiment, and b) the percent of signal above threshold and the average signal intensity was not different between groups for neither GluA1 or GluA2 in either experiment. Thus, it is unlikely that differences in signal intensity contributed to our findings, but rather that the observed effects are due to cocaine-induced adaptations in the compartmentalization of AMPA receptors in these neurons.

Conclusions

The PrL cortex represents an important hub for the integration of sensory and motivational computations and is a critical node in which encoded information engages motor programs. Cocaine-induced structural plasticity in the PrL cortex has not been heavily investigated, largely due to experimental obstacles in imaging the full length of deep layer pyramidal neurons. The data described herein suggest that the previously described biphasic alterations in glutamatergic signaling that occur globally in the PrL cortex during early withdrawal and early abstinence are

associated with adaptations in the PrL-NAc core pathway. These adaptations occur not only at the level of the nucleus, but also at the level of individual dendritic spines, leading to differential compartmentalization of AMPA receptors in spines. Given that the two timepoints show remarkable dichotomy in PrL-NAc core adaptations, it is plausible that the altered structure and presumably diminished function of PrL-NAc core neurons during early withdrawal is likely required for the subsequent enlargement of dendritic spines, induction of p-CREB, and accumulation of AMPA receptors in enlarged spines after one week of abstinence. Thus, the abstinence duration-dependent adaptations in PrL-NAc core neurons provide a novel way of looking at corticostriatal dysfunction as it relates to relapse vulnerability. Future studies should investigate the precise timescale of these events as they occur over one week of abstinence. Furthermore, it is not clear whether structural and synaptic adaptations in PrL-NAc neurons are required for context-induced relapse. Future studies should address this question utilizing chemogenetic-mediated silencing of the PrL-NAc core pathway prior to context-induced relapse.

Chapter 5: General discussion

Summary of findings

The data described in this dissertation show that the dephosphorylation of ERK2 in the PrL cortex during early withdrawal is mediated by cocaine-induced activation of STEP that is critical to subsequent relapse to cocaine seeking after abstinence. Moreover, stimulation of the PrL cortex or the PrL-NAc core pathway immediately after SA leads to a transient suppression of cocaine seeking after abstinence, with differential effects depending on the stimuli used to induce cocaine seeking, suggesting that the ability to suppress subsequent cocaine seeking by intervening during early withdrawal is more complex than merely stimulating PrL output to the NAc core. Finally, cocaine SA decreases PrL-NAc core distal apical tuft dendritic spine head diameter, nuclear p-CREB and Fos, as well as GluA1/2 AMPA receptor expression in specific subsets of dendritic spines during early withdrawal. However, one week of abstinence elevated dendritic spine head diameter, but decreased density, and elevated GluA1/2 expression in dendritic spine heads and p-CREB-IR in the nucleus. Thus, cocaine-induced adaptations in glutamatergic transmission in the PrL-NAc core pathway emerge during early withdrawal, and induce subsequent circuit remodeling during abstinence, ultimately facilitating relapse to cocaine seeking.

Brain region-specific effects of drug-induced regulation of STEP function

Relative to several other neuropsychological and neurodegenerative disorders, far less is known about the involvement of STEP in addiction-related disorders. The little that is known clearly shows that STEP activation plays different roles in

regulation of psychostimulant-induced synaptic transmission and glutamatergic signaling depending on the brain region investigated, whether investigators measure acute versus chronic effects of drugs of abuse, and whether drug administration is contingent or non-contingent (Valjent et al., 2000).

Acute cocaine and amphetamine are well-documented to engage ERK2 phosphorylation in the ventral striatum, which is important for the expression of behavioral sensitization, through concomitant activation of dopamine D1 and NMDA receptors. The effect is complex, involving augmented dopamine interactions with ambient glutamate, PKA-mediated phosphorylation of DARRP-32, activation of PP1, dephosphorylation (inactivation) of STEP, elevations in dendritic spine density, and Src Family Kinase (SFK)-mediated augmentation of GluN2B-containing NMDA receptors (Zhang et al., 2001; Valjent et al., 2005; Girault et al., 2007; Pascoli et al., 2011; Cahill et al., 2014; Dos Santos et al., 2017).

Although reinstatement/relapse following chronic cocaine SA and the expression of locomotor sensitization to cocaine share some overlapping characteristics (Kalivas et al., 1998), there are also clear differences between the two paradigms pertaining to the operant conditioning nature of cocaine SA. Remarkably, it is unknown how chronic cocaine SA alters STEP activity in the NAc following cocaine SA. However, ERK phosphorylation is elevated in the NAc core of cocaine SA animals following three weeks of withdrawal, which is not present after one day of withdrawal, when reintroduced into the cocaine-paired context (Edwards et al., 2011). This finding suggests that STEP activity in the NAc core

may undergo abstinence duration-dependent inhibition of activity to drive relapse, although other ERK phosphatases, such as MKP3, may be involved.

In the prefrontal cortex, a rather different picture emerges and, in general, far less is known. In contrast to the NAc, acute cocaine-induced elevations in ERK phosphorylation do not require PKA-mediated phosphorylation of DAARP-32 (Valjent et al., 2005), suggesting alternative pathways are involved. We have previously found that cocaine SA leads to ERK, GluN2A/B-containing NMDA receptor, and CREB dephosphorylation in the PrL cortex during early withdrawal (Whitfield et al., 2011; Sun et al., 2013; Barry and McGinty, 2017). These changes are associated with dephosphorylation and activation of STEP (Sun et al., 2013). BDNF-mediated attenuation of cocaine seeking requires normalization of ERK phosphorylation (Whitfield et al., 2011). The results presented herein posit that STEP mediates the cocaine-induced dephosphorylation of ERK and plays a role in relapse after abstinence and extinction training depending on whether STEP is inhibited globally or specifically within the PrL cortex during early withdrawal. Thus, STEP-mediated ERK dephosphorylation in the PrL cortex is a critical regulator of cocaine-induced plasticity during early withdrawal that may ultimately facilitate dysfuntional corticostriatal glutamate transmission that drives relapse, perhaps through dysregulated gene expression.

Divergent prelimbic cortical pathways and their encoding of reward-predictive stimuli

The PrL cortex is a highly organized structure that contains heterogenous pyramidal neurons that project to multiple diverse subcortical targets. Layer II/III pyramidal neurons are generally believed to be made up of projection neurons

innervating the contralateral medial prefrontal cortex. In addition, a small number of neurons project to subcortical structures implicated in assignment of stimulus valence, such as the NAc and BLA (Gabbott et al., 2005; Little and Carter, 2013). A few layer V projection neurons also project to contralateral mPFC, but the majority of layer V neurons project to subcortical structures implicated in reinforcement learning and conditioned reward seeking, including the NAc core (Gabbott et al., 2005). Finally layer VI neurons encompass corticothalamic neurons innervating the mediodorsal nucleus of the thalamus as well as midline thalamic nuclei, such as the PVT (Otis et al., 2017). These glutamatergic projection neurons are fundamentally regulated by an array of GABAergic inhibitory interneurons and disruptions in this regulation have been implicated in numerous neuropsychiatric disorders (Lodge et al., 2009; Hervig et al., 2016).

Recent evidence indicates that layer V corticostriatal neurons (including the PrL-NAc core pathway) and layer VI neurons projecting to the midline thalamus, particularly the PVT, produce dichotomous encoding of reward-related information following learning (Otis et al., 2017). Moreover, recent data from our lab indicate that chemogenetic-mediated inhibition of the PrL cortex immediately following SA provides an enduring reduction in cocaine-seeking after abstinence or extinction training. Specifically, selectively inhibiting the PrL-NAc core pathway during early withdrawal had no effect on relapse to cocaine seeking whereas selective inhibition of the PrL-PVT pathway replicated the suppression of cocaine seeking following global PrL output inhibition (Giannotti et al., submitted).

STEP mRNA is expressed in all layers of the PrL cortex (Lein et al., 2007). Thus it is likely that intra-PrL STEP inhibition during early withdrawal from cocaine SA inhibits STEP activity in the majority of pyramidal neurons in the PrL cortex. However, it is unknown to what degree STEP is expressed in a pathway-specific manner. It would be interesting to examine whether the effect of intra-PrL STEP inhibition during early withdrawal is dependent on inhibiting STEP activity specifically in the PrL efferents projecting to the NAc core.

In the experiments presented herein, we found that global chemogenetic activation of the PrL cortex during early withdrawal transiently suppressed cue-induced reinstatement after extinction. In contrast, selective activation of the PrL-NAc core pathway transiently suppressed post-abstinence context-induced relapse but not cue-, or cocaine prime-, induced reinstatement. The relatively low dose of CNO used may account for the transient suppression in each case although alternative explanations, as discussed in Chapter 3, are possible. However, the differential, transient, suppression of relapse depending on the stimulus used to induce cocaine seeking after non-selective vs. pathway-specific activation of PrL cortex may be because global chemogenetic activation of the PrL cortex activates pyramidal neurons in all layers of the PrL cortex whereas selective activation of the PrL-NAc core pathway is preferentially infecting layer V PrL neurons projecting to the NAc core. Although PrL cortical STEP inhibition and Gq-DREADD activation showed vastly different behavioral effects, it can be postulated that the two interventions combined may provide a more enduring normalization of

ERK phosphorylation in the PrL cortex during early withdrawal more akin to BDNF, allowing hM3Dq to provide a sustained suppression of relapse (Fig. 5.1).

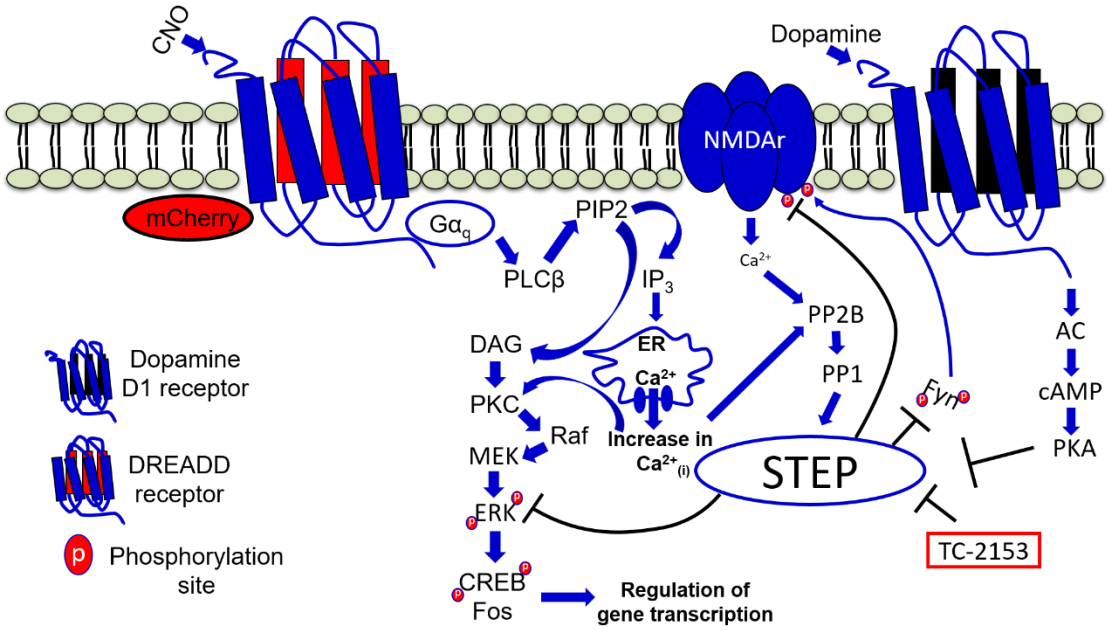

Figure 5.1. TC-2153 and Gq-DREADD interact at the level of ERK. The cocaine-induced dephosphorylation of ERK by STEP represents a critical adaptation that facilitates relapse. The synergistic action of the two to drive ERK phosphorylation may provide a more enduring suppression of relapse behavior in cocaine SA animals.

Cyotoarchitecture of layer V pyramidal neurons: Implications for activity-dependent structural remodeling

Pyramidal neurons make up the majority of glutamatergic projection neurons and are characterized by two distinct dendritic domains: basal and apical dendrites. Layer V-VI pyramidal neurons have a distinct primary apical dendrite that extends ~ 600 µm towards the pial surface, passing through layer III before bifurcating and ultimately producing a tuft of apical dendrites in layers II and layer I. Importantly, the apical tuft receives inputs from different origins relative to the proximal apical or basal dendrites (Spruston, 2008). For example, serotonin application to medial prefrontal cortical layer V distal apical tufts, but not basal dendrites, increases

excitatory post synaptic currents (EPSCs-(Aghajanian and Marek, 1997). Moreover, orexin (hypocretin) inputs to thalamocortical projection neuron axon boutons arising from intralaminar and midline thalamic nuclei elicits glutamate release onto distal apical tuft dendritic spines of layer V pyramidal neurons in the prefrontal cortex. Interestingly, this was associated with large Ca^{2+} transients in only a subset of dendritic spines (Lambe and Aghajanian, 2003). Stimulation of α4β2 nicotinic acetylcholine receptors (nAchRs) also induces glutamate release onto layer V prefrontal cortical pyramidal neurons due to actions at axon terminals of the same thalamocortical neurons (Lambe et al., 2003). Thus, it is possible that altered glutamatergic neurotransmission arising from thalamic neurons and regulated by orexinergic, serotonergic, or cholinergic inputs may induce altered glutamatergic plasticity in layer V PrL-NAc core neurons. Ultimately, this may lead to circuit level remodeling and sensitivity of these neurons to glutamate inputs that may drive relapse after abstinence.

It is well known that layer I-III of mPFC contains massive innervation by TH^{+} (presumably dopaminergic) fibers, at least in the primate PFC (Goldman-Rakic et al., 1989). Moreover, dendritic spines of distal apical tufts of layer V pyramidal neurons show an abundance of hyperpolarization-activated cyclic nucleotide-gated channel (HCN) immunoreactivity, which colocalize with D1 receptors preferentially on long thin spines (Paspalas et al., 2013). Thus, although it has not been definitively shown, the latter finding suggests that, in addition to serotonergic and orexinergic inputs, layer V prefrontal cortical distal apical tufts also receive dopaminergic inputs, presumably arising from the VTA. In contrast, glutamatergic

inputs arising from the BLA preferentially innervate basal dendrites of layer V PrL cortical pyramidal neurons (Liu et al., 2015). Furthermore, during development, proximal apical dendrites of layer V prefrontal cortical neurons undergo a transformational shift in NMDA receptor-dependent excitatory neurotransmission characterized by an emergence of GluN2B-containing NMDA receptors, which requires PKA and D1 activity. Such an emergence provides sustained plasticity in response to ventral hippocampal, but not BLA, inputs (Flores-Barrera et al., 2014). These findings provide insight into the potential anatomical inputs onto layer V PrL cortical distal apical tufts which may undergo plasticity following chronic cocaine SA, ultimately driving post synaptic alterations in form (structural plasticity) and function (glutamatergic signaling).

In the context of psychopathology, chronic mild stress paradigms have been shown to reduce the percentage of mushroom-type spines of distal apical dendrites, but not basal dendrites, in both the CA3 region of the hippocampus as well as the mPFC (Bessa et al., 2009). Moreover, distal apical tufts of layer V pyramidal neurons undergo hypotrophic structural plasticity (i.e. loss of dendritic spines) following chronic stress, which is associated with a loss of orexin and sertonin-induced EPSCs (Liu and Aghajanian, 2008). Chronic stress also decreases the surface expression of GluA1 and GluA2 subunits of AMPA receptors in the mPFC, effects which occur through activation of glucocorticoid receptors (Yuen et al., 2012). Finally, layer II/III PrL cortical neurons show reduced spine density, but increased spine volume, following two weeks of abstinence; alterations which are associated with heightened corticosterone as well as working

memory deficits following cocaine SA (Radley et al., 2015). This latter finding has also been shown following chronic stress (Radley et al., 2006), suggesting that cocaine SA and chronic stress induce similar neuroadaptations, perhaps ultimately leading to a shared inability of top-down control of behavior. Thus, it is possible that acute cocaine withdrawal following chronic SA may engage the rodent stress response which sensitizes during more prolonoged abstinence, ultimately leading to prefrontal cortical impairments and dysregulation of downstream structures such as the NAc core.

Time-dependent regulation of structural plasticity: Role of experience-dependent circuit remodeling

The majority of mature dendritic spines in various brain regions are relatively stable during adulthoood (Trachtenberg et al., 2002). However, several experiments have shown that structural remodeling of neurons occurs following learning. In the hippocampus, contextual fear conditioning alters morphological plasticity 24 hours after learning, specifically in neurons activated during fear conditioning relative to neurons that were inactive during fear conditioning (Sanders et al., 2012). Moreover, contextual fear conditioning leads to a hippocampal-dependent progressive reorganization of anterior cingulate neuron apical dendritic spine density characterized by elevated density 36 days, but not 24 hours, after conditioning. Lesions of the hippocampus immediately after conditioning prevent this elevated spine density weeks after conditioning (Restivo et al., 2009). In the barrel cortex, dendritic spine formation and pruning occurs following paradigms that induce functional reorganization, such as contralateral whisker trimming. Specifically, whisker trimming destablizaes nascent spines, while stabilizing spines

that were persistent during repeated two-photon imaging (Holtmaat et al., 2006). It is therefore plausbile that the initial spine head shrinkage observed in PrL-NAc core neurons during early withdrawal, and the subsequent enlargement of spines coupled with the elimination of spines after one week of abstinence, may lead to stabilization of synapses that have a greater influence on PrL-NAc core transmission, leading to heightened encoding of cocaine-paired stimuli.

What might be the molecular substrates of activity-dependent structural remodeling? Several lines of evidence point to altered gene transcription in structural remodeling following associative learning. For example, prolonged whisker trimming elevates the proportion of thin spines in the contralateral barrel cortex in wild type, but not CREB-knockout mice. Moreover, in the ipsilateral barrel cortex, there is a CREB-dependent enlargement of dendritic spines (Pignataro et al., 2015). Furthermore, in the CA1 field of the hippocampus, CREB inhibition impairs contextual fear conditioning and leads to actin depolymerization resulting in the collapse of dendritic spines (Middei et al., 2012). BDNF has been recognized as a major upstream regulator of CREB-mediated gene transcription and spine morphogenesis. In the mPFC, BDNF mice containing the knockin Val66Met polymorphism, that hinders intracellular BDNF transport and secretion (Chen et al., 2004) show distal apical dendrite atrophy of layer V neurons, characterized by decreased density and spine head width. They also display decrements in evoked EPSCs, which is consistent with the above-mentioned effects of stress on apical dendrites of layer V mPFC neurons (Liu et al., 2012). Thus, it is likely that BDNF and CREB act in concert to regulate time-dependent changes in structural

plasticity. Moreover, these two signaling molecules likely exist as core tenants of activity-dependent structural remodeling, ultimately resulting in a stabilization of newly formed synapses, and perhaps the coordinated and parallel pruning of other synapses.

Potential cellular mechanisms mediating PrL-NAc core apical dendrite structural plasticity: Role of STEP and BDNF

It is possible that the cocaine-induced activation of STEP in the PrL cortex during early withdrawal serves as a potential mediator of dendritic spine changes in PrL-NAc core neurons. Previous work indicates that activation of STEP leads to the dephosphorylation and inactivation of a key inhibitor of cofilin-mediated actin depolymerization, SPIN 90, in cultured neurons (Cho et al., 2013), although this is yet to be demonstrated *in vivo*. This agrees with findings that STEP suppresses LTP induction (Pelkey et al., 2002), which is generally associated with enlargement of dendritic spine heads (Huganir and Nicoll, 2013). Importantly, chronic inhibition of STEP ameliorates dendritic spine adaptations in a Fmr1 knockout mouse model of Fragile X syndrome (Chatterjee et al., 2018). Moreover, chronic inhibition of the upstream activator of STEP, PP2B (calcineurin), has been shown to increase dendritic branching and spine density in naïve mouse neocortex (Spires-Jones et al., 2011), although this effect could be due to alterations in other systems downstream of PP2B, and not necessarily at the level of STEP. Regarding regulation of AMPA receptors, STEP dephosphorylates tyrosine residues in the intracellular C-terminal domain of GluA2, promoting endocytosis (Zhang et al., 2008). Finally, STEP knock-out mice crossed with Tg2576 Alzheimer's disease transgenic mice show an attenuation of Amyloidβ-mediated GluA1/2 endocytosis

in cortical tissue normally present in Tg2576 mice alone (Zhang et al., 2011). These findings suggest the possible involvement of STEP activation in cocaine-induced structural plasticity and AMPA receptor alterations in PrL-NAc core neurons. Given the role of STEP-mediated dephosphorylation of p-ERK2 in the PrL cortex during early withdrawal, leading to subsequent relapse, it would be interesting to examine whether transient inhibition of STEP specifically in PrL-NAc core neurons immediately after SA is sufficient to suppress relapse after abstinence.

Acute stimulation of neuronal cultures *in vitro* with BDNF leads to a sustained incorporation of synaptic AMPA receptors through increased association of GluA2 with Glutamate Receptor-Interacting Protein 1 (GRIP1) and GluA1 with synapse-associated protein 97 (SAP97) (Jourdi and Kabbaj, 2013). Moreover, BDNF promotes actin polymerization and dendritic spine growth (Horch et al., 1999; Tanaka et al., 2008; Bennett and Lagopoulos, 2014). Because the suppressive effect of intra-PrL BDNF on cocaine seeking is ERK dependent (Whitfield et al., 2011) and AMPA receptor exocytosis and lateral diffusion into stimulated synapses during LTP induction is ERK-dependent (Patterson et al., 2010), it is plausible that one mechanism of action by which an intra-PrL BDNF microinfusion suppresses relapse is through increased incorporation of AMPA receptors in dendritic spines of PrL-NAc core neurons during early withdrawal as has been demonstrated in the NAc (Li and Wolf, 2011). Future studies should investigate whether this intervention normalizes the cocaine-induced depression

of dendritic spine head size as well as GluA-IR in large spines of PrL-NAc core neurons.

Are all PrL-NAc core neurons created equal?

The PrL-NAc core pathway represents a critical node in regulating cocaine-seeking, as discussed in detail above. Using a rabies monosynaptic tracing technique, it was found that the NAc receives input from ~50 different brain regions. Cortical inputs (including cingulate, orbitofrontal, PrL, IL, insular, perirhinal, entorhinal, and motor cortices) were found to constitute ~25% of brain-wide inputs to the NAc core. PrL cortical neurons innervating the NAc core project evenly to D1 and D2 MSN's, whereas medial orbitofrontal cortical neurons innervate a significantly greater proportion of D1 relative to D2 MSNs (Barrientos et al., 2018). Both D1 and D2-expressing MSNs innervate the ventral pallidum (Kupchik et al., 2015), and D1 versus D2 activation differentially regulates cocaine-seeking (Lobo et al., 2010) via actions in the ventral pallidum (Heinsbroek et al., 2017).

Thus, it is plausible that hM3Dq-mediated PrL-NAc core activation immediately after SA is activating both PrL-NAc core neurons innervating D1-expressing MSNs as well as D2-expressing MSNs. Because these accumbens neurons have different effects on cocaine-seeking when stimulated or inhibited, it is possible that the overall lack of effect of hM3Dq activation on cocaine-seeking may be due to differential effects on these divergent NAc MSN subtypes. This differential activation is further supported by the finding that the majority of hM3Dq-expressing PrL-NAc core neurons were Fos activated, indicating that PrL-NAc core

neurons innervating both D1 and D2 expressing MSNs were likely to be activated by CNO during early withdrawal. Furthermore, the experiments performed by Barrientos and colleagues demonstrated that PrL-NAc core neurons innervating D1 MSNs preferentially showed reduced apical dendrite spine density following 14, but not 5, days of withdrawal from daily non-contingent cocaine injections. Thus, our findings that PrL-NAc core neurons show decreased spine density following one week of abstinence from cocaine SA agree and suggest that our effects may be specific to PrL neurons innervating D1-expressing MSNs, a subject for future investigation. Moreover, because Barrientos and colleagues found structural alterations after 14, but not 5 days, implies that these changes occur as a result of abstinence duration and not necessarily because of the pharmacological effect of daily cocaine injections.

Conclusions

Pyramidal neurons within the mPFC are well-positioned to integrate multiple sensory and neuromodulatory inputs that guide motivated behavior to ensure survival of a given species. In naïve animals, it could be postulated that the mPFC acts as a gate that allows for stimuli to induce adaptive, or inhibit maladaptive, behaviors that facilitate behavioral activation in response to cues that predict rewards, likely through innervation of the NAc core. The ability to adapt to an ever-changing environment likely involves transient alterations in structural plasticity, glutamatergic signaling, and ultimately gene transcription in PrL neurons innervating limbic regions that interact with motor programs, such as the NAc core (Fig. 5.2).

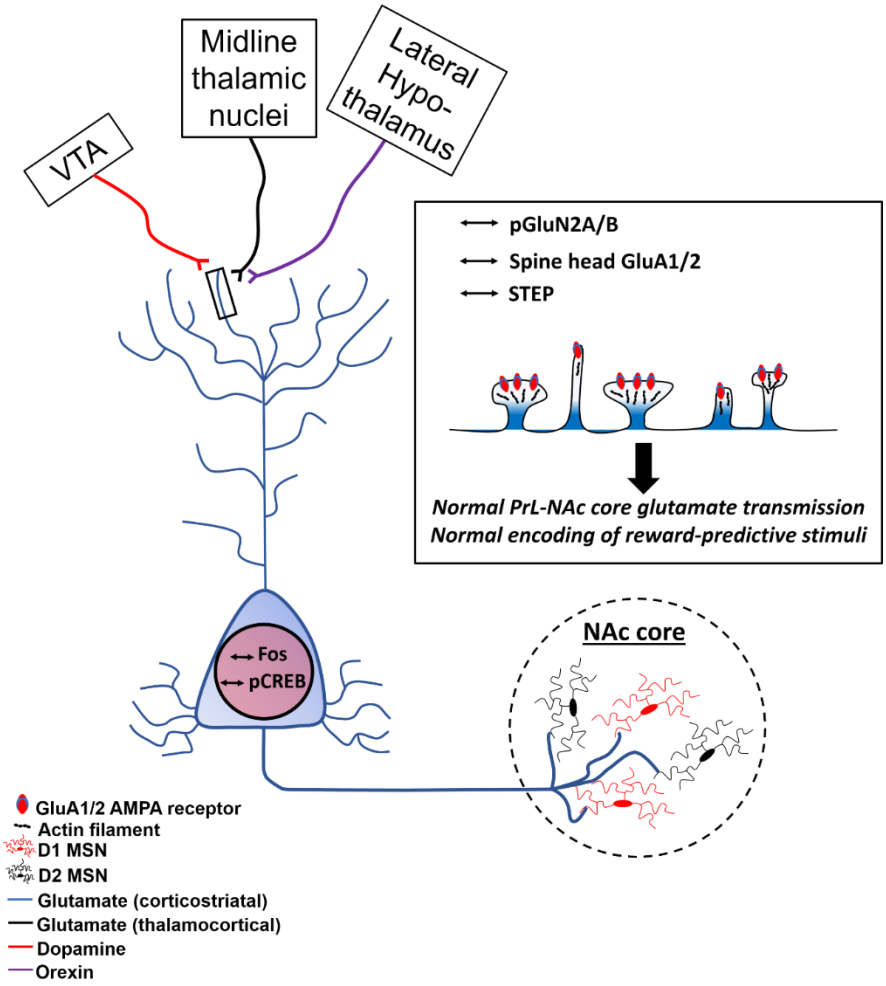

Figure 5.2. Schematic illustrating "normal" PrL-NAc core neuronal activity. Layer V PrL cortical neurons' distal apical tufts receive input from various excitatory and neuromodulatory regions, facilitating activity-dependent synaptic and structural remodeling in response to these inputs. These changes may be both upstream and downstream of transcriptional activity in the nucleus. Specifically, PrL neurons projecting to the NAc core may undergo activity-dependent alterations in response to stimuli associated with rewards, ultimately facilitating motor activation via interactions with D1 and D2-expressing MSNs in the NAc core.

However, following chronic cocaine SA, the PrL-NAc core pathway undergoes maladaptive plasticity within the first few hours of withdrawal. This is characterized by decreased CREB phosphorylation, decreased nuclear Fos expression, as well as decreased GluA1/2 expression in mature dendritic spines of PrL-NAc core neurons. These neurons may also make up a proportion of those

that show elevated STEP activity, leading to decreased phosphorylation of ERK2 and GluN2A/B-containing NMDA receptors. It is likely that these effects rely on altered glutamatergic inputs to PrL-NAc core neurons that may also undergo maladaptive plasticity (Fig. 5.3).

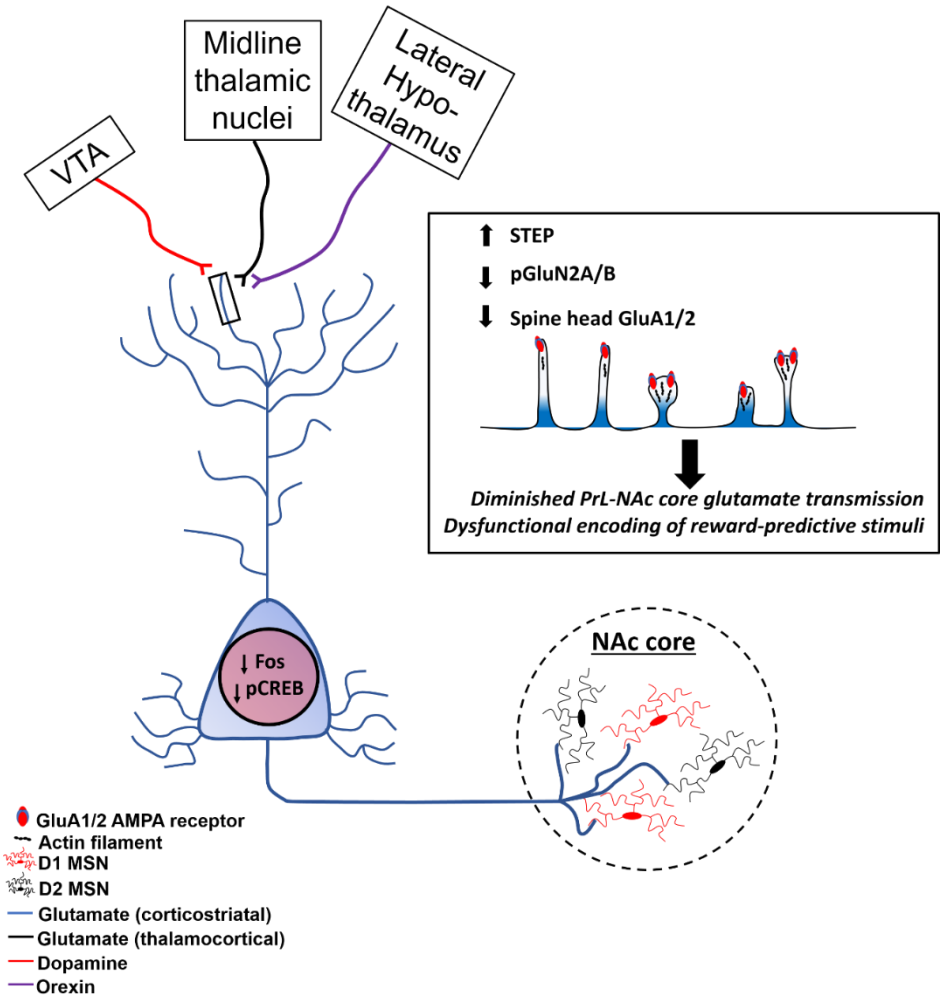

Figure 5.3. Schematic illustrating dysfuntional PrL-NAc core transmission during early withdrawal. Chronic cocaine exposure may alter the excitatory and modulatory inputs to PrL-NAc core distal apical tufts. These inputs result in hypotrophic structural alterations, which may be due to an imbalance in kinase-phosphatase activity (i.e. increased STEP). Ultimately, this may facilitate dysfunctional PrL-NAc core glutamate transmission during early withdrawal from cocaine SA.

Moreover, the altered plasticity in PrL-NAc core neurons is time-dependent, such that after one week of abstinence (i.e. immediately prior to a context-induced relapse test), PrL-NAc core neurons may exist in a state of hyper-responsiveness to glutamate inputs, characterized by elevated GluA1/2 expression in dendritic spines, as well as increased nuclear p-CREB (Fig. 5.4). Ultimately, this chain of maladaptive plasticity likely facilitates preferential encoding of drug-associated stimuli, facilitating the seeking for cocaine, perhaps at the expense of natural rewards, a key characteristic of addictive disorders.

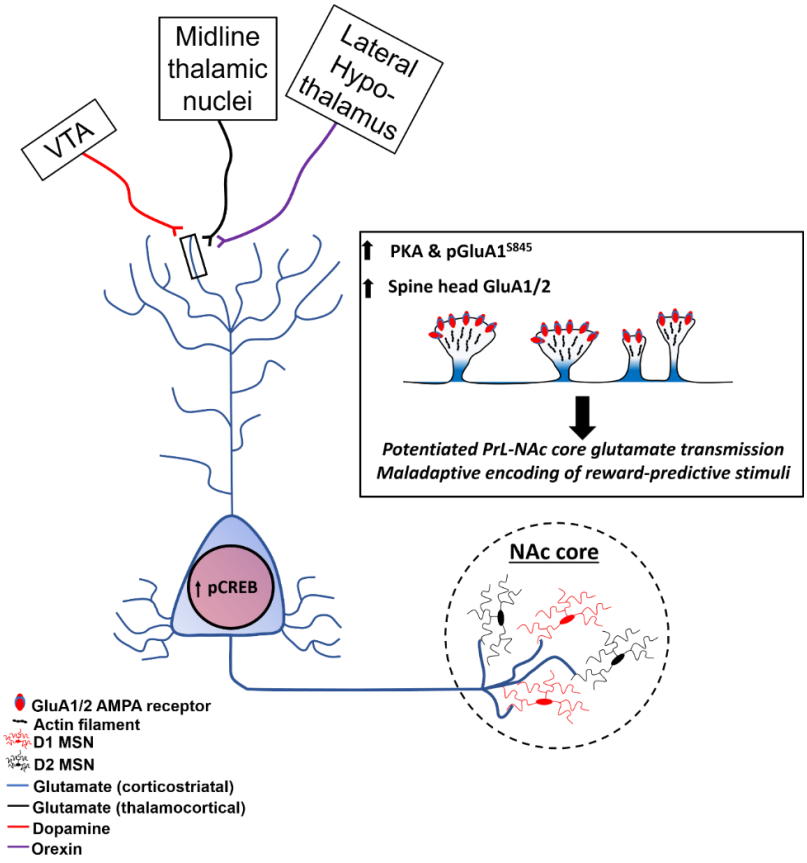

Figure 5.4. Schematic illustrating dysfuntional PrL-NAc core transmission after one week of abstinence. Chronic cocaine SA may alter encoding of cocaine-related stimuli by layer V PrL cortical neurons via hypertrophic enlargements in spine heads and AMPA receptor accumulation in spine heads, as well as elevated p-CREB-dependent transcription of plasticity-related genes. This likely facilitates increased PrL-NAc core glutamate transmission, perhaps preferentially in PrL neurons innervating D1-expressing MSNs in the NAc core.

Future directions

Most of the experiments described herein have taken advantage of traditional behavioral pharmacology and biochemical techniques, as well as the recent advent of pathway-specific viral vector techniques and high-resolution confocal microscopy. However, the findings from these experiments would be greatly enhanced by electrophysiological and Ca^{2+} imaging experiments that would further reveal mechanisms involved in producing the transient and enduring PrL adaptations following chronic cocaine exposure, as well as providing a physiological readout of activity. Moreover, the precise mechanisms mediating these adaptive effects are unknown. As described above, it is possible that STEP activation during early withdrawal is involved in these adaptations. Furthermore, it is probable that one mechanism of action of the suppressive effect of BDNF on cocaine seeking involves normalizing structural and glutamate signaling adaptations in PrL-NAc core neurons. Furthermore, future studies should examine whether the spine changes are positively correlated with p-CREB-IR using two-photon imaging in behaving animals.

An often-underappreciated aspect of glutamate transmission is the involvement of astroglial cells. Astrocytes play a critical role in glutamate uptake at synapses through the actions of the high-affinity glutamate transporter GLT1 (Anderson and Swanson, 2000; Shen et al., 2014b), and cocaine-induced alterations in the proximity of astrocytes to synapses in the NAc core has been suggested to play a role in altered glutamate transmission implicated in relapse to various drugs of abuse (Scofield et al., 2016a; Scofield et al., 2016b). Indeed,

drugs that have shown promise in the treatment of addiction-related disorders, such as N-acetyl-cysteine, exert most of their effects on astrocytes, particularly by normalizing drug-induced downregulation in GLT1 (Reissner et al., 2015). Emerging evidence indicates that perisynaptic astrocytic processes (PAPs) interdigitate with individual dendritic spines where they regulate the fidelity of neuronal communication and ensheathe synapses in response to bouts of high activity (Bernardinelli et al., 2014). An advantage of our pathway-specific labeling of dendritic spines is that viruses used to label neurons can be co-injected with viruses that label the fine membrane of astrocytes. Indeed, using this multi-viral labeling technique, we can observe the degree to which astrocytes associate with neurons at the level of individual dendritic spines (Fig. 5.5).

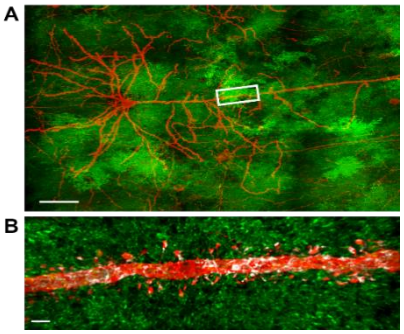

Figure 5.5. Representative PAP association with PrL-NAc core dendrite. **A.** PrL-NAc core mCherry-labeled neuron (red) surrounded by field of GFAP-Lck-GFP which preferentially labels asrocytic plasma membranes (green). **B.** High magnification inset of boxed region in A. Note the dense array of dendritic spine heads surrounded by astrocyte PAPs. Instances where astrocyte PAPs are within 150 nm of the dendritic shaft and spines are shown in white. Scale bars = 50 μm (A), 3 μm (B).

Thus, future experiments should determine whether a) STEP inhibition alters astrocyte-neuron interactions at spines of PrL-NAc core neurons during early withdrawal, b) hM3Dq-mediated activation of PrL-NAc core neurons is associated with altered astrocyte contact, and c) whether PrL-NAc core neuron structural plasticity and dendritic AMPA receptor expression is associated with altered astrocyte contact, particularly at enlarged mushroom-type spines. Ultimately, these experiments would synergize with those presented within this dissertation

by providing a greater understanding of how drug-induced adaptations in synaptic plasticity in the PrL-NAc core circuit drive subsequent relapse after abstinence.

Works cited

Aghajanian GK, Marek GJ (1997) Serotonin induces excitatory postsynaptic potentials in apical dendrites of neocortical pyramidal cells. Neuropharmacology 36:589-599.

Alcacer C, Andreoli L, Sebastianutto I, Jakobsson J, Fieblinger T, Cenci MA (2017) Chemogenetic stimulation of striatal projection neurons modulates responses to Parkinson's disease therapy. J Clin Invest 127:720-734.

Alexander GM, Rogan SC, Abbas AI, Armbruster BN, Pei Y, Allen JA, Nonneman RJ, Hartmann J, Moy SS, Nicolelis MA, McNamara JO, Roth BL (2009) Remote control of neuronal activity in transgenic mice expressing evolved G protein-coupled receptors. Neuron 63:27-39.

Anderson CM, Swanson RA (2000) Astrocyte glutamate transport: review of properties, regulation, and physiological functions. Glia 32:1-14.

Anggono V, Huganir RL (2012) Regulation of AMPA receptor trafficking and synaptic plasticity. Curr Opin Neurobiol 22:461-469.

Atwal JK, Massie B, Miller FD, Kaplan DR (2000) The TrkB-Shc site signals neuronal survival and local axon growth via MEK and P13-kinase. Neuron 27:265-277.

Augur IF, Wyckoff AR, Aston-Jones G, Kalivas PW, Peters J (2016) Chemogenetic Activation of an Extinction Neural Circuit Reduces Cue-Induced Reinstatement of Cocaine Seeking. J Neurosci 36:10174-10180.

Ball KT, Wellman CL, Fortenberry E, Rebec GV (2009) Sensitizing regimens of (+/-)3, 4-methylenedioxymethamphetamine (ecstasy) elicit enduring and differential structural alterations in the brain motive circuit of the rat. Neuroscience 160:264-274.

Banke TG, Bowie D, Lee H, Huganir RL, Schousboe A, Traynelis SF (2000) Control of GluR1 AMPA receptor function by cAMP-dependent protein kinase. J Neurosci 20:89-102.

Barrientos C, Knowland D, Wu MMJ, Lilascharoen V, Huang KW, Malenka RC, Lim BK (2018) Cocaine induced structural plasticity in input regions to distinct cell types in nucleus accumbens. Biological Psychiatry 10.1016/j.biopsych.2018.04.019.

Barry SM, McGinty JF (2017) Role of Src Family Kinases in BDNF-Mediated Suppression of Cocaine-Seeking and Prevention of Cocaine-Induced ERK, GluN2A, and GluN2B Dephosphorylation in the Prelimbic Cortex. Neuropsychopharmacology 42:1972-1980.

Bellocchio L, Ruiz-Calvo A, Chiarlone A, Cabanas M, Resel E, Cazalets JR, Blazquez C, Cho YH, Galve-Roperh I, Guzman M (2016) Sustained Gq-

Protein Signaling Disrupts Striatal Circuits via JNK. J Neurosci 36:10611-10624.

Bellot A, Guivernau B, Tajes M, Bosch-Morato M, Valls-Comamala V, Munoz FJ (2014) The structure and function of actin cytoskeleton in mature glutamatergic dendritic spines. Brain Res 1573:1-16.

Bennett MR, Lagopoulos J (2014) Stress and trauma: BDNF control of dendritic-spine formation and regression. Prog Neurobiol 112:80-99.

Berglind WJ, Whitfield TW, Jr., LaLumiere RT, Kalivas PW, McGinty JF (2009) A single intra-PFC infusion of BDNF prevents cocaine-induced alterations in extracellular glutamate within the nucleus accumbens. J Neurosci 29:3715-3719.

Berglind WJ, See RE, Fuchs RA, Ghee SM, Whitfield TW, Jr., Miller SW, McGinty JF (2007) A BDNF infusion into the medial prefrontal cortex suppresses cocaine seeking in rats. Eur J Neurosci 26:757-766.

Bernardinelli Y, Randall J, Janett E, Nikonenko I, Konig S, Jones EV, Flores CE, Murai KK, Bochet CG, Holtmaat A, Muller D (2014) Activity-dependent structural plasticity of perisynaptic astrocytic domains promotes excitatory synapse stability. Curr Biol 24:1679-1688.

Bessa JM, Ferreira D, Melo I, Marques F, Cerqueira JJ, Palha JA, Almeida OF, Sousa N (2009) The mood-improving actions of antidepressants do not depend on neurogenesis but are associated with neuronal remodeling. Mol Psychiatry 14:764-773, 739.

Blaustein MP, Golovina VA (2001) Structural complexity and functional diversity of endoplasmic reticulum Ca(2+) stores. Trends Neurosci 24:602-608.

Boudreau AC, Ferrario CR, Glucksman MJ, Wolf ME (2009) Signaling pathway adaptations and novel protein kinase A substrates related to behavioral sensitization to cocaine. J Neurochem 110:363-377.

Boulanger LM, Lombroso PJ, Raghunathan A, During MJ, Wahle P, Naegele JR (1995) Cellular and molecular characterization of a brain-enriched protein tyrosine phosphatase. J Neurosci 15:1532-1544.

Braithwaite SP, Paul S, Nairn AC, Lombroso PJ (2006) Synaptic plasticity: one STEP at a time. Trends Neurosci 29:452-458.

Brewer JA, Worhunsky PD, Carroll KM, Rounsaville BJ, Potenza MN (2008) Pretreatment brain activation during stroop task is associated with outcomes in cocaine-dependent patients. Biol Psychiatry 64:998-1004.

Brown TC, Correia SS, Petrok CN, Esteban JA (2007) Functional compartmentalization of endosomal trafficking for the synaptic delivery of AMPA receptors during long-term potentiation. J Neurosci 27:13311-13315.

Cahill E, Salery M, Vanhoutte P, Caboche J (2014) Convergence of dopamine and glutamate signaling onto striatal ERK activation in response to drugs of abuse. Front Pharmacol 4:172.

Carreno FR, Walch JD, Dutta M, Nedungadi TP, Cunningham JT (2011) Brain-derived neurotrophic factor-tyrosine kinase B pathway mediates NMDA receptor NR2B subunit phosphorylation in the supraoptic nuclei following progressive dehydration. J Neuroendocrinol 23:894-905.

Chatterjee M, Kurup PK, Lundbye CJ, Hugger Toft AK, Kwon J, Benedict J, Kamceva M, Banke TG, Lombroso PJ (2018) STEP inhibition reverses behavioral, electrophysiologic, and synaptic abnormalities in Fmr1 KO mice. Neuropharmacology 128:43-53.

Chen BT, Yau HJ, Hatch C, Kusumoto-Yoshida I, Cho SL, Hopf FW, Bonci A (2013) Rescuing cocaine-induced prefrontal cortex hypoactivity prevents compulsive cocaine seeking. Nature 496:359-362.

Chen ZY, Patel PD, Sant G, Meng CX, Teng KK, Hempstead BL, Lee FS (2004) Variant brain-derived neurotrophic factor (BDNF) (Met66) alters the intracellular trafficking and activity-dependent secretion of wild-type BDNF in neurosecretory cells and cortical neurons. J Neurosci 24:4401-4411.

Cho IH, Lee MJ, Kim DH, Kim B, Bae J, Choi KY, Kim SM, Huh YH, Lee KH, Kim CH, Song WK (2013) SPIN90 dephosphorylation is required for cofilin-mediated actin depolymerization in NMDA-stimulated hippocampal neurons. Cell Mol Life Sci 70:4369-4383.

Conrad KL, Tseng KY, Uejima JL, Reimers JM, Heng LJ, Shaham Y, Marinelli M, Wolf ME (2008) Formation of accumbens GluR2-lacking AMPA receptors mediates incubation of cocaine craving. Nature 454:118-121.

Cornish JL, Kalivas PW (2000) Glutamate transmission in the nucleus accumbens mediates relapse in cocaine addiction. J Neurosci 20:RC89.

Dailey ME, Smith SJ (1996) The dynamics of dendritic structure in developing hippocampal slices. J Neurosci 16:2983-2994.

Degenhardt L, Hall W (2012) Extent of illicit drug use and dependence, and their contribution to the global burden of disease. Lancet 379:55-70.

Dennis TS, Jhou TC, McGinty JF (2018) Cocaine Self-Administration and Time-dependent Decreases in Prelimbic Activity. bioRxiv 10.1101/255455.

Dong Y, Nasif FJ, Tsui JJ, Ju WY, Cooper DC, Hu XT, Malenka RC, White FJ (2005) Cocaine-induced plasticity of intrinsic membrane properties in prefrontal cortex pyramidal neurons: adaptations in potassium currents. J Neurosci 25:936-940.

Dos Santos M, Salery M, Forget B, Garcia Perez MA, Betuing S, Boudier T, Vanhoutte P, Caboche J, Heck N (2017) Rapid Synaptogenesis in the Nucleus Accumbens Is Induced by a Single Cocaine Administration and

Stabilized by Mitogen-Activated Protein Kinase Interacting Kinase-1 Activity. Biol Psychiatry 82:806-818.

Dragunow M, Faull R (1989) The use of c-fos as a metabolic marker in neuronal pathway tracing. J Neurosci Methods 29:261-265.

Edwards S, Bachtell RK, Guzman D, Whisler KN, Self DW (2011) Emergence of context-associated GluR(1) and ERK phosphorylation in the nucleus accumbens core during withdrawal from cocaine self-administration. Addict Biol 16:450-457.

Ehlers MD, Heine M, Groc L, Lee MC, Choquet D (2007) Diffusional trapping of GluR1 AMPA receptors by input-specific synaptic activity. Neuron 54:447-460.

Ersche KD, Barnes A, Jones PS, Morein-Zamir S, Robbins TW, Bullmore ET (2011) Abnormal structure of frontostriatal brain systems is associated with aspects of impulsivity and compulsivity in cocaine dependence. Brain 134:2013-2024.

Everitt BJ, Wolf ME (2002) Psychomotor stimulant addiction: a neural systems perspective. J Neurosci 22:3312-3320.

Fifkova E, Delay RJ (1982) Cytoplasmic actin in neuronal processes as a possible mediator of synaptic plasticity. J Cell Biol 95:345-350.

Flores-Barrera E, Thomases DR, Heng LJ, Cass DK, Caballero A, Tseng KY (2014) Late adolescent expression of GluN2B transmission in the prefrontal cortex is input-specific and requires postsynaptic protein kinase A and D1 dopamine receptor signaling. Biol Psychiatry 75:508-516.

Fu M, Zuo Y (2011) Experience-dependent structural plasticity in the cortex. Trends Neurosci 34:177-187.

Fuchs RA, Branham RK, See RE (2006) Different neural substrates mediate cocaine seeking after abstinence versus extinction training: a critical role for the dorsolateral caudate-putamen. J Neurosci 26:3584-3588.

Gabbott PL, Warner TA, Jays PR, Salway P, Busby SJ (2005) Prefrontal cortex in the rat: projections to subcortical autonomic, motor, and limbic centers. J Comp Neurol 492:145-177.

Gao P, Limpens JH, Spijker S, Vanderschuren LJ, Voorn P (2017) Stable immediate early gene expression patterns in medial prefrontal cortex and striatum after long-term cocaine self-administration. Addict Biol 22:354-368.

Garavan H, Pankiewicz J, Bloom A, Cho JK, Sperry L, Ross TJ, Salmeron BJ, Risinger R, Kelley D, Stein EA (2000) Cue-induced cocaine craving: neuroanatomical specificity for drug users and drug stimuli. Am J Psychiatry 157:1789-1798.

Garcia AF, Nakata KG, Ferguson SM (2017) Viral strategies for targeting cortical circuits that control cocaine-taking and cocaine-seeking in rodents. Pharmacol Biochem Behav 10.1016/j.pbb.2017.05.009.

Garcia Pardo MP, Roger Sanchez C, De la Rubia Orti JE, Aguilar Calpe MA (2017) Animal models of drug addiction. Adicciones 29:278-292.

Gipson CD, Kupchik YM, Shen H, Reissner KJ, Thomas CA, Kalivas PW (2013) Relapse induced by cues predicting cocaine depends on rapid, transient synaptic potentiation. Neuron 77:867-872.

Girault JA, Valjent E, Caboche J, Herve D (2007) ERK2: a logical AND gate critical for drug-induced plasticity? Curr Opin Pharmacol 7:77-85.

Go BS, Barry SM, McGinty JF (2016) Glutamatergic neurotransmission in the prefrontal cortex mediates the suppressive effect of intra-prelimbic cortical infusion of BDNF on cocaine-seeking. Eur Neuropsychopharmacol 26:1989-1999.

Goebel-Goody SM, Baum M, Paspalas CD, Fernandez SM, Carty NC, Kurup P, Lombroso PJ (2012) Therapeutic implications for striatal-enriched protein tyrosine phosphatase (STEP) in neuropsychiatric disorders. Pharmacol Rev 64:65-87.

Goldman-Rakic PS, Leranth C, Williams SM, Mons N, Geffard M (1989) Dopamine synaptic complex with pyramidal neurons in primate cerebral cortex. Proc Natl Acad Sci U S A 86:9015-9019.

Goldstein RZ, Volkow ND (2011) Dysfunction of the prefrontal cortex in addiction: neuroimaging findings and clinical implications. Nat Rev Neurosci 12:652-669.

Gomez JL, Bonaventura J, Lesniak W, Mathews WB, Sysa-Shah P, Rodriguez LA, Ellis RJ, Richie CT, Harvey BK, Dannals RF, Pomper MG, Bonci A, Michaelides M (2017) Chemogenetics revealed: DREADD occupancy and activation via converted clozapine. Science 357:503-507.

Graybiel AM, Moratalla R, Robertson HA (1990) Amphetamine and cocaine induce drug-specific activation of the c-fos gene in striosome-matrix compartments and limbic subdivisions of the striatum. Proc Natl Acad Sci U S A 87:6912-6916.

Hardingham GE, Arnold FJ, Bading H (2001) A calcium microdomain near NMDA receptors: on switch for ERK-dependent synapse-to-nucleus communication. Nat Neurosci 4:565-566.

Hardingham GE, Fukunaga Y, Bading H (2002) Extrasynaptic NMDARs oppose synaptic NMDARs by triggering CREB shut-off and cell death pathways. Nat Neurosci 5:405-414.

Hearing M, Kotecki L, Marron Fernandez de Velasco E, Fajardo-Serrano A, Chung HJ, Lujan R, Wickman K (2013) Repeated cocaine weakens GABA(B)-Girk

signaling in layer 5/6 pyramidal neurons in the prelimbic cortex. Neuron 80:159-170.

Hearing MC, Miller SW, See RE, McGinty JF (2008) Relapse to cocaine seeking increases activity-regulated gene expression differentially in the prefrontal cortex of abstinent rats. Psychopharmacology (Berl) 198:77-91.

Heinsbroek JA, Neuhofer DN, Griffin WC, 3rd, Siegel GS, Bobadilla AC, Kupchik YM, Kalivas PW (2017) Loss of Plasticity in the D2-Accumbens Pallidal Pathway Promotes Cocaine Seeking. J Neurosci 37:757-767.

Hemby SE, Horman B, Tang W (2005) Differential regulation of ionotropic glutamate receptor subunits following cocaine self-administration. Brain Res 1064:75-82.

Hervig ME, Thomsen MS, Kallo I, Mikkelsen JD (2016) Acute phencyclidine administration induces c-Fos-immunoreactivity in interneurons in cortical and subcortical regions. Neuroscience 334:13-25.

Hollander JA, Carelli RM (2005) Abstinence from cocaine self-administration heightens neural encoding of goal-directed behaviors in the accumbens. Neuropsychopharmacology 30:1464-1474.

Hollmann M, Heinemann S (1994) Cloned glutamate receptors. Annu Rev Neurosci 17:31-108.

Holtmaat A, Wilbrecht L, Knott GW, Welker E, Svoboda K (2006) Experience-dependent and cell-type-specific spine growth in the neocortex. Nature 441:979-983.

Hope BT, Crombag HS, Jedynak JP, Wise RA (2005) Neuroadaptations of total levels of adenylate cyclase, protein kinase A, tyrosine hydroxylase, cdk5 and neurofilaments in the nucleus accumbens and ventral tegmental area do not correlate with expression of sensitized or tolerant locomotor responses to cocaine. J Neurochem 92:536-545.

Horch HW, Kruttgen A, Portbury SD, Katz LC (1999) Destabilization of cortical dendrites and spines by BDNF. Neuron 23:353-364.

Hu H, Real E, Takamiya K, Kang MG, Ledoux J, Huganir RL, Malinow R (2007) Emotion enhances learning via norepinephrine regulation of AMPA-receptor trafficking. Cell 131:160-173.

Huang YZ, McNamara JO (2010) Mutual regulation of Src family kinases and the neurotrophin receptor TrkB. J Biol Chem 285:8207-8217.

Huganir RL, Nicoll RA (2013) AMPARs and synaptic plasticity: the last 25 years. Neuron 80:704-717.

Ide JS, Zhang S, Hu S, Sinha R, Mazure CM, Li CR (2014) Cerebral gray matter volumes and low-frequency fluctuation of BOLD signals in cocaine

dependence: duration of use and gender difference. Drug Alcohol Depend 134:51-62.

Ivanov A, Pellegrino C, Rama S, Dumalska I, Salyha Y, Ben-Ari Y, Medina I (2006) Opposing role of synaptic and extrasynaptic NMDA receptors in regulation of the extracellular signal-regulated kinases (ERK) activity in cultured rat hippocampal neurons. J Physiol 572:789-798.

James MH, McGlinchey EM, Vattikonda A, Mahler SV, Aston-Jones G (2018) Cued Reinstatement of Cocaine but Not Sucrose Seeking Is Dependent on Dopamine Signaling in Prelimbic Cortex and Is Associated with Recruitment of Prelimbic Neurons That Project to Contralateral Nucleus Accumbens Core. Int J Neuropsychopharmacol 21:89-94.

Jasinska AJ, Chen BT, Bonci A, Stein EA (2015) Dorsal medial prefrontal cortex (MPFC) circuitry in rodent models of cocaine use: implications for drug addiction therapies. Addict Biol 20:215-226.

Jourdi H, Kabbaj M (2013) Acute BDNF treatment upregulates GluR1-SAP97 and GluR2-GRIP1 interactions: implications for sustained AMPA receptor expression. PLoS One 8:e57124.

Junyent F, Kremer EJ (2015) CAV-2--why a canine virus is a neurobiologist's best friend. Curr Opin Pharmacol 24:86-93.

Kalivas PW (2009) The glutamate homeostasis hypothesis of addiction. Nat Rev Neurosci 10:561-572.

Kalivas PW, O'Brien C (2008) Drug addiction as a pathology of staged neuroplasticity. Neuropsychopharmacology 33:166-180.

Kalivas PW, Volkow ND (2011) New medications for drug addiction hiding in glutamatergic neuroplasticity. Mol Psychiatry 16:974-986.

Kalivas PW, Volkow N, Seamans J (2005) Unmanageable motivation in addiction: a pathology in prefrontal-accumbens glutamate transmission. Neuron 45:647-650.

Kalivas PW, Pierce RC, Cornish J, Sorg BA (1998) A role for sensitization in craving and relapse in cocaine addiction. J Psychopharmacol 12:49-53.

Kasai H, Matsuzaki M, Noguchi J, Yasumatsu N, Nakahara H (2003) Structure-stability-function relationships of dendritic spines. Trends Neurosci 26:360-368.

Kaufmann A, Keim A, Thiel G (2013) Regulation of immediate-early gene transcription following activation of Galpha(q)-coupled designer receptors. J Cell Biochem 114:681-696.

Keifer OP, Jr., Hurt RC, Gutman DA, Keilholz SD, Gourley SL, Ressler KJ (2015) Voxel-based morphometry predicts shifts in dendritic spine density and morphology with auditory fear conditioning. Nat Commun 6:7582.

Kelly MP (2018) Cyclic nucleotide signaling changes associated with normal aging and age-related diseases of the brain. Cell Signal 42:281-291.

Kerstetter KA, Wunsch AM, Nakata KG, Donckels E, Neumaier JF, Ferguson SM (2016) Corticostriatal Afferents Modulate Responsiveness to Psychostimulant Drugs and Drug-Associated Stimuli. Neuropsychopharmacology 41:1128-1137.

Kim MJ, Dunah AW, Wang YT, Sheng M (2005) Differential roles of NR2A- and NR2B-containing NMDA receptors in Ras-ERK signaling and AMPA receptor trafficking. Neuron 46:745-760.

Krapivinsky G, Krapivinsky L, Manasian Y, Ivanov A, Tyzio R, Pellegrino C, Ben-Ari Y, Clapham DE, Medina I (2003) The NMDA receptor is coupled to the ERK pathway by a direct interaction between NR2B and RasGRF1. Neuron 40:775-784.

Kupchik YM, Brown RM, Heinsbroek JA, Lobo MK, Schwartz DJ, Kalivas PW (2015) Coding the direct/indirect pathways by D1 and D2 receptors is not valid for accumbens projections. Nat Neurosci 18:1230-1232.

Kurup P, Zhang Y, Xu J, Venkitaramani DV, Haroutunian V, Greengard P, Nairn AC, Lombroso PJ (2010) A -Mediated NMDA Receptor Endocytosis in Alzheimer's Disease Involves Ubiquitination of the Tyrosine Phosphatase STEP61. Journal of Neuroscience 30:5948-5957.

Kurup PK, Xu J, Videira RA, Ononenyi C, Baltazar G, Lombroso PJ, Nairn AC (2015) STEP61 is a substrate of the E3 ligase parkin and is upregulated in Parkinson's disease. Proc Natl Acad Sci U S A 112:1202-1207.

Lambe EK, Aghajanian GK (2003) Hypocretin (orexin) induces calcium transients in single spines postsynaptic to identified thalamocortical boutons in prefrontal slice. Neuron 40:139-150.

Lambe EK, Picciotto MR, Aghajanian GK (2003) Nicotine induces glutamate release from thalamocortical terminals in prefrontal cortex. Neuropsychopharmacology 28:216-225.

Lein ES et al. (2007) Genome-wide atlas of gene expression in the adult mouse brain. Nature 445:168-176.

Leveille F, El Gaamouch F, Gouix E, Lecocq M, Lobner D, Nicole O, Buisson A (2008) Neuronal viability is controlled by a functional relation between synaptic and extrasynaptic NMDA receptors. FASEB J 22:4258-4271.

Li X, Wolf ME (2011) Brain-derived neurotrophic factor rapidly increases AMPA receptor surface expression in rat nucleus accumbens. Eur J Neurosci 34:190-198.

Little JP, Carter AG (2013) Synaptic mechanisms underlying strong reciprocal connectivity between the medial prefrontal cortex and basolateral amygdala. J Neurosci 33:15333-15342.

Liu D, Gu X, Zhu J, Zhang X, Han Z, Yan W, Cheng Q, Hao J, Fan H, Hou R, Chen Z, Chen Y, Li CT (2014) Medial prefrontal activity during delay period contributes to learning of a working memory task. Science 346:458-463.

Liu RJ, Aghajanian GK (2008) Stress blunts serotonin- and hypocretin-evoked EPSCs in prefrontal cortex: role of corticosterone-mediated apical dendritic atrophy. Proc Natl Acad Sci U S A 105:359-364.

Liu RJ, Ota KT, Dutheil S, Duman RS, Aghajanian GK (2015) Ketamine Strengthens CRF-Activated Amygdala Inputs to Basal Dendrites in mPFC Layer V Pyramidal Cells in the Prelimbic but not Infralimbic Subregion, A Key Suppressor of Stress Responses. Neuropsychopharmacology 40:2066-2075.

Liu RJ, Lee FS, Li XY, Bambico F, Duman RS, Aghajanian GK (2012) Brain-derived neurotrophic factor Val66Met allele impairs basal and ketamine-stimulated synaptogenesis in prefrontal cortex. Biol Psychiatry 71:996-1005.

Lobo MK, Covington HE, 3rd, Chaudhury D, Friedman AK, Sun H, Damez-Werno D, Dietz DM, Zaman S, Koo JW, Kennedy PJ, Mouzon E, Mogri M, Neve RL, Deisseroth K, Han MH, Nestler EJ (2010) Cell type-specific loss of BDNF signaling mimics optogenetic control of cocaine reward. Science 330:385-390.

Lodge DJ, Behrens MM, Grace AA (2009) A loss of parvalbumin-containing interneurons is associated with diminished oscillatory activity in an animal model of schizophrenia. J Neurosci 29:2344-2354.

Lombroso PJ, Naegele JR, Sharma E, Lerner M (1993) A protein tyrosine phosphatase expressed within dopaminoceptive neurons of the basal ganglia and related structures. J Neurosci 13:3064-3074.

Lu H, Cheng PL, Lim BK, Khoshnevisrad N, Poo MM (2010) Elevated BDNF after cocaine withdrawal facilitates LTP in medial prefrontal cortex by suppressing GABA inhibition. Neuron 67:821-833.

Lu L, Koya E, Zhai H, Hope BT, Shaham Y (2006) Role of ERK in cocaine addiction. Trends Neurosci 29:695-703.

Magill CK, Moore AM, Borschel GH, Mackinnon SE (2010) A new model for facial nerve research: the novel transgenic Thy1-GFP rat. Arch Facial Plast Surg 12:315-320.

Mahler SV, Aston-Jones G (2018) CNO Evil? Considerations for the Use of DREADDs in Behavioral Neuroscience. Neuropsychopharmacology 43:934-936.

Mao XY, Cao YG, Ji Z, Zhou HH, Liu ZQ, Sun HL (2015) Topiramate protects against glutamate excitotoxicity via activating BDNF/TrkB-dependent ERK

pathway in rodent hippocampal neurons. Prog Neuropsychopharmacol Biol Psychiatry 60:11-17.

Marron Fernandez de Velasco E, Carlblom N, Xia Z, Wickman K (2017) Suppression of inhibitory G protein signaling in forebrain pyramidal neurons triggers plasticity of glutamatergic neurotransmission in the nucleus accumbens core. Neuropharmacology 117:33-40.

Matsuo N, Reijmers L, Mayford M (2008) Spine-type-specific recruitment of newly synthesized AMPA receptors with learning. Science 319:1104-1107.

Matsuzaki M, Honkura N, Ellis-Davies GC, Kasai H (2004) Structural basis of long-term potentiation in single dendritic spines. Nature 429:761-766.

Matsuzaki M, Ellis-Davies GC, Nemoto T, Miyashita Y, Iino M, Kasai H (2001) Dendritic spine geometry is critical for AMPA receptor expression in hippocampal CA1 pyramidal neurons. Nat Neurosci 4:1086-1092.

McClure EA, Gipson CD, Malcolm RJ, Kalivas PW, Gray KM (2014) Potential role of N-acetylcysteine in the management of substance use disorders. CNS Drugs 28:95-106.

McFarland K, Kalivas PW (2001) The circuitry mediating cocaine-induced reinstatement of drug-seeking behavior. J Neurosci 21:8655-8663.

McFarland K, Lapish CC, Kalivas PW (2003) Prefrontal glutamate release into the core of the nucleus accumbens mediates cocaine-induced reinstatement of drug-seeking behavior. J Neurosci 23:3531-3537.

McGinty JF, Zelek-Molik A, Sun WL (2015) Cocaine self-administration causes signaling deficits in corticostriatal circuitry that are reversed by BDNF in early withdrawal. Brain Res 1628:82-87.

McGlinchey EM, James MH, Mahler SV, Pantazis C, Aston-Jones G (2016) Prelimbic to Accumbens Core Pathway Is Recruited in a Dopamine-Dependent Manner to Drive Cued Reinstatement of Cocaine Seeking. J Neurosci 36:8700-8711.

Middei S, Houeland G, Cavallucci V, Ammassari-Teule M, D'Amelio M, Marie H (2013) CREB is necessary for synaptic maintenance and learning-induced changes of the AMPA receptor GluA1 subunit. Hippocampus 23:488-499.

Middei S, Spalloni A, Longone P, Pittenger C, O'Mara SM, Marie H, Ammassari-Teule M (2012) CREB selectively controls learning-induced structural remodeling of neurons. Learn Mem 19:330-336.

Miszkiel J, Detka J, Cholewa J, Frankowska M, Nowak E, Budziszewska B, Przegalinski E, Filip M (2014) The effect of active and passive intravenous cocaine administration on the extracellular signal-regulated kinase (ERK) activity in the rat brain. Pharmacol Rep 66:630-637.

Moussawi K, Pacchioni A, Moran M, Olive MF, Gass JT, Lavin A, Kalivas PW (2009) N-Acetylcysteine reverses cocaine-induced metaplasticity. Nat Neurosci 12:182-189.

Nagappan G, Lu B (2005) Activity-dependent modulation of the BDNF receptor TrkB: mechanisms and implications. Trends Neurosci 28:464-471.

National Drug Intelligence Center (2011) The Economic Impact of Illicit Drug Use on American Society. Washington D.C. United States Department of Justice.

Nguyen TH, Liu J, Lombroso PJ (2002) Striatal enriched phosphatase 61 dephosphorylates Fyn at phosphotyrosine 420. J Biol Chem 277:24274-24279.

Oh MC, Derkach VA, Guire ES, Soderling TR (2006) Extrasynaptic membrane trafficking regulated by GluR1 serine 845 phosphorylation primes AMPA receptors for long-term potentiation. J Biol Chem 281:752-758.

Otis JM, Mueller D (2017) Reversal of Cocaine-Associated Synaptic Plasticity in Medial Prefrontal Cortex Parallels Elimination of Memory Retrieval. Neuropsychopharmacology 42:2000-2010.

Otis JM, Namboodiri VM, Matan AM, Voets ES, Mohorn EP, Kosyk O, McHenry JA, Robinson JE, Resendez SL, Rossi MA, Stuber GD (2017) Prefrontal cortex output circuits guide reward seeking through divergent cue encoding. Nature 543:103-107.

Parvaz MA, Moeller SJ, d'Oleire Uquillas F, Pflumm A, Maloney T, Alia-Klein N, Goldstein RZ (2017) Prefrontal gray matter volume recovery in treatment-seeking cocaine-addicted individuals: a longitudinal study. Addict Biol 22:1391-1401.

Pascoli V, Besnard A, Herve D, Pages C, Heck N, Girault JA, Caboche J, Vanhoutte P (2011) Cyclic adenosine monophosphate-independent tyrosine phosphorylation of NR2B mediates cocaine-induced extracellular signal-regulated kinase activation. Biol Psychiatry 69:218-227.

Paspalas CD, Wang M, Arnsten AF (2013) Constellation of HCN channels and cAMP regulating proteins in dendritic spines of the primate prefrontal cortex: potential substrate for working memory deficits in schizophrenia. Cereb Cortex 23:1643-1654.

Passafaro M, Nakagawa T, Sala C, Sheng M (2003) Induction of dendritic spines by an extracellular domain of AMPA receptor subunit GluR2. Nature 424:677-681.

Patterson MA, Szatmari EM, Yasuda R (2010) AMPA receptors are exocytosed in stimulated spines and adjacent dendrites in a Ras-ERK-dependent manner during long-term potentiation. Proc Natl Acad Sci U S A 107:15951-15956.

Paul S, Connor JA (2010) NR2B-NMDA receptor-mediated increases in intracellular Ca2+ concentration regulate the tyrosine phosphatase, STEP, and ERK MAP kinase signaling. J Neurochem 114:1107-1118.

Paul S, Nairn AC, Wang P, Lombroso PJ (2003) NMDA-mediated activation of the tyrosine phosphatase STEP regulates the duration of ERK signaling. Nat Neurosci 6:34-42.

Paul S, Snyder GL, Yokakura H, Picciotto MR, Nairn AC, Lombroso PJ (2000) The Dopamine/D1 receptor mediates the phosphorylation and inactivation of the protein tyrosine phosphatase STEP via a PKA-dependent pathway. J Neurosci 20:5630-5638.

Pei Y, Rogan SC, Yan F, Roth BL (2008) Engineered GPCRs as tools to modulate signal transduction. Physiology (Bethesda) 23:313-321.

Pelkey KA, Askalan R, Paul S, Kalia LV, Nguyen TH, Pitcher GM, Salter MW, Lombroso PJ (2002) Tyrosine phosphatase STEP is a tonic brake on induction of long-term potentiation. Neuron 34:127-138.

Pignataro A, Borreca A, Ammassari-Teule M, Middei S (2015) CREB Regulates Experience-Dependent Spine Formation and Enlargement in Mouse Barrel Cortex. Neural Plast 2015:651469.

Pozo K, Cingolani LA, Bassani S, Laurent F, Passafaro M, Goda Y (2012) beta3 integrin interacts directly with GluA2 AMPA receptor subunit and regulates AMPA receptor expression in hippocampal neurons. Proc Natl Acad Sci U S A 109:1323-1328.

Prithviraj R, Kelly KM, Espinoza-Lewis R, Hexom T, Clark AB, Inglis FM (2008) Differential regulation of dendrite complexity by AMPA receptor subunits GluR1 and GluR2 in motor neurons. Dev Neurobiol 68:247-264.

Pulipparacharuvil S, Renthal W, Hale CF, Taniguchi M, Xiao G, Kumar A, Russo SJ, Sikder D, Dewey CM, Davis MM, Greengard P, Nairn AC, Nestler EJ, Cowan CW (2008) Cocaine regulates MEF2 to control synaptic and behavioral plasticity. Neuron 59:621-633.

Quintero GC (2013) Role of nucleus accumbens glutamatergic plasticity in drug addiction. Neuropsychiatr Dis Treat 9:1499-1512.

Radley JJ, Anderson RM, Cosme CV, Glanz RM, Miller MC, Romig-Martin SA, LaLumiere RT (2015) The Contingency of Cocaine Administration Accounts for Structural and Functional Medial Prefrontal Deficits and Increased Adrenocortical Activation. J Neurosci 35:11897-11910.

Radley JJ, Rocher AB, Miller M, Janssen WG, Liston C, Hof PR, McEwen BS, Morrison JH (2006) Repeated stress induces dendritic spine loss in the rat medial prefrontal cortex. Cereb Cortex 16:313-320.

Rasakham K, Schmidt HD, Kay K, Huizenga MN, Calcagno N, Pierce RC, Spires-Jones TL, Sadri-Vakili G (2014) Synapse density and dendritic complexity

are reduced in the prefrontal cortex following seven days of forced abstinence from cocaine self-administration. PLoS One 9:e102524.

Reissner KJ, Gipson CD, Tran PK, Knackstedt LA, Scofield MD, Kalivas PW (2015) Glutamate transporter GLT-1 mediates N-acetylcysteine inhibition of cocaine reinstatement. Addict Biol 20:316-323.

Restivo L, Vetere G, Bontempi B, Ammassari-Teule M (2009) The formation of recent and remote memory is associated with time-dependent formation of dendritic spines in the hippocampus and anterior cingulate cortex. J Neurosci 29:8206-8214.

Robbins SJ, Ehrman RN, Childress AR, O'Brien CP (1999) Comparing levels of cocaine cue reactivity in male and female outpatients. Drug Alcohol Depend 53:223-230.

Robinson TE, Gorny G, Mitton E, Kolb B (2001) Cocaine self-administration alters the morphology of dendrites and dendritic spines in the nucleus accumbens and neocortex. Synapse 39:257-266.

Roche KW, O'Brien RJ, Mammen AL, Bernhardt J, Huganir RL (1996) Characterization of multiple phosphorylation sites on the AMPA receptor GluR1 subunit. Neuron 16:1179-1188.

Rogan SC, Roth BL (2011) Remote control of neuronal signaling. Pharmacol Rev 63:291-315.

Ruan H, Yao WD (2017) Cocaine Promotes Coincidence Detection and Lowers Induction Threshold during Hebbian Associative Synaptic Potentiation in Prefrontal Cortex. J Neurosci 37:986-997.

Russo SJ, Dietz DM, Dumitriu D, Morrison JH, Malenka RC, Nestler EJ (2010) The addicted synapse: mechanisms of synaptic and structural plasticity in nucleus accumbens. Trends Neurosci 33:267-276.

Rutherford LC, Nelson SB, Turrigiano GG (1998) BDNF has opposite effects on the quantal amplitude of pyramidal neuron and interneuron excitatory synapses. Neuron 21:521-530.

Saavedra A, Puigdellivol M, Tyebji S, Kurup P, Xu J, Gines S, Alberch J, Lombroso PJ, Perez-Navarro E (2016) BDNF Induces Striatal-Enriched Protein Tyrosine Phosphatase 61 Degradation Through the Proteasome. Mol Neurobiol 53:4261-4273.

Saglietti L, Dequidt C, Kamieniarz K, Rousset MC, Valnegri P, Thoumine O, Beretta F, Fagni L, Choquet D, Sala C, Sheng M, Passafaro M (2007) Extracellular interactions between GluR2 and N-cadherin in spine regulation. Neuron 54:461-477.

Sala C, Segal M (2014) Dendritic spines: the locus of structural and functional plasticity. Physiol Rev 94:141-188.

Sanders J, Cowansage K, Baumgartel K, Mayford M (2012) Elimination of dendritic spines with long-term memory is specific to active circuits. J Neurosci 32:12570-12578.

Sargin D, Mercaldo V, Yiu AP, Higgs G, Han JH, Frankland PW, Josselyn SA (2013) CREB regulates spine density of lateral amygdala neurons: implications for memory allocation. Front Behav Neurosci 7:209.

Scofield MD, Heinsbroek JA, Gipson CD, Kupchik YM, Spencer S, Smith AC, Roberts-Wolfe D, Kalivas PW (2016a) The Nucleus Accumbens: Mechanisms of Addiction across Drug Classes Reflect the Importance of Glutamate Homeostasis. Pharmacol Rev 68:816-871.

Scofield MD, Li H, Siemsen BM, Healey KL, Tran PK, Woronoff N, Boger HA, Kalivas PW, Reissner KJ (2016b) Cocaine Self-Administration and Extinction Leads to Reduced Glial Fibrillary Acidic Protein Expression and Morphometric Features of Astrocytes in the Nucleus Accumbens Core. Biol Psychiatry 80:207-215.

Sepulveda-Orengo MT, Healey KL, Kim R, Auriemma AC, Rojas J, Woronoff N, Hyppolite R, Reissner KJ (2017) Riluzole Impairs Cocaine Reinstatement and Restores Adaptations in Intrinsic Excitability and GLT-1 Expression. Neuropsychopharmacology 10.1038/npp.2017.244.

Sharma E, Zhao F, Bult A, Lombroso PJ (1995) Identification of two alternatively spliced transcripts of STEP: a subfamily of brain-enriched protein tyrosine phosphatases. Brain Res Mol Brain Res 32:87-93.

Shen H, Sesack SR, Toda S, Kalivas PW (2008) Automated quantification of dendritic spine density and spine head diameter in medium spiny neurons of the nucleus accumbens. Brain Struct Funct 213:149-157.

Shen HW, Gipson CD, Huits M, Kalivas PW (2014a) Prelimbic cortex and ventral tegmental area modulate synaptic plasticity differentially in nucleus accumbens during cocaine-reinstated drug seeking. Neuropsychopharmacology 39:1169-1177.

Shen HW, Scofield MD, Boger H, Hensley M, Kalivas PW (2014b) Synaptic glutamate spillover due to impaired glutamate uptake mediates heroin relapse. J Neurosci 34:5649-5657.

Shepherd JD, Huganir RL (2007) The cell biology of synaptic plasticity: AMPA receptor trafficking. Annu Rev Cell Dev Biol 23:613-643.

Shi SH, Hayashi Y, Petralia RS, Zaman SH, Wenthold RJ, Svoboda K, Malinow R (1999) Rapid spine delivery and redistribution of AMPA receptors after synaptic NMDA receptor activation. Science 284:1811-1816.

Shi Y, Ethell IM (2006) Integrins control dendritic spine plasticity in hippocampal neurons through NMDA receptor and Ca2+/calmodulin-dependent protein kinase II-mediated actin reorganization. J Neurosci 26:1813-1822.

Sinha R (2011) New findings on biological factors predicting addiction relapse vulnerability. Curr Psychiatry Rep 13:398-405.

Smith AC, Kupchik YM, Scofield MD, Gipson CD, Wiggins A, Thomas CA, Kalivas PW (2014) Synaptic plasticity mediating cocaine relapse requires matrix metalloproteinases. Nat Neurosci 17:1655-1657.

Smith KS, Bucci DJ, Luikart BW, Mahler SV (2016) DREADDS: Use and application in behavioral neuroscience. Behav Neurosci 130:137-155.

Snyder EM, Nong Y, Almeida CG, Paul S, Moran T, Choi EY, Nairn AC, Salter MW, Lombroso PJ, Gouras GK, Greengard P (2005) Regulation of NMDA receptor trafficking by amyloid-beta. Nat Neurosci 8:1051-1058.

Spires-Jones TL, Kay K, Matsouka R, Rozkalne A, Betensky RA, Hyman BT (2011) Calcineurin inhibition with systemic FK506 treatment increases dendritic branching and dendritic spine density in healthy adult mouse brain. Neurosci Lett 487:260-263.

Spruston N (2008) Pyramidal neurons: dendritic structure and synaptic integration. Nat Rev Neurosci 9:206-221.

Stankeviciute NM, Scofield MD, Kalivas PW, Gipson CD (2014) Rapid, transient potentiation of dendritic spines in context-induced relapse to cocaine seeking. Addict Biol 19:972-974.

Stefanik MT, Kalivas PW (2013) Optogenetic dissection of basolateral amygdala projections during cue-induced reinstatement of cocaine seeking. Front Behav Neurosci 7:213.

Stefanik MT, Kupchik YM, Kalivas PW (2016) Optogenetic inhibition of cortical afferents in the nucleus accumbens simultaneously prevents cue-induced transient synaptic potentiation and cocaine-seeking behavior. Brain Struct Funct 221:1681-1689.

Stefanik MT, Moussawi K, Kupchik YM, Smith KC, Miller RL, Huff ML, Deisseroth K, Kalivas PW, LaLumiere RT (2013) Optogenetic inhibition of cocaine seeking in rats. Addict Biol 18:50-53.

Substance Abuse and Mental Health Services Administration, Drug Abuse Warning Network (2011) National Estimates of Drug-Related Emergency Department Visits. HHS Publication No. (SMA) 13-4760, DAWN Series D-39. Rockville, MD

Sun W, Rebec GV (2006) Repeated cocaine self-administration alters processing of cocaine-related information in rat prefrontal cortex. J Neurosci 26:8004-8008.

Sun WL, Zelek-Molik A, McGinty JF (2013) Short and long access to cocaine self-administration activates tyrosine phosphatase STEP and attenuates GluN expression but differentially regulates GluA expression in the prefrontal cortex. Psychopharmacology (Berl) 229:603-613.

Sun WL, Eisenstein SA, Zelek-Molik A, McGinty JF (2014a) A single brain-derived neurotrophic factor infusion into the dorsomedial prefrontal cortex attenuates cocaine self-administration-induced phosphorylation of synapsin in the nucleus accumbens during early withdrawal. Int J Neuropsychopharmacol 18.

Sun WL, Coleman NT, Zelek-Molik A, Barry SM, Whitfield TW, Jr., McGinty JF (2014b) Relapse to cocaine-seeking after abstinence is regulated by cAMP-dependent protein kinase A in the prefrontal cortex. Addict Biol 19:77-86.

Sun X, Zhao Y, Wolf ME (2005) Dopamine receptor stimulation modulates AMPA receptor synaptic insertion in prefrontal cortex neurons. J Neurosci 25:7342-7351.

Swanson AM, DePoy LM, Gourley SL (2017) Inhibiting Rho kinase promotes goal-directed decision making and blocks habitual responding for cocaine. Nat Commun 8:1861.

Szepesi Z, Hosy E, Ruszczycki B, Bijata M, Pyskaty M, Bikbaev A, Heine M, Choquet D, Kaczmarek L, Wlodarczyk J (2014) Synaptically released matrix metalloproteinase activity in control of structural plasticity and the cell surface distribution of GluA1-AMPA receptors. PLoS One 9:e98274.

Tanaka J, Horiike Y, Matsuzaki M, Miyazaki T, Ellis-Davies GC, Kasai H (2008) Protein synthesis and neurotrophin-dependent structural plasticity of single dendritic spines. Science 319:1683-1687.

Taniguchi M, Carreira MB, Cooper YA, Bobadilla AC, Heinsbroek JA, Koike N, Larson EB, Balmuth EA, Hughes BW, Penrod RD, Kumar J, Smith LN, Guzman D, Takahashi JS, Kim TK, Kalivas PW, Self DW, Lin Y, Cowan CW (2017) HDAC5 and Its Target Gene, Npas4, Function in the Nucleus Accumbens to Regulate Cocaine-Conditioned Behaviors. Neuron 96:130-144 e136.

Taniguchi S, Nakazawa T, Tanimura A, Kiyama Y, Tezuka T, Watabe AM, Katayama N, Yokoyama K, Inoue T, Izumi-Nakaseko H, Kakuta S, Sudo K, Iwakura Y, Umemori H, Inoue T, Murphy NP, Hashimoto K, Kano M, Manabe T, Yamamoto T (2009) Involvement of NMDAR2A tyrosine phosphorylation in depression-related behaviour. EMBO J 28:3717-3729.

Tao X, Finkbeiner S, Arnold DB, Shaywitz AJ, Greenberg ME (1998) Ca2+ influx regulates BDNF transcription by a CREB family transcription factor-dependent mechanism. Neuron 20:709-726.

Terraneo A, Leggio L, Saladini M, Ermani M, Bonci A, Gallimberti L (2016) Transcranial magnetic stimulation of dorsolateral prefrontal cortex reduces cocaine use: A pilot study. Eur Neuropsychopharmacol 26:37-44.

Tervo DG, Hwang BY, Viswanathan S, Gaj T, Lavzin M, Ritola KD, Lindo S, Michael S, Kuleshova E, Ojala D, Huang CC, Gerfen CR, Schiller J, Dudman JT, Hantman AW, Looger LL, Schaffer DV, Karpova AY (2016) A

Designer AAV Variant Permits Efficient Retrograde Access to Projection Neurons. Neuron 92:372-382.

Tian M, Xu J, Lei G, Lombroso PJ, Jackson MF, MacDonald JF (2016) STEP activation by Galphaq coupled GPCRs opposes Src regulation of NMDA receptors containing the GluN2A subunit. Sci Rep 6:36684.

Tonnesen J, Katona G, Rozsa B, Nagerl UV (2014) Spine neck plasticity regulates compartmentalization of synapses. Nat Neurosci 17:678-685.

Trachtenberg JT, Chen BE, Knott GW, Feng G, Sanes JR, Welker E, Svoboda K (2002) Long-term in vivo imaging of experience-dependent synaptic plasticity in adult cortex. Nature 420:788-794.

Trantham-Davidson H, Centanni SW, Garr SC, New NN, Mulholland PJ, Gass JT, Glover EJ, Floresco SB, Crews FT, Krishnan HR, Pandey SC, Chandler LJ (2017) Binge-Like Alcohol Exposure During Adolescence Disrupts Dopaminergic Neurotransmission in the Adult Prelimbic Cortex. Neuropsychopharmacology 42:1024-1036.

Valjent E, Corvol JC, Pages C, Besson MJ, Maldonado R, Caboche J (2000) Involvement of the extracellular signal-regulated kinase cascade for cocaine-rewarding properties. J Neurosci 20:8701-8709.

Valjent E, Pascoli V, Svenningsson P, Paul S, Enslen H, Corvol JC, Stipanovich A, Caboche J, Lombroso PJ, Nairn AC, Greengard P, Herve D, Girault JA (2005) Regulation of a protein phosphatase cascade allows convergent dopamine and glutamate signals to activate ERK in the striatum. Proc Natl Acad Sci U S A 102:491-496.

Vissavajjhala P, Janssen WG, Hu Y, Gazzaley AH, Moran T, Hof PR, Morrison JH (1996) Synaptic distribution of the AMPA-GluR2 subunit and its colocalization with calcium-binding proteins in rat cerebral cortex: an immunohistochemical study using a GluR2-specific monoclonal antibody. Exp Neurol 142:296-312.

Volkow ND, Wise RA, Baler R (2017) The dopamine motive system: implications for drug and food addiction. Nat Rev Neurosci 18:741-752.

Volkow ND, Hitzemann R, Wang GJ, Fowler JS, Wolf AP, Dewey SL, Handlesman L (1992) Long-term frontal brain metabolic changes in cocaine abusers. Synapse 11:184-190.

West EA, Saddoris MP, Kerfoot EC, Carelli RM (2014) Prelimbic and infralimbic cortical regions differentially encode cocaine-associated stimuli and cocaine-seeking before and following abstinence. Eur J Neurosci 39:1891-1902.

Whitfield TW, Jr., Shi X, Sun WL, McGinty JF (2011) The suppressive effect of an intra-prefrontal cortical infusion of BDNF on cocaine-seeking is Trk receptor

and extracellular signal-regulated protein kinase mitogen-activated protein kinase dependent. J Neurosci 31:834-842.

Williams JM, Steketee JD (2004) Cocaine increases medial prefrontal cortical glutamate overflow in cocaine-sensitized rats: a time course study. Eur J Neurosci 20:1639-1646.

Wilmot CA, Szczepanik AM (1989) Effects of acute and chronic treatments with clozapine and haloperidol on serotonin (5-HT2) and dopamine (D2) receptors in the rat brain. Brain Res 487:288-298.

Wise RA, Wang B, You ZB (2008) Cocaine serves as a peripheral interoceptive conditioned stimulus for central glutamate and dopamine release. PLoS One 3:e2846.

Xu J, Kurup P, Baguley TD, Foscue E, Ellman JA, Nairn AC, Lombroso PJ (2016) Inhibition of the tyrosine phosphatase STEP61 restores BDNF expression and reverses motor and cognitive deficits in phencyclidine-treated mice. Cell Mol Life Sci 73:1503-1514.

Xu J, Kurup P, Zhang Y, Goebel-Goody SM, Wu PH, Hawasli AH, Baum ML, Bibb JA, Lombroso PJ (2009) Extrasynaptic NMDA receptors couple preferentially to excitotoxicity via calpain-mediated cleavage of STEP. J Neurosci 29:9330-9343.

Xu J et al. (2014) Inhibitor of the tyrosine phosphatase STEP reverses cognitive deficits in a mouse model of Alzheimer's disease. PLoS Biol 12:e1001923.

Xu J et al. (2018) Inhibition of STEP61 ameliorates deficits in mouse and hiPSC-based schizophrenia models. Mol Psychiatry 23:271-281.

Yap CC, Digilio L, McMahon L, Garcia DA, Winckler B (2017) Bulk degradation of dendritic cargos requires Rab7-dependent transport in Rab7-positive/LAMP1-negative endosomes to somatic lysosomes. bioRxiv 10.1101/215970.

Yau JO, McNally GP (2015) Pharmacogenetic excitation of dorsomedial prefrontal cortex restores fear prediction error. J Neurosci 35:74-83.

Yuen EY, Wei J, Liu W, Zhong P, Li X, Yan Z (2012) Repeated stress causes cognitive impairment by suppressing glutamate receptor expression and function in prefrontal cortex. Neuron 73:962-977.

Zahm DS, Becker ML, Freiman AJ, Strauch S, Degarmo B, Geisler S, Meredith GE, Marinelli M (2010) Fos after single and repeated self-administration of cocaine and saline in the rat: emphasis on the Basal forebrain and recalibration of expression. Neuropsychopharmacology 35:445-463.

Zhai H, Li Y, Wang X, Lu L (2008) Drug-induced alterations in the extracellular signal-regulated kinase (ERK) signalling pathway: implications for reinforcement and reinstatement. Cell Mol Neurobiol 28:157-172.

Zhai S, Ark ED, Parra-Bueno P, Yasuda R (2013) Long-distance integration of nuclear ERK signaling triggered by activation of a few dendritic spines. Science 342:1107-1111.

Zhang Y, Loonam TM, Noailles PA, Angulo JA (2001) Comparison of cocaine- and methamphetamine-evoked dopamine and glutamate overflow in somatodendritic and terminal field regions of the rat brain during acute, chronic, and early withdrawal conditions. Ann N Y Acad Sci 937:93-120.

Zhang Y, Kurup P, Xu J, Anderson GM, Greengard P, Nairn AC, Lombroso PJ (2011) Reduced levels of the tyrosine phosphatase STEP block beta amyloid-mediated GluA1/GluA2 receptor internalization. J Neurochem 119:664-672.

Zhang Y, Venkitaramani DV, Gladding CM, Zhang Y, Kurup P, Molnar E, Collingridge GL, Lombroso PJ (2008) The tyrosine phosphatase STEP mediates AMPA receptor endocytosis after metabotropic glutamate receptor stimulation. J Neurosci 28:10561-10566.

Zhang Z, Fan J, Ren Y, Zhou W, Yin G (2013) The release of glutamate from cortical neurons regulated by BDNF via the TrkB/Src/PLC-gamma1 pathway. J Cell Biochem 114:144-151.

Zuo Y, Lin A, Chang P, Gan WB (2005) Development of long-term dendritic spine stability in diverse regions of cerebral cortex. Neuron 46:181-189.